Interactions between biosphere and atmosphere as an important source of nitrous acid

Dissertation
zur Erlangung des Grades
‘Doktor rerum naturalium (Dr. rer. nat.)’
im Promotionsfach Chemie
am Fachbereich Chemie, Pharmazie und Geowissenschaften
der Johannes Gutenberg-Universität in Mainz,
Max Planck Graduate School

Hannah Meusel
geb. am 07.05.1986 in Ludwigshafen/Rhein

Mainz, Mai 2017

I hereby declare that I wrote the dissertation without any unauthorized external assistance. I used only sources acknowledged in the work. All textual passages which are appropriated verbatim or paraphrased from published and unpublished texts as well as all information obtained from oral sources are duly indicated and listed in accordance with bibliographical rules. In carrying out this research, I complied with the rules of standard scientific practice as formulated in the statutes of Johannes Gutenberg-University Mainz to insure standard scientific practice.

Abstract

Interactions between biosphere, lithosphere, hydrosphere and atmosphere are important processes in the Earth´s environment. There are several elements which are distributed in each compartment, e.g., nitrogen and carbon. Biogeochemical cycles describe the partition and the pathways of those compounds between environmental compartments. In this PhD project the partition of nitrous acid between the lithosphere/biosphere and atmosphere has been studied. Nitrous acid (HONO) is not only part of the nitrogen cycle, but also an important precursor of the OH radical, the key oxidant in the atmosphere. The current knowledge of atmospheric HONO sources is still unsatisfactory. Thus, more research on HONO sources is needed to improve simulations of the oxidative capacity of the atmosphere.

One main focus of this work is on biological emissions of reactive nitrogen (HONO and NO) from soil and biological soil crusts which cover the soil surface in semi-arid regions. The PhD study shows that natural ground surface emission can be the major source of atmospheric HONO in rural/remote regions. This was indicated by field measurements in Cyprus, a rural island in the East Mediterranean Sea, which detected much higher daytime HONO concentrations than expected by budget analysis and photostationary state calculations. While observed NO_2 concentrations were low, demonstrating that heterogeneous NO_2 conversion couldn´t account significantly for the HONO budget, the missing HONO source correlated well with NO and its missing source indicating a common origin. Laboratory based measurements of reactive nitrogen emission from local soil and biological soil crust samples (chlorolichen-, moss- and cyanobacteria-dominated types) showed a wide range of emission rates, which extrapolation, nevertheless, revealed a share of ~75% of the unaccounted HONO source. On the other hand, only 8% of the missing NO source could be attributed to soil/crust emissions and the NO source remained unclear.
Although the low NO_2 concentrations observed in Cyprus are not sufficient to explain the missing HONO source by heterogeneous uptake and conversion, the unexpected high HONO to NO_x ratio (mean 0.33) may indicate a highly efficient pathway to convert NO_2 into HONO. In addition, the good correlation of the missing HONO source with the product of the NO_2 photolysis rate and ambient NO_2 concentrations suggests photo-induced HONO formation. Hence, light enhanced heterogeneous conversion of NO_2 on biological surfaces, using proteins as a proxy, was studied in detail. Proteins exposed to NO_2 and light were shown to be nitrated and decompose, accompanied by simultaneous HONO production. Nitration of proteins enhances their allergenic potential. Initial NO_2 uptake coefficients on bovine serum albumin are comparable with NO_2 uptake coefficients reported for other surfaces like humic acid, several aromatic compounds or soot. Unlike in other studies, persistent HONO formation over a long time was observed, indicative of a catalytic surface reactivity.

In conclusion, the biosphere can play an important role in the atmospheric HONO budget, either by biological production and subsequent emission or by acting as a reactive surface for heterogeneous NO_2 conversion.

Zusammenfassung

Wechselwirkungen zwischen Biosphäre, Lithosphäre, Hydrosphäre und Atmosphäre sind wichtige Prozesse in der Umwelt der Erde. Es gibt einige Elemente, wie z.B. Stickstoff und Kohlenstoff, die in jedem dieser Bereiche vorkommen. Biogeochemische Kreisläufe beschreiben die Verteilung und die Pfade solcher Stoffe zwischen den Umweltbereichen. In dieser Doktorarbeit wird die Verteilung von salpetriger Säure zwischen Lithosphäre/ Biosphäre und Atmosphäre untersucht. Salpetrige Säure (HONO) ist nicht nur Teil des Stickstoffkreislaufs sondern auch ein wichtiger Vorläufer des OH Radikals, des Hauptoxidationsmittels in der Atmosphäre. Der derzeitige Wissensstand über atmosphärische HONO Quellen ist noch ungenügend. Demzufolge sind weitere Untersuchungen von HONO Quellen nötig um das Oxidationsvermögen der Atmosphäre besser simulieren zu können.

Ein Schwerpunkt dieser Doktorarbeit liegt bei der Untersuchung biologischer Emissionen von reaktivem Stickstoff (HONO und NO) aus Böden und biologischen Bodenkrusten, die die Bodenoberfläche in semiariden Regionen bedecken. Die Doktorarbeit zeigt, dass Emissionen aus natürlichen Bodenoberflächen die Hauptquelle von atmosphärischem HONO in ländlichen oder abgeschiedenen Gegenden sein können. Dies wurde anhand von Feldmessungen auf Zypern, einer ländlichen geprägten Insel im östlichen Mittelmeer gezeigt, welche viel höhere HONO-Tageskonzentrationen detektierten als durch Budgetanalysen und photostationäre Gleichgewichtsberechnungen zu erwarten waren. Während beobachtete NO_2 Konzentrationen gering waren und folglich heterogene NO_2 Umwandlungen nicht bedeutend zum HONO Budget beitragen konnten, korrelierte die fehlende HONO Quelle mit NO und dessen fehlender Quelle, was auf einen gemeinsamen Ursprung hindeutete. Laborbasierte Emissionsmessungen von reaktivem Stickstoff aus lokalen Boden- und biologischen Bodenkrustenproben (Grünalgenflechten, Moose und Cyanobakterien dominierende Typen) ergaben eine große Spanne an Emissionsraten, deren Hochrechnung dennoch einen Anteil von etwa 75% der fehlenden HONO Quelle abdeckten. Anderseits konnten nur 8% der fehlenden NO Quelle den Boden-und Bodenkrustenemissionen zugeschrieben werden und die NO Quelle blieb unklar.
Obwohl die geringen NO_2 Konzentrationen, die in Zypern beobachtet wurden, nicht ausreichten um die fehlende HONO Quelle durch heterogene Aufnahme und Umsetzung zu erklären, könnte das unerwartet hohe HONO-NO_x-Verhältnis (im Mittel 0.33) auf einen sehr effizienten Weg zur Umwandlung von NO_2 zu HONO hinweisen. Zusätzlich deutet die gute Korrelation von der fehlenden HONO Quelle mit dem Produkt aus der NO_2 Photolyserate und der NO_2-Umgebungskonzentration auf eine durch Licht initiierte HONO Bildung. Folglich wurde die durch Licht verstärkte heterogene NO_2-Umwandlung an Proteinen, stellvertretend für biologische Oberflächen, genauer untersucht. Es wurde gezeigt, dass Proteine, die NO_2 und Licht ausgesetzt sind, nitriert und unter gleichzeitiger HONO Bildung abgebaut werden. Nitrierung von Proteinen verstärkt deren Potential Allergien auszulösen. Anfängliche NO_2 Aufnahmekoeffizienten von Rinderserumalbumin sind mit berichteten NO_2 Aufnahmekoeffizienten von verschiedenen Oberflächen wie Huminsäure, einige aromatische Verbindungen oder Ruß vergleichbar. Anders als in anderen Studien, wurde eine stabile HONO Bildung über einen langen Zeitraum beobachtet, was auf eine katalytische Oberflächenaktivität hinweist.

Schlussfolgernd kann die Biosphäre, entweder durch biologische Produktion und folgender Emission oder durch Bereitstellung einer reaktiven Oberfläche für NO_2 Umwandlung, eine wichtige Rolle im atmosphärischem HONO-Budget spielen.

Content

1. Introduction

The composition of the atmosphere is influenced by biological processes in soil, vegetation and ocean interacting with physical and chemical reactions within the atmosphere. The physical surface-atmosphere exchange of many trace gases is often coupled with biological production. To understand the Earth system it is important to know the production, destruction and exchange processes.

An alteration of the atmospheric composition, being underway since the industrial revolution, causes changes in climate, biodiversity and biogeochemical cycling of nitrogen, carbon and sulphur. Biochemical cycles are influenced directly by anthropogenic impact like changes in land use or combustion. The emission of reactive nitrogen by human activities, for example, exceeds that from natural process by a factor of 4 at the end of the 20th century (Fowler et al., 2009; Galloway et al., 2004). But also the input of nitrogen into the soil increased caused by increased application of fertilizer. In general surfaces can act as sinks but also as sources of trace gases, depending on the equilibrium of those trace gases between biosphere surface and atmosphere.

In this PhD study I focused on the biosphere-atmosphere exchange of nitrous acid, an exemplary constituent of the nitrogen cycle, and particularly the emission from soil and biological soil crusts. The biosphere-atmosphere interactions were further investigated on the basis of light-induced heterogeneous reactions of nitrogen dioxide on biological surfaces, i.e., proteins.

1.1 Nitrous acid

Nitrous acid (HONO) is an important precursor of the OH radical. In the atmosphere the OH radical plays an important role (Levy, 1971). It is the main oxidant and is often called detergent of the troposphere. Reacting with volatile organic compounds or SO_2, particles are formed, as in general the products have lower vapor pressure and condense subsequently (Arey et al., 1990; Zhou et al., 2013). During the day OH is mainly generated by photolysis of O_3. But during the mornings photolysis of O_3 is usually low and photolysis of nitrous acid (HONO) becomes a more relevant source contributing up to 30% to the OH budget (Kleffmann et al., 2005; Alicke et al., 2002; Ren et al., 2006). Nitrite (NO_2^-) is part of the nitrogen cycle being widespread in the environment. In its protonated form (HNO_2 or HONO) it is mainly partitioned in the gas-phase but as NO_2^- it can also be found in aerosol particles, clouds and dew droplets, seawater, sediments and soil (Foster et al., 1990; Rubio et al., 2002; Acker et al., 2008; Bianchi et al., 1997). Ambient gas-phase mixing ratios range from several parts per trillion (ppt) in rural regions to some parts per billion (ppb) in polluted sites (Acker et al., 2006; Costabile et al., 2010, Michoud et al., 2014; Spataro et al., 2013; Su et al., 2008). Simulated atmospheric HONO concentrations are frequently lower than observed concentrations in field studies showing that not all sources of HONO have been described, yet (Kleffmann et al., 2005; Su et al., 2008; Sörgel et al., 2011; Michoud et al., 2014; Oswald et al., 2015). It can be derived from the gas-phase reaction of OH and NO, the reverse reaction of the depletion by photolysis. Direct HONO emissions during fossil fuel combustion are low,

only 0.8% of the NOx emitted by car engines consist of HONO (Kurtenbach et al., 2001). Recent studies observed heterogeneous NO_2 conversion on different surfaces, e.g., soot and organic-coated particles (Kalberer et al., 1999, Kleffmann et al., 1999; Arens et al., 2001, 2002; Ammann et al., 1998, 2005). Others found light-enhanced or light-induced HONO formation either via heterogeneous reactions of NO_2 or by photolysis of nitrated organic substances (e.g., nitrophenol) or nitric acid and nitrate (Monge et al., 2010; Sosedova et al., 2011; George et al., 2005; Ramazan et al., 2004; Stemmler et al., 2006, 2007; Bejan et al., 2006; Zhou et al., 2001, 2002, 2003). Nevertheless, these sources cannot explain HONO concentrations found in the environment (Elshorbany et al., 2012). Budget analyses reveal a missing source of about $5x10^5$ – $4x10^7$ cm^{-3} s^{-1} (Acker et al., 2006; Soergel et al., 2011; Kleffmann et al., 2005; Su et al., 2008; Wong et al., 2012). Vertical gradient measurements and simulations indicate a ground level HONO source (Kleffmann et al., 2003; Vogel et al., 2003; VandenBoer et al., 2013; Villena et al., 2011; Ren et al., 2011).

1.2 Biosphere

Soil, biological soil crusts (subsequently called biocrusts) and primary biological aerosols including proteins are important constituents of the biosphere and have direct contact to the atmosphere. It is known that soil can act as sink but also as source of many trace gases. Soil and soil biota represent a major environmental compartment of the biochemical cycle of nitrogen. Soil can emit reactive nitrogen like NO and N_2O (Meixner and Yang, 2006), and recently HONO emissions from soil were also observed (Oswald et al., 2013; Su et al., 2011). It was shown that biological activities, e.g., biological N fixation and subsequent nitrification and denitrification processes enhanced by cyanobacteria dominated and other biocrusts, can increase reactive nitrogen emissions (Abed et al., 2013; Weber et al., 2015). During biologic N fixation, atmospheric N_2 is fixed and transformed into ammonium (NH_4^+) via the enzyme nitrogenase. Ammonium is then oxidized in a stepwise manner into NO_2^- and nitrate (NO_3^-; nitrification). Denitrification enzymes reduce nitrate and nitrite to nitric oxide (NO), nitrous oxide (N_2O) and nitrogen (N_2). In dark cyanobacteria dominated biocrusts a higher biological activity was found compared to light cyanobacteria or lichen dominated biocrusts (Abed et al., 2013; Barger et al., 2013). Consistently, Weber et al. (2015) observed highest NO and HONO emissions from dark cyanobacteria dominated biocrusts followed by light cynobacteria, chlorolichen and moss dominated biocrusts sampled from South Africa. Bare soil had lowest emissions. Biocrusts are mainly found in arid and semi-arid ecosystems and grow within the uppermost millimeters to centimeters of soil. They are composed of photoautotrophic cyanobacteria, algae, lichens, and bryophytes, growing together with heterotrophic bacteria, fungi and archaea in varying proportions (Belnap et al., 2016).

Besides soil and biocrusts proteins are important constituents of the biosphere as they can be found in the whole environment and can affect human health, e.g., they cause allergies (D'Amato et al., 2007). They are part of aerosols in all size ranges. In form of pollen, fungal spores, plant debris and fragments of those they contribute to coarse particles (diameter > 2.5 µm). In fine particulate matter (diameter < 2.5 µm) proteins are dissolved in hydrometeors, mixed with fine dust and other particles (Miguel et al., 1999; Riediker et al., 2000; Zhang and

Anastasio, 2003). Up to 5% of particle mass in airborne particles is constituted by proteins (Franze et al., 2003; Menetrez et al., 2007). But proteins can also cover plants and soil. Proteins can be nitrated by air pollutants enhancing their allergenic potential (Shiraiwa et al., 2012; Gruijthuijsen et al., 2006). Nitration of proteins usually occurs at aromatic amino acids like tyrosine, tryptophan and phenylalanine. These aromatic amino acids are photosensitive and can be activated by UV-light which generates reactive radical intermediates which subsequently can react with NO_2 (Houee-Levin et al., 2015). Hence, irradiation of proteins might enhance nitration by air pollutants similar to the elevated NO_2 uptake of proteins which were initially exposed to O_3, forming also a radical intermediate (Shiraiwa et al., 2012). Nitrotyrosine has the same chemical structure as 3-nitrophenol, which photolysis forms HONO (Bejan et al., 2006). Therefore it is likely that irradiated nitrated proteins also produce HONO. On the other hand, as proteins are ubiquitously found in the environment, they might provide a reactive surface for heterogeneous reactions of NO_2.

1.3 Research objectives

It is important to get a better insight into atmospheric and multiphase processes like aerosol chemistry but also atmosphere-biosphere or atmosphere-lithosphere interactions and study their effects on climate change, air quality and public health.

This PhD thesis will help to better understand the oxidizing capacity of the atmosphere as it focuses on the unexplored sources of HONO a relevant precursor of the major tropospheric oxidant, the OH radical. On the one hand the (biological) emissions of HONO and NO from soils and biological soil crusts are studied. There are several studies which observe and quantify HONO and NO fluxes from soil but only a few compare them with observed missing sources or evaluate their contributions to the HONO budget. In this work ambient measurements, HONO budget analysis and lab-based flux measurements from soil samples from the same site are performed. Hence, an evaluation of the significance of soil emission on the local HONO budget is assessed. On the other hand HONO formation from heterogeneous NO_2 conversion on proteins (as an example of biosphere surfaces) and photolysis of nitrated proteins releasing HONO are studied. Simultaneously light initiated nitration of intact proteins is investigated.

1.4 Methods

In this PhD study three different methods were applied:

a) field measurements during a four week lasting extensive campaign on the East Mediterranean island Cyprus,
b) dynamic chamber studies (on emission fluxes from Cyprus soil and biological soil crust samples), and
c) coated-wall flow tube measurements (on light-induced protein nitration and degradation with HONO emission).

In summer 2014 an extensive field campaign took place in Cyprus, a rural island in the East Mediterranean Sea. The chosen measurement site was on a small hill, in 5.5-8 km distance from the sea. The population in the surrounded area of about 15 km was weak. With low anthropogenic activity and emission the site was ideal to study unknown HONO sources, and its contribution to the OH budget. During the campaign many trace gases like, NOx, O_3, and CO were detected, but also several volatile organic compounds (VOC) and hydrocarbons. Reactive species like OH, HO_2, NO_3 and N_2O_5 were measured. Besides the usual meteorological parameters (temperature, relative humidity, precipitation, wind direction and wind speed) also photolysis frequencies were recorded. Aerosol composition and particle size were measured, too.

Next to the measurement site 50 grids were placed at randomly selected spots for systematic ground cover assessment and totally 43 samples, with 6-10 replicates of each found cover species (bare soil, dark or light cyanobacteria dominated biocusts, chlorolichen or moss dominated biological biocrusts) were taken. Emission flux measurements of those samples were performed in dynamic Teflon chambers in temperature controlled laboratories. Measurements followed the well-proven method for emission studies. Therefore the sample was wetted till full water holding capacity, placed into the chamber and then dried completely by flushing with dry purified air. The measured flux or concentrations were transformed into an atmospheric/environmental flux according to Su et al., (2011) and converted into a corresponding ground source and compared to the observed missing source.

In the third part coated wall flow tubes were used. The proteins, here bovine serum albumin (BSA) and nitrated ovalbumin (n-OVA) were therefore coated to the inner wall of the glass flow tube (length 50 cm, inner diameter 8.1 mm). To study the light effects the coated tube was exposed to maximum 7 lamps in a circular arrangement surrounding the tube. The heating caused by illuminating lights was prevented by sheath air. The coated proteins were purged with humidified pure air or mixed with atmospheric relevant concentrations of NO_2. After the flow tube experiment the proteins were extracted from the wall with pure water and nitration degrees were analyzed by means of high performance liquid chromatography with diode array detection.

In all three studies HONO was analyzed with a commercial long path absorption photometer (LOPAP, QUMA, Wuppertal, Germany). Using an effective light path of 1.5 m and a time resolution of 30 s, LOPAP had a detection limit of 2-5 ppt. The instrument is based on a wet chemical analytical method. HONO is trapped efficiently in a stripping coil flushed with an acidic aqueous solution of sulfanilamide. There are two stripping coils in series to reduce known interfering signals (Heland et al., 2001). In the first coil HONO is quantitatively collected with an efficiency of about 99%. Interfering species are collected in both channels but only in small amounts. After a second reaction with N-(1-naphthyl)ethylenediamine-dihydrochloride forming an azo dye the concentration is determined via absorption photometry in a long Teflon tubing. The true concentration of HONO is obtained by subtracting the inferences quantified in the second channel from the total signal obtained from the first channel. This correction of chemical interferences showed excellent agreement with the differential optical absorption spectroscopy (DOAS) measurements, both in a smog chamber and under urban atmospheric conditions (Kleffmann et al., 2006).

For NOx measurements different instruments were used. But all three are based on chemiluminescence of the reaction between NO and O_3. Infrared light is emitted when electronically excited NO_2 molecules decay to lower energy levels. While NO can directly be detected via this reaction NO_2 must be initially transformed into NO. During the field campaign in Cyprus a modified commercial detector (CLD 790 SR), originally manufactured by ECO Physics (Duernten, Switzerland) with a photolytic NO_2 converter was applied. In the follow up study on emission fluxes from soil a commercial detector (42i) by Thermo Scientific (Watham, USA) modified with a photolytic converter was used. In the third study the NOx analyzer was a commercial CLD 77 AM (Eco Physics) with a molybdenum converter. A photolytic converter is more selective as NO_2 is converted via UV radiation but is less efficient than a molybdenum converter. In a molybdenum converter which is heated to about 325 °C NO_2 is converted with almost 100% efficiency but also other nitrogen species like HNO_3, NH_3 or peroxyacetyl nitrate are transformed. Limits of detection of the field measurements were lower than those of lab studies (NO: 5 – 50 ppt, NO_2: 20 – 65 ppt).
The specifications of the additional instruments applied during CYPHEX of which data were used for budget analysis are described in my publication (Meusel et al., 2016; see Appendix B1).

2 Results and discussion

2.1 Overview

The PhD project is divided into two parts with three first-author publications and five co-authored publications on related studies. The primary topic is about soil-atmosphere trace gas exchange. The second part is related to protein modification. Figure 1 shows an overview and the relation of the two topics and the single studies. The first study is based on field measurements in a rural site of Cyprus, in which a variety of trace gases and aerosols were detected. A large daytime missing HONO source was found which couldn´t be explained by NO_2 conversion only. A follow-up study deals with the possible suggested HONO source of soil emission. Therefore local soil and biological soil crust samples and their emission fluxes were analyzed by means of dynamic chamber studies. In a similar study reactive nitrogen emission from soil and biocrust samples from South Africa was measured. Furthermore I joined a study on soil-air trace gas exchange measurements of formaldehyde by means of the flow tube technique and I accompanied a technical study on the influence of surface roughness on coated-flow tube experiments for gas uptake analysis. These two ancillary studies are linked with the second PhD topic via the shared technical method of flow tube measurements. The second part of the PhD work focus on protein modification by air pollutants, i.e., light-induced protein nitration and decomposition. Both PhD topics share the common context of studying HONO sources. While in the first part HONO is directly emitted from soil, in the second part HONO is formed during decomposition of nitrated proteins and via light enhanced heterogeneous conversion of NO_2 on proteins, used as a proxy for biological surfaces.. Two publications with minor contribution deal with protein nitration and oligomerization upon O_3 and NO_2 exposure in darkness.

The results of the three main studies are summarized in the next chapter.

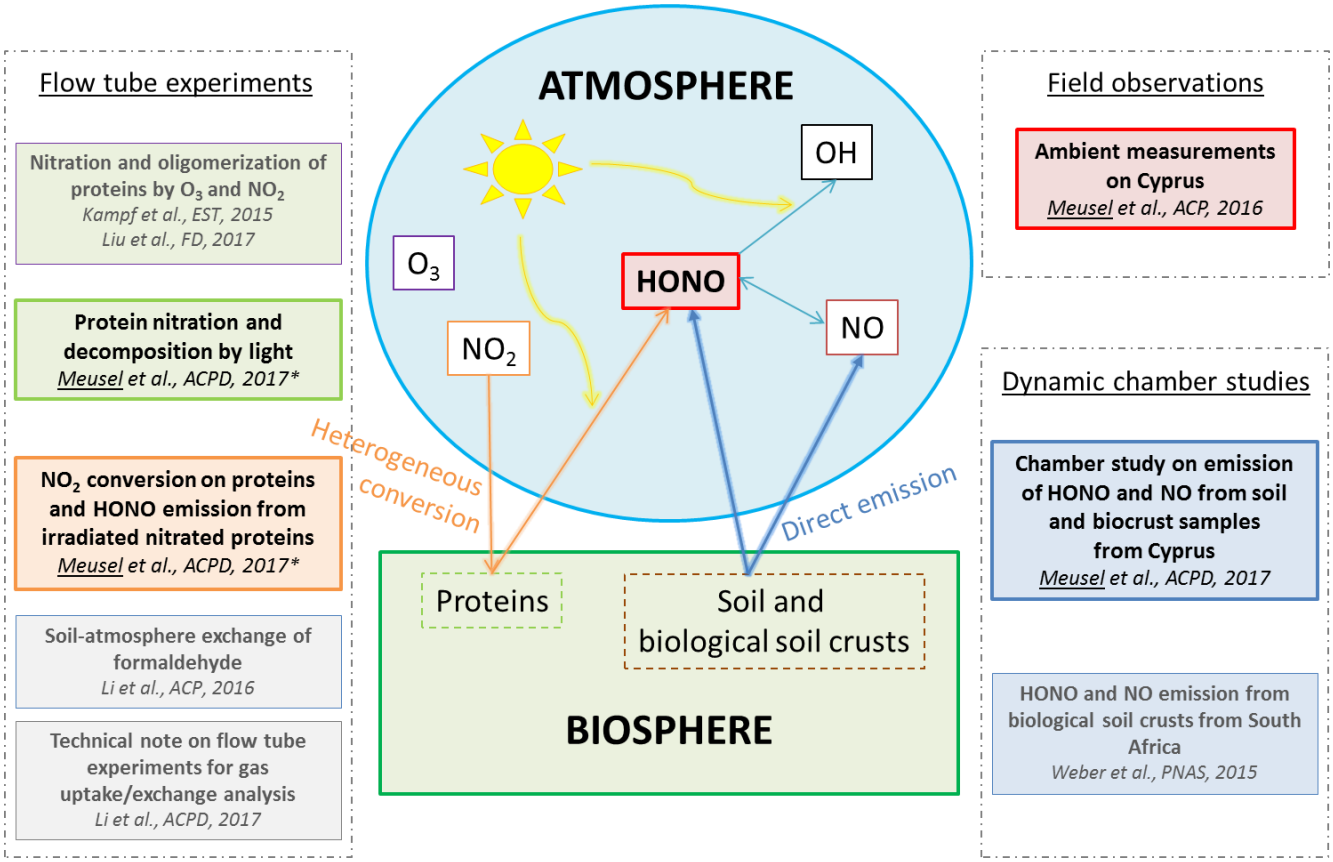

Fig.1: Structure of PhD thesis. In the middle the topic of the project of biosphere-atmosphere exchange is schematically presented. On the left and on the right side single studies, associated with peer-reviewed publications in international scientific journals are shown, separated based on the applied experimental method. Here, thick boxes indicate first-author publications and thin boxes (with grey text) indicate co-authored publication. Colors represent relations between publication and exchange process. The asterisk indicates the same publication.

2.2 Single studies

2.2.1 Nitrous acid on Cyprus

Cyprus, as a rural island in the East Mediterranean Sea with low local anthropogenic impact and low NO_x levels but with high solar radiation, was ideal to study unknown HONO sources. During the campaign the wind came from South-West bringing clean marine air to the site. In the low NOx environment (NOx < 1 ppb; NO_2 < 800 ppt, mean 150 ppt; NO < 100 ppt, mean 25 ppt) HONO mixing ratios of up to 150 ppt were found with unusual higher concentrations during day than night and strong morning peaks. High HONO to NOx ratios (mean 0.33) indicate HONO daytime sources independent from NO_2 or rather a highly effective pathway to convert NO_2 to HONO. The slight increase in HONO concentrations during night can be explained by heterogeneous NO_2 reactions with a conversion rate between 0.4-1.6% h^{-1}. Budget analysis revealed an unknown HONO source of a daytime mean of 1.3×10^6 cm^{-3} s^{-1}. Although the unknown HONO source correlated well with photolytic reactions of NO_2

(J_{NO2}*[NO_2], J_{NO2}*[NO_2]*RH) theses reactions cannot account prominently to the unknown HONO source as the NO_2 levels were too low. But good correlations of HONO and NO as well as the high correlations of their unknown sources indicate a common source. Emissions from soil and production of HONO and NO by biological soil crusts were considered to be a major source of HONO. The contribution of HONO to the local primary OH production was calculated to be about 40% in the morning hours with peak values of up to 65%.
For more details see Appendix B.1, Meusel et al., Atmos. Chem. Phys., 2016.

2.2.2 Emission of nitrous acid from Cyprus soil and biological soil crusts

In order to proof the above concluded hypothesis that soil and biocrusts from Cyprus emit HONO and NO and that these can be the major HONO source the emission fluxes of 25 samples from the same region were analyzed in chamber measurements. All samples showed both HONO and NO emissions with slightly higher HONO emissions. Bare soil samples emitted highest HONO-N and NO-N followed by light and dark cyanobacteria dominated biocrusts (BSC). Emissions from chlorolichen and moss dominated biocrusts were lowest. Emissions highly correlated with nutrient content, especially nitrite and nitrate. An environmental flux was calculated according to a standard formalism describing the atmosphere-soil exchange of trace gases as a function of the difference between atmospheric concentrations and the equilibrium concentration at the soil surface (Su et al., 2011). Considering the abundance of the biocrusts an overall flux of 2-19 ng m^{-2} s^{-1} HONO-N and 2-16 ng m^{-2} s^{-1} NO-N could be estimated for optimum soil water content and 25°C soil temperature. As bare soil had lowest and moss BSC highest abundance the contributions of each surface type to the total flux did not resemble the order of flux rates of the single surface type. In the high total emission range the contribution of light BSC was highest (HONO: 43%, NO: 50%), followed by bare soil (HONO: 25%, NO: 13%) and dark BSC (HONO: 20%, NO: 23%). Conversion of the environmental flux rate (at a soil water content of 10% water holding capacity, somewhat lower than the optimum soil water content as during CYPHEX no precipitation but high relative humidity was observed) into the estimated ground source exhibit that ground emissions can explain up to 75% of the missing source found during CYPHEX. But soil NO emissions only cover 8% of the observed missing source. During daytime soil temperature was detected to be higher than 25°C likely leading to higher HONO and NO emissions.
For more information see Appendix B.2, Meusel et al., Atmos. Chem. Phys. Disc. 2017a.

2.2.3 Heterogeneous reaction of NO_2 on light activated proteins

In high NOx level environment (contrary to Cyprus) heterogeneous reactions of NO_2 are proposed to be an important HONO source. This reaction could also be light enhanced which is also suggested by the Cyprus study as well as by several other publications. The unexpected high HONO to NOx ratio found during the CYPHEX campaign might also indicate a highly efficient conversion of NO_2 to HONO. In this chapter the heterogeneous conversion of NO_2 on light activated proteins (as an example of important biosphere surfaces) and the light-induced decomposition of nitrated proteins were studied. After some hours of NO_2 exposure

under irradiated conditions proteins were found to be slightly nitrated but mainly decomposed. Proteins which were nitrated in liquid phase (by tetranitromethane) prior to the flow tube experiments released HONO when irradiated even without NO_2 exposure and also degraded. HONO formation was strongly dependent on NO_2 concentration, coating thickness, relative humidity and light intensity. Results indicate that not only reactions on the surface but also in the bulk occur. Stable HONO formation was observed over 20 hours of light and NO_2 exposure. The estimated effective rate constant of the NO_2 conversion on untreated proteins is in the same range as NO_2 uptake coefficients on different irradiated surfaces like humic acid and other organic compounds but also soot.
The detailed study is shown in Appendix B.3, Meusel et al., Atmos. Chem. Phys. Disc. 2017b.

2.3 Conclusion

The PhD study focused on biosphere-atmosphere exchange of HONO and amplified the understanding in HONO chemistry and its unaccounted sources. It combined field measurements and lab studies. Ambient measurements on rural Cyprus provided a good first insight into the topic and showed that more research on HONO sources needs to be done as budget analysis reveal a big missing source. Dynamic chamber studies on emission fluxes of local soil and biological soil crusts verified that the major fraction of the missing HONO source derived from biological soil emissions. Contrary the contribution of NO emissions from soil to the missing source was only about 8%. Similar combined studies (ambient measurements, budget analysis and soil and biocrust emission studies) should be performed in different sites with different soil type and cover all over the world to better quantify emission rates and its contribution to the HONO budget. A modification of the chamber measurements, e.g., not wetting the soil samples but flushing with air of different humidity levels while measuring the emissions, should be considered to better simulate reactive nitrogen emissions in regions with few precipitation.
Another proposed HONO source of photochemical driven heterogeneous NO_2 conversion was investigated together with light-induced protein nitration. Light enhanced NO_2 uptake and HONO formation was already observed on several surfaces like humic acid, soot or phenolic compounds. Here irradiated proteins provided a highly reactive surface for the heterogeneous NO_2 conversion with stable HONO formation over a long time. Proteins can coat/cover different surfaces and are therefore likely to be an important medium for heterogeneous reactions. Simultaneously the proteins were nitrated and decomposed. Nitrated proteins enhance their allergenic potential but are likely to degrade under sunlight. Therefore the health effects of degraded proteins or single nitrated amino acids or peptides should be investigated carefully. More studies on photo-enhanced heterogeneous NO_2 reactions should be done as it seems to be a potential source of HONO.
It is important to improve the quality of simulations of atmospheric HONO and hence OH radical concentration, as OH measurements are extremely difficult due to its short lifetime, and a proper evaluation by models is crucial to ensure realistic representation of the oxidation pathways in the atmosphere.

References

Abed, R. M. M., Lam, P., de Beer, D., and Stief, P.: High rates of denitrification and nitrous oxide emission in arid biological soil crusts from the Sultanate of Oman, Isme Journal, 7, 1862-1875, 10.1038/ismej.2013.55, 2013.

Acker, K., Moller, D., Wieprecht, W., Meixner, F. X., Bohn, B., Gilge, S., Plass-Dulmer, C., and Berresheim, H.: Strong daytime production of OH from HNO2 at a rural mountain site, Geophysical Research Letters, 33, 10.1029/2005gl024643, 2006.

Acker, K., Beysens, D., and Moeller, D.: Nitrite in dew, fog, cloud and rain water: An indicator for heterogeneous processes on surfaces, Atmospheric Research, 87, 200-212, 10.1016/j.atmosres.2007.11.002, 2008.

Alicke, B., Platt, U., and Stutz, J.: Impact of nitrous acid photolysis on the total hydroxyl radical budget during the Limitation of Oxidant Production/Pianura Padana Produzione di Ozono study in Milan, Journal of Geophysical Research-Atmospheres, 107, 10.1029/2000jd000075, 2002.

Ammann, M., Kalberer, M., Jost, D. T., Tobler, L., Rossler, E., Piguet, D., Gaggeler, H. W., and Baltensperger, U.: Heterogeneous production of nitrous acid on soot in polluted air masses, Nature, 395, 157-160, 10.1038/25965, 1998.

Ammann, M., Rossler, E., Strekowski, R., and George, C.: Nitrogen dioxide multiphase chemistry: Uptake kinetics on aqueous solutions containing phenolic compounds, Physical Chemistry Chemical Physics, 7, 2513-2518, 10.1039/B501808K, 2005.

Arens, F., Gutzwiller, L., Baltensperger, U., Gaggeler, H. W., and Ammann, M.: Heterogeneous reaction of NO2 on diesel soot particles, Environmental Science & Technology, 35, 2191-2199, 10.1021/es000207s, 2001.

Arens, F., Gutzwiller, L., Gaggeler, H. W., and Ammann, M.: The reaction of NO2 with solid anthrarobin (1,2,10-trihydroxy-anthracene), Physical Chemistry Chemical Physics, 4, 3684-3690, 10.1039/B201713J, 2002.

Arey, J., Atkinson, R., and Aschmann, S. M.: Product study of the gas-phase reactions of monoterpenes with the OH radical in the presence of NO x, Journal of Geophysical Research: Atmospheres, 95, 18539-18546, 10.1029/JD095iD11p18539, 1990.

Barger, N. N., Castle, S. C., and Dean, G. N.: Denitrification from nitrogen-fixing biologically crusted soils in a cool desert environment, southeast Utah, USA, Ecological Processes, 2, 16, 10.1186/2192-1709-2-16, 2013.

Bejan, I., Abd El Aal, Y., Barnes, I., Benter, T., Bohn, B., Wiesen, P., and Kleffmann, J.: The photolysis of ortho-nitrophenols: a new gas phase source of HONO, Physical Chemistry Chemical Physics, 8, 2028-2035, 10.1039/b516590c, 2006.

Belnap, J., Weber, B., and Büdel, B.: Biological Soil Crusts as an Organizing Principle in Drylands, in: Biological Soil Crusts: An Organizing Principle in Drylands, 1 ed., edited by: Weber, B., Büdel, B., and Belnap, J., Ecological Studies, 226, Springer International Publishing, 3-13, 2016.

Bianchi, M., Feliatra, F., Tréguer, P., Vincendeau, M.-A., and Morvan, J.: Nitrification rates, ammonium and nitrate distribution in upper layers of the water column and in sediments of the Indian sector of the Southern Ocean, Deep Sea Research Part II: Topical Studies in Oceanography, 44, 1017-1032, 10.1016/S0967-0645(96)00109-9, 1997.

Costabile, F., Amoroso, A., and Wang, F.: Sub-mu m particle size distributions in a suburban Mediterranean area. Aerosol populations and their possible relationship with HONO mixing ratios, Atmospheric Environment, 44, 5258-5268, 10.1016/j.atmosenv.2010.08.018, 2010.

D'Amato, G., Cecchi, L., Bonini, S., Nunes, C., Annesi-Maesano, I., Behrendt, H., Liccardi, G., Popov, T., and Van Cauwenberge, P.: Allergenic pollen and pollen allergy in Europe, Allergy, 62, 976-990, 10.1111/j.1398-9995.2007.01393.x, 2007.

Elshorbany, Y. F., Steil, B., Brühl, C., and Lelieveld, J.: Impact of HONO on global atmospheric chemistry calculated with an empirical parameterization in the EMAC model, Atmos. Chem. Phys., 12, 9977-10000, 10.5194/acp-12-9977-2012, 2012.

Foster, J. R., Pribush, R. A., and Carter, B. H.: The chemistry of dews and frosts in Indianapolis, Indiana, Atmospheric Environment Part a-General Topics, 24, 2229-2236, 10.1016/0960-1686(90)90254-k, 1990.

Fowler, D., Pilegaard, K., Sutton, M. A., Ambus, P., Raivonen, M., Duyzer, J., Simpson, D., Fagerli, H., Fuzzi, S., Schjoerring, J. K., Granier, C., Neftel, A., Isaksen, I. S. A., Laj, P., Maione, M., Monks, P. S., Burkhardt, J., Daemmgen, U., Neirynck, J., Personne, E., Wichink-Kruit, R., Butterbach-Bahl, K., Flechard, C., Tuovinen, J. P., Coyle, M., Gerosa, G., Loubet, B., Altimir, N., Gruenhage, L., Ammann, C., Cieslik, S., Paoletti, E., Mikkelsen, T. N., Ro-Poulsen, H., Cellier, P., Cape, J. N., Horváth, L., Loreto, F., Niinemets, Ü., Palmer, P. I., Rinne, J., Misztal, P., Nemitz, E., Nilsson, D., Pryor, S., Gallagher, M. W., Vesala, T., Skiba, U., Brüggemann, N., Zechmeister-Boltenstern, S., Williams, J., O'Dowd, C., Facchini, M. C., de Leeuw, G., Flossman, A., Chaumerliac, N., and Erisman, J. W.: Atmospheric composition change: Ecosystems–Atmosphere interactions, Atmospheric Environment, 43, 5193-5267, 10.1016/j.atmosenv.2009.07.068, 2009.

Franze, T., Krause, K., Niessner, R., and Poeschl, U.: Proteins and amino acids in air particulate matter, Journal of Aerosol Science, 34, S777-S778, 10.1016/S0021-8502(03)00155-1, 2003.

Galloway, J. N., Dentener, F. J., Capone, D. G., Boyer, E. W., Howarth, R. W., Seitzinger, S. P., Asner, G. P., Cleveland, C. C., Green, P. A., Holland, E. A., Karl, D. M., Michaels, A. F., Porter, J. H., Townsend, A. R., and Vöosmarty, C. J.: Nitrogen cycles: past, present, and future, Biogeochemistry, 70, 153-226, 10.1007/s10533-004-0370-0, 2004.

George, C., Strekowski, R. S., Kleffmann, J., Stemmler, K., and Ammann, M.: Photoenhanced uptake of gaseous NO2 on solid-organic compounds: a photochemical source of HONO?, Faraday Discussions, 130, 195-210, 10.1039/b417888m, 2005.

Gruijthuijsen, Y. K., Grieshuber, I., Stoecklinger, A., Tischler, U., Fehrenbach, T., Weller, M. G., Vogel, L., Vieths, S., Poeschl, U., and Duschl, A.: Nitration enhances the allergenic potential of proteins, International Archives of Allergy and Immunology, 141, 265-275, 10.1159/000095296, 2006.

Heland, J., Kleffmann, J., Kurtenbach, R., and Wiesen, P.: A new instrument to measure gaseous nitrous acid (HONO) in the atmosphere, Environmental Science & Technology, 35, 3207-3212, 10.1021/es000303t, 2001.

Houee-Levin, C., Bobrowski, K., Horakova, L., Karademir, B., Schoneich, C., Davies, M. J., and Spickett, C. M.: Exploring oxidative modifications of tyrosine: An update on

mechanisms of formation, advances in analysis and biological consequences, Free Radical Research, 49, 347-373, 10.3109/10715762.2015.1007968, 2015.

Kalberer, M., Ammann, M., Arens, F., Gaggeler, H. W., and Baltensperger, U.: Heterogeneous formation of nitrous acid (HONO) on soot aerosol particles, Journal of Geophysical Research-Atmospheres, 104, 13825-13832, 10.1029/1999jd900141, 1999.

Kampf, C. J., Liu, F., Reinmuth-Selzle, K., Berkemeier, T., Meusel, H., Shiraiwa, M., and Pöschl, U.: Protein Cross-Linking and Oligomerization through Dityrosine Formation upon Exposure to Ozone, Environmental Science & Technology, 49, 10859-10866, 10.1021/acs.est.5b02902, 2015.

Kleffmann, J., H. Becker, K., Lackhoff, M., and Wiesen, P.: Heterogeneous conversion of NO2 on carbonaceous surfaces, Physical Chemistry Chemical Physics, 1, 5443-5450, 10.1039/A905545B, 1999.

Kleffmann, J., Kurtenbach, R., Lorzer, J., Wiesen, P., Kalthoff, N., Vogel, B., and Vogel, H.: Measured and simulated vertical profiles of nitrous acid - Part I: Field measurements, Atmospheric Environment, 37, 2949-2955, 10.1016/s1352-2310(03)00242-5, 2003.

Kleffmann, J., Gavriloaiei, T., Hofzumahaus, A., Holland, F., Koppmann, R., Rupp, L., Schlosser, E., Siese, M., and Wahner, A.: Daytime formation of nitrous acid: A major source of OH radicals in a forest, Geophysical Research Letters, 32, 10.1029/2005gl022524, 2005.

Kleffmann, J., Lörzer, J. C., Wiesen, P., Kern, C., Trick, S., Volkamer, R., Rodenas, M., and Wirtz, K.: Intercomparison of the DOAS and LOPAP techniques for the detection of nitrous acid (HONO), Atmospheric Environment, 40, 3640-3652, 10.1016/j.atmosenv.2006.03.027, 2006.

Kurtenbach, R., Becker, K. H., Gomes, J. A. G., Kleffmann, J., Lorzer, J. C., Spittler, M., Wiesen, P., Ackermann, R., Geyer, A., and Platt, U.: Investigations of emissions and heterogeneous formation of HONO in a road traffic tunnel, Atmospheric Environment, 35, 3385-3394, 10.1016/s1352-2310(01)00138-8, 2001.

Levy, H.: Normal Atmosphere: Large Radical and Formaldehyde Concentrations Predicted, Science, 173, 141-143, 10.1126/science.173.3992.141, 1971.

Li, G., Su, H., Li, X., Kuhn, U., Meusel, H., Hoffmann, T., Ammann, M., Pöschl, U., Shao, M., and Cheng, Y.: Uptake of gaseous formaldehyde by soil surfaces: a combination of adsorption/desorption equilibrium and chemical reactions, Atmos. Chem. Phys., 16, 10299-10311, 10.5194/acp-16-10299-2016, 2016.

Li, G., Su, H., Kuhn, U., Meusel, H., Ammann, M., Shao, M., Pöschl, U., and Cheng, Y.: Technical Note: Influence of surface roughness and local turbulence on coated-wall flow tube experiments for gas uptake and kinetic studies, Atmos. Chem. Phys. Discuss., 2017, 1-27, 10.5194/acp-2017-232, 2017.

Liu, F., Lakey, P., Berkemeier, T., Tong, H., Kunert, A. T., Meusel, H., Su, H., Cheng, Y., Frohlich-Nowoisky, J., Lai, S., Weller, M. G., Shiraiwa, M., Poschl, U., and Kampf, C. J.: Atmospheric protein chemistry influenced by anthropogenic air pollutants: nitration and oligomerization upon exposure to ozone and nitrogen dioxide, Faraday Discussions, 10.1039/C7FD00005G, 2017.

Mamtimin, B., Meixner, F. X., Behrendt, T., Badawy, M., and Wagner, T.: The contribution of soil biogenic NO and HONO emissions from a managed hyperarid ecosystem to the

regional NOx emissions during growing season, Atmos. Chem. Phys., 16, 10175-10194, 10.5194/acp-16-10175-2016, 2016.

Meixner, FX., and Yang, WX.: Biogenic emissions of nitric oxide and nitrous oxide from arid and semi-arid land, in: Dryland Ecohydrology, edited by: D'Odorico, P., and Porporato, A., Springer Netherlands, Dordrecht, 233-255, 2006.

Menetrez, M. Y., Foarde, K. K., Dean, T. R., Betancourt, D. A., and Moore, S. A.: An evaluation of the protein mass of particulate matter, Atmospheric Environment, 41, 8264-8274, 10.1016/j.atmosenv.2007.06.021, 2007.

Meusel, H., Kuhn, U., Reiffs, A., Mallik, C., Harder, H., Martinez, M., Schuladen, J., Bohn, B., Parchatka, U., Crowley, J. N., Fischer, H., Tomsche, L., Novelli, A., Hoffmann, T., Janssen, R. H. H., Hartogensis, O., Pikridas, M., Vrekoussis, M., Bourtsoukidis, E., Weber, B., Lelieveld, J., Williams, J., Pöschl, U., Cheng, Y., and Su, H.: Daytime formation of nitrous acid at a coastal remote site in Cyprus indicating a common ground source of atmospheric HONO and NO, Atmos. Chem. Phys., 16, 14475-14493, 10.5194/acp-16-14475-2016, 2016.

Meusel, H., Tamm, A., Kuhn, U., Wu, D., Leifke, A. L., Fiedler, S., Ruckteschler, N., Yordanova, P., Lang-Yona, N., Lelieveld, J., Hoffmann, T., Pöschl, U., Su, H., Weber, B., and Cheng, Y.: Emission of nitrous acid from soil and biological soil crusts represents a dominant source of HONO in the remote atmosphere in Cyprus, Atmos. Chem. Phys. Discuss., 2017, 1-21, 10.5194/acp-2017-356, 2017a.

Meusel, H., Elshorbany, Y., Kuhn, U., Bartels-Rausch, T., Reinmuth-Selzle, K., Kampf, C. J., Li, G., Wang, X., Lelieveld, J., Pöschl, U., Hoffmann, T., Su, H., Ammann, M., and Cheng, Y.: Light-induced protein nitration and degradation with HONO emission, Atmos. Chem. Phys. Discuss., 2017, 1-22, 10.5194/acp-2017-277, 2017b.

Michoud, V., Colomb, A., Borbon, A., Miet, K., Beekmann, M., Camredon, M., Aumont, B., Perrier, S., Zapf, P., Siour, G., Ait-Helal, W., Afif, C., Kukui, A., Furger, M., Dupont, J. C., Haeffelin, M., and Doussin, J. F.: Study of the unknown HONO daytime source at a European suburban site during the MEGAPOLI summer and winter field campaigns, Atmospheric Chemistry and Physics, 14, 2805-2822, 10.5194/acp-14-2805-2014, 2014.

Miguel, A. G., Cass, G. R., Glovsky, M. M., and Weiss, J.: Allergens in paved road dust and airborne particles, Environmental Science & Technology, 33, 4159-4168, 10.1021/es9904890, 1999.

Monge, M. E., D'Anna, B., Mazri, L., Giroir-Fendler, A., Ammann, M., Donaldson, D. J., and George, C.: Light changes the atmospheric reactivity of soot, Proceedings of the National Academy of Sciences of the United States of America, 107, 6605-6609, 10.1073/pnas.0908341107, 2010.

Oswald, R., Behrendt, T., Ermel, M., Wu, D., Su, H., Cheng, Y., Breuninger, C., Moravek, A., Mougin, E., Delon, C., Loubet, B., Pommerening-Roeser, A., Soergel, M., Poeschl, U., Hoffmann, T., Andreae, M. O., Meixner, F. X., and Trebs, I.: HONO emissions from soil bacteria as a major source of atmospheric reactive nitrogen, Science, 341, 1233-1235, 10.1126/science.1242266, 2013.

Oswald, R., Ermel, M., Hens, K., Novelli, A., Ouwersloot, H. G., Paasonen, P., Petaja, T., Sipila, M., Keronen, P., Back, J., Konigstedt, R., Beygi, Z. H., Fischer, H., Bohn, B., Kubistin, D., Harder, H., Martinez, M., Williams, J., Hoffmann, T., Trebs, I., and Soergel,

M.: A comparison of HONO budgets for two measurement heights at a field station within the boreal forest in Finland, Atmospheric Chemistry and Physics, 15, 799-813, 10.5194/acp-15-799-2015, 2015.

Ramazan, K. A., Syomin, D., and Finlayson-Pitts, B. J.: The photochemical production of HONO during the heterogeneous hydrolysis of NO2, Physical Chemistry Chemical Physics, 6, 3836-3843, 10.1039/b402195a, 2004.

Ren, X., Brune, W. H., Oliger, A., Metcalf, A. R., Simpas, J. B., Shirley, T., Schwab, J. J., Bai, C., Roychowdhury, U., Li, Y., Cai, C., Demerjian, K. L., He, Y., Zhou, X., Gao, H., and Hou, J.: OH, HO2, and OH reactivity during the PMTACS-NY Whiteface Mountain 2002 campaign: Observations and model comparison, Journal of Geophysical Research-Atmospheres, 111, 10.1029/2005jd006126, 2006.

Ren, X., Sanders, J. E., Rajendran, A., Weber, R. J., Goldstein, A. H., Pusede, S. E., Browne, E. C., Min, K. E., and Cohen, R. C.: A relaxed eddy accumulation system for measuring vertical fluxes of nitrous acid, Atmospheric Measurement Techniques, 4, 2093-2103, 10.5194/amt-4-2093-2011, 2011.

Riediker, Koller, and Monn: Differences in size selective aerosol sampling for pollen allergen detection using high-volume cascade impactors, Clinical & Experimental Allergy, 30, 867-873, 10.1046/j.1365-2222.2000.00792.x, 2000.

Rubio, M. A., Lissi, E., and Villena, G.: Nitrite in rain and dew in Santiago city, Chile. Its possible impact on the early morning start of the photochemical smog, Atmospheric Environment, 36, 293-297, 10.1016/s1352-2310(01)00356-9, 2002.

Shiraiwa, M., Selzle, K., Yang, H., Sosedova, Y., Ammann, M., and Poeschl, U.: Multiphase chemical kinetics of the nitration of aerosolized protein by ozone and nitrogen dioxide, Environmental Science & Technology, 46, 6672-6680, 10.1021/es300871b, 2012.

Soergel, M., Regelin, E., Bozem, H., Diesch, J. M., Drewnick, F., Fischer, H., Harder, H., Held, A., Hosaynali-Beygi, Z., Martinez, M., and Zetzsch, C.: Quantification of the unknown HONO daytime source and its relation to NO2, Atmospheric Chemistry and Physics, 11, 10433-10447, 10.5194/acp-11-10433-2011, 2011a.

Sosedova, Y., Rouviere, A., Bartels-Rausch, T., and Ammann, M.: UVA/Vis-induced nitrous acid formation on polyphenolic films exposed to gaseous NO2, Photochemical & Photobiological Sciences, 10, 1680-1690, 10.1039/c1pp05113j, 2011.

Spataro, F., Ianniello, A., Esposito, G., Allegrini, I., Zhu, T., and Hu, M.: Occurrence of atmospheric nitrous acid in the urban area of Beijing (China), The Science of the total environment, 447, 210-224, 10.1016/j.scitotenv.2012.12.065, 2013.

Stemmler, K., Ammann, M., Donders, C., Kleffmann, J., and George, C.: Photosensitized reduction of nitrogen dioxide on humic acid as a source of nitrous acid, Nature, 440, 195-198, 10.1038/nature04603, 2006.

Stemmler, K., Ndour, M., Elshorbany, Y., Kleffmann, J., D'Anna, B., George, C., Bohn, B., and Ammann, M.: Light induced conversion of nitrogen dioxide into nitrous acid on submicron humic acid aerosol, Atmospheric Chemistry and Physics, 7, 4237-4248, 2007.

Su, H., Cheng, Y. F., Shao, M., Gao, D. F., Yu, Z. Y., Zeng, L. M., Slanina, J., Zhang, Y. H., and Wiedensohler, A.: Nitrous acid (HONO) and its daytime sources at a rural site during the 2004 PRIDE-PRD experiment in China, Journal of Geophysical Research-Atmospheres, 113, 10.1029/2007jd009060, 2008b.

Su, H., Cheng, Y., Oswald, R., Behrendt, T., Trebs, I., Meixner, F. X., Andreae, M. O., Cheng, P., Zhang, Y., and Poeschl, U.: Soil nitrite as a source of atmospheric HONO and OH radicals, Science, 333, 1616-1618, 10.1126/science.1207687, 2011.

VandenBoer, T. C., Brown, S. S., Murphy, J. G., Keene, W. C., Young, C. J., Pszenny, A. A. P., Kim, S., Warneke, C., de Gouw, J. A., Maben, J. R., Wagner, N. L., Riedel, T. P., Thornton, J. A., Wolfe, D. E., Dubé, W. P., Öztürk, F., Brock, C. A., Grossberg, N., Lefer, B., Lerner, B., Middlebrook, A. M., and Roberts, J. M.: Understanding the role of the ground surface in HONO vertical structure: High resolution vertical profiles during NACHTT-11, Journal of Geophysical Research: Atmospheres, 118, 10,155-110,171, 10.1002/jgrd.50721, 2013.

Villena, G., Kleffmann, J., Kurtenbach, R., Wiesen, P., Lissi, E., Rubio, M. A., Croxatto, G., and Rappenglueck, B.: Vertical gradients of HONO, NOx and O3 in Santiago de Chile, Atmospheric Environment, 45, 3867-3873, 10.1016/j.atmosenv.2011.01.073, 2011.

Vogel, B., Vogel, H., Kleffmann, J., and Kurtenbach, R.: Measured and simulated vertical profiles of nitrous acid - Part II. Model simulations and indications for a photolytic source, Atmospheric Environment, 37, 2957-2966, 10.1016/s1352-2310(03)00243-7, 2003.

Weber, B., Wu, D., Tamm, A., Ruckteschler, N., Rodriguez-Caballero, E., Steinkamp, J., Meusel, H., Elbert, W., Behrendt, T., Soergel, M., Cheng, Y., Crutzen, P. J., Su, H., and Poeschi, U.: Biological soil crusts accelerate the nitrogen cycle through large NO and HONO emissions in drylands, Proceedings of the National Academy of Sciences of the United States of America, 112, 15384-15389, 10.1073/pnas.1515818112, 2015.

Wong, K. W., Tsai, C., Lefer, B., Haman, C., Grossberg, N., Brune, W. H., Ren, X., Luke, W., and Stutz, J.: Daytime HONO vertical gradients during SHARP 2009 in Houston, TX, Atmospheric Chemistry and Physics, 12, 635-652, 10.5194/acp-12-635-2012, 2012.

Zhang, Q., and Anastasio, C.: Free and combined amino compounds in atmospheric fine particles (PM2.5) and fog waters from Northern California, Atmospheric Environment, 37, 2247-2258, 10.1016/s1352-2310(03)00127-4, 2003.

Zhou, X. L., Beine, H. J., Honrath, R. E., Fuentes, J. D., Simpson, W., Shepson, P. B., and Bottenheim, J. W.: Snowpack photochemical production of HONO: a major source of OH in the Arctic boundary layer in springtime, Geophysical Research Letters, 28, 4087-4090, 10.1029/2001gl013531, 2001.

Zhou, X. L., Civerolo, K., Dai, H. P., Huang, G., Schwab, J., and Demerjian, K.: Summertime nitrous acid chemistry in the atmospheric boundary layer at a rural site in New York State, Journal of Geophysical Research-Atmospheres, 107, 10.1029/2001jd001539, 2002.

Zhou, X. L., Gao, H. L., He, Y., Huang, G., Bertman, S. B., Civerolo, K., and Schwab, J.: Nitric acid photolysis on surfaces in low-NOx environments: Significant atmospheric implications, Geophysical Research Letters, 30, 10.1029/2003gl018620, 2003.

Zhou, Y., Rosen, E. P., Zhang, H., Rattanavaraha, W., Wang, W., and Kamens, R. M.: SO2 oxidation and nucleation studies at near-atmospheric conditions in outdoor smog chamber, Environmental Chemistry, 10, 210-220, 10.1071/EN13024, 2013.

A. Personal List of Publications

A.1 Journal articles

Bandowe, B. A. M., Meusel, H., Huang, R.-j., Ho, K., Cao, J., Hoffmann, T., and Wilcke, W.: PM2.5-bound oxygenated PAHs, nitro-PAHs and parent-PAHs from the atmosphere of a Chinese megacity: Seasonal variation, sources and cancer risk assessment, Science of The Total Environment, 473–474, 77-87, 10.1016/j.scitotenv.2013.11.108, 2014.

Bandowe, B. A. M., Meusel, H., Huang, R., Hoffmann, T., Cao, J., and Ho, K.: Azaarenes in fine particulate matter from the atmosphere of a Chinese megacity, Environmental Science and Pollution Research, 23, 16025-16036, 10.1007/s11356-016-6740-z, 2016.

Bandowe, B. A. M., and Meusel, H.: Nitrated polycyclic aromatic hydrocarbons (nitro-PAHs) in the environment – A review, Science of The Total Environment, 581–582, 237-257, 10.1016/j.scitotenv.2016.12.115, 2017.

Bandowe, B. A. M., and Meusel, H.: Nitrierte polyzyklische aromatische Kohlenwasserstoffe (Nitro-PAK), in: Bodengefährdende Stoffe: Bewertung - Stoffdaten - Ökotoxikologie - Sanierung, Wiley-VCH Verlag GmbH & Co. KGaA, 10.1002/9783527678501.bgs2014001.

Kampf, C. J., Liu, F., Reinmuth-Selzle, K., Berkemeier, T., Meusel, H., Shiraiwa, M., and Pöschl, U.: Protein Cross-Linking and Oligomerization through Dityrosine Formation upon Exposure to Ozone, Environmental Science & Technology, 49, 10859-10866, 10.1021/acs.est.5b02902, 2015.

Li, G., Su, H., Li, X., Kuhn, U., Meusel, H., Hoffmann, T., Ammann, M., Pöschl, U., Shao, M., and Cheng, Y.: Uptake of gaseous formaldehyde by soil surfaces: a combination of adsorption/desorption equilibrium and chemical reactions, Atmos. Chem. Phys., 16, 10299-10311, 10.5194/acp-16-10299-2016, 2016.

Li, G., Su, H., Kuhn, U., Meusel, H., Ammann, M., Shao, M., Pöschl, U., and Cheng, Y.: Technical Note: Influence of surface roughness and local turbulence on coated-wall flow tube experiments for gas uptake and kinetic studies, Atmos. Chem. Phys. Discuss., 2017, 1-27, 10.5194/acp-2017-232, 2017.

Liu, F., Lakey, P., Berkemeier, T., Tong, H., Kunert, A. T., Meusel, H., Su, H., Cheng, Y., Frohlich-Nowoisky, J., Lai, S., Weller, M. G., Shiraiwa, M., Poschl, U., and Kampf, C. J.: Atmospheric protein chemistry influenced by anthropogenic air pollutants: nitration and oligomerization upon exposure to ozone and nitrogen dioxide, Faraday Discussions, 10.1039/C7FD00005G, 2017.

Mallik, C., Tomsche, L., Bourtsoukidis, E., Crowley, J.N., Derstroff, B., Fischer, H., Hafermann, S., Hueser, I., Javed, U., Jones, P., Kessel, S., Lelieveld, J., Martinez, M., Meusel, H., Novelli, A., Phillips, G.J., Pozzer, A., Reiffs, A., Sander, R., Sauvage, C., Schuladen, J., Su, H., Williams, J., and Harder, H.: Oxidation processes in the Eastern Mediterranean atmosphere: Evidences from the modelling of HOx measurements over Cyprus, to be submitted to ACP.

Meusel, H., Kuhn, U., Reiffs, A., Mallik, C., Harder, H., Martinez, M., Schuladen, J., Bohn, B., Parchatka, U., Crowley, J. N., Fischer, H., Tomsche, L., Novelli, A., Hoffmann, T., Janssen, R. H. H., Hartogensis, O., Pikridas, M., Vrekoussis, M., Bourtsoukidis, E., Weber, B., Lelieveld, J., Williams, J., Pöschl, U., Cheng, Y., and Su, H.: Daytime formation of

nitrous acid at a coastal remote site in Cyprus indicating a common ground source of atmospheric HONO and NO, Atmos. Chem. Phys., 16, 14475-14493, 10.5194/acp-16-14475-2016, 2016.

Meusel, H., Tamm, A., Kuhn, U., Wu, D., Leifke, A. L., Fiedler, S., Ruckteschler, N., Yordanova, P., Lang-Yona, N., Lelieveld, J., Hoffmann, T., Pöschl, U., Su, H., Weber, B., and Cheng, Y.: Emission of nitrous acid from soil and biological soil crusts represents a dominant source of HONO in the remote atmosphere in Cyprus, Atmos. Chem. Phys. Discuss., 2017, 1-21, 10.5194/acp-2017-356, 2017a.

Meusel, H., Elshorbany, Y., Kuhn, U., Bartels-Rausch, T., Reinmuth-Selzle, K., Kampf, C. J., Li, G., Wang, X., Lelieveld, J., Pöschl, U., Hoffmann, T., Su, H., Ammann, M., and Cheng, Y.: Light-induced protein nitration and degradation with HONO emission, Atmos. Chem. Phys. Discuss., 2017, 1-22, 10.5194/acp-2017-277, 2017b.

Weber, B., Wu, D., Tamm, A., Ruckteschler, N., Rodriguez-Caballero, E., Steinkamp, J., Meusel, H., Elbert, W., Behrendt, T., Soergel, M., Cheng, Y., Crutzen, P. J., Su, H., and Poeschi, U.: Biological soil crusts accelerate the nitrogen cycle through large NO and HONO emissions in drylands, Proceedings of the National Academy of Sciences of the United States of America, 112, 15384-15389, 10.1073/pnas.1515818112, 2015.

A.2 Oral presentations

Meusel, H.: HONO on a Mediterranean island – unusual diurnal course and possible daytime sources, IMPRS PhD Symposium, December 2014.

Meusel, H.: HONO on a Mediterranean island – unusual diurnal course and possible daytime sources, Earth System Science Conference, Mainz, Germany, 25-27 March 2015.

Meusel, H. et al: Emission of nitrous acid from soil and biological soil crusts as a major source of atmospheric HONO on Cyprus, General Assembly of the European Geoscience Union, Vienna, Austria, 23-28 April 2017.

A.3 Poster presentations

Meusel, H., Elshorbany, Y., Bartels-Rausch, T., Selzle, K., Lelieveld, J., Amman, M., Pöschl, U., Su, H., Cheng, Y.: Photo-induced formation of nitrous acid (HONO) on protein surfaces, General Assembly of the European Geoscience Union, Vienna, Austria, 27 April - 02 May 2014

B. Selected Publications

Meusel, H., Kuhn, U., Reiffs, A., Mallik, C., Harder, H., Martinez, M., Schuladen, J., Bohn, B., Parchatka, U., Crowley, J. N., Fischer, H., Tomsche, L., Novelli, A., Hoffmann, T., Janssen, R. H. H., Hartogensis, O., Pikridas, M., Vrekoussis, M., Bourtsoukidis, E., Weber, B., Lelieveld, J., Williams, J., Pöschl, U., Cheng, Y., and Su, H.: Daytime formation of nitrous acid at a coastal remote site in Cyprus indicating a common ground source of atmospheric HONO and NO, Atmos. Chem. Phys., 16, 14475-14493, 10.5194/acp-16-14475-2016, 2016.

Meusel, H., Tamm, A., Kuhn, U., Wu, D., Leifke, A. L., Fiedler, S., Ruckteschler, N., Yordanova, P., Lang-Yona, N., Lelieveld, J., Hoffmann, T., Pöschl, U., Su, H., Weber, B., and Cheng, Y.: Emission of nitrous acid from soil and biological soil crusts represents a dominant source of HONO in the remote atmosphere in Cyprus, Atmos. Chem. Phys. Discuss., 2017, 1-21, 10.5194/acp-2017-356, 2017a.

Meusel, H., Elshorbany, Y., Kuhn, U., Bartels-Rausch, T., Reinmuth-Selzle, K., Kampf, C. J., Li, G., Wang, X., Lelieveld, J., Pöschl, U., Hoffmann, T., Su, H., Ammann, M., and Cheng, Y.: Light-induced protein nitration and degradation with HONO emission, Atmos. Chem. Phys. Discuss., 2017, 1-22, 10.5194/acp-2017-277, 2017b.

B.1 Meusel et al., Atmos. Chem. Phys., 2016

Daytime formation of nitrous acid at a coastal remote site in Cyprus indicating a common ground source of atmospheric HONO and NO

Hannah Meusel[1], Uwe Kuhn[1], Andreas Reiffs[2], Chinmay Mallik[2], Hartwig Harder[2], Monica Martinez[2], Jan Schuladen[2], Birger Bohn[3], Uwe Parchatka[2], John N. Crowley[2], Horst Fischer[2], Laura Tomsche[2], Anna Novelli[2,3], Thorsten Hoffmann[4], Ruud Janssen[2,], Oscar Hartogensis[5], Michael Pikridas[6], Mihalis Vrekoussis[6,7,8], Efstratios Bourtsoukidis[2], Bettina Weber[1], Jos Lelieveld[2], Jonathan Williams[2], Ulrich Pöschl[1], Yafang Cheng[1], and Hang Su[1]

[1]Max Planck Institute for Chemistry, Multiphase Chemistry Department, Mainz, Germany
[2]Max Planck Institute for Chemistry, Atmospheric Chemistry Department, Mainz, Germany
[3]Institute for Energy and Climate Research (IEK-8), Research Center Jülich, Jülich, Germany
[4]Johannes Gutenberg University, Inorganic and Analytical Chemistry, Mainz, Germany
[5]Wageningen University and Research Center, Meteorology and Air Quality, Wageningen, Netherlands
[6]Cyprus Institute, Energy, Environment and Water Research Center, Nicosia, Cyprus
[7]Institute of Environmental Physics and Remote Sensing – IUP, University of Bremen, Germany
[8]Center of Marine Environmental Sciences – MARUM, University of Bremen, Germany

Atmospheric Chemistry and Physics, **16**, 14475-14493, (2016)
DOI: 10.5194/acp-16-14475-2016.

Author contributions:

HM and HS designed the research.
HM performed the study.
AR, CM, HH, MM, JS, BB, UPa, HF, LT, AN, RJ, OH, MP, MV, EB, JW provided relevant data.
HM, UK, HS, YC, BW, HF, HH, UPö, TH discussed the results.
HM, UK, HS, CM, JNC, HF, EB, JL wrote the paper.

Atmos. Chem. Phys., 16, 14475–14493, 2016
www.atmos-chem-phys.net/16/14475/2016/
doi:10.5194/acp-16-14475-2016

Atmospheric Chemistry and Physics Open Access EGU

Daytime formation of nitrous acid at a coastal remote site in Cyprus indicating a common ground source of atmospheric HONO and NO

Hannah Meusel[1], Uwe Kuhn[1], Andreas Reiffs[2], Chinmay Mallik[2], Hartwig Harder[2], Monica Martinez[2], Jan Schuladen[2], Birger Bohn[3], Uwe Parchatka[2], John N. Crowley[2], Horst Fischer[2], Laura Tomsche[2], Anna Novelli[2,3], Thorsten Hoffmann[4], Ruud H. H. Janssen[2], Oscar Hartogensis[5], Michael Pikridas[6], Mihalis Vrekoussis[6,7,8], Efstratios Bourtsoukidis[2], Bettina Weber[1], Jos Lelieveld[2], Jonathan Williams[2], Ulrich Pöschl[1], Yafang Cheng[1], and Hang Su[1]

[1]Max Planck Institute for Chemistry, Multiphase Chemistry Department, Mainz, Germany
[2]Max Planck Institute for Chemistry, Atmospheric Chemistry Department, Mainz, Germany
[3]Institute for Energy and Climate Research (IEK-8), Research Center Jülich, Jülich, Germany
[4]Johannes Gutenberg University, Inorganic and Analytical Chemistry, Mainz, Germany
[5]Wageningen University and Research Center, Meteorology and Air Quality, Wageningen, the Netherlands
[6]Cyprus Institute, Energy, Environment and Water Research Center, Nicosia, Cyprus
[7]Institute of Environmental Physics and Remote Sensing – IUP, University of Bremen, Bremen, Germany
[8]Center of Marine Environmental Sciences – MARUM, University of Bremen, Bremen, Germany

Correspondence to: Hang Su (h.su@mpic.de)

Received: 24 June 2016 – Published in Atmos. Chem. Phys. Discuss.: 25 July 2016
Revised: 27 October 2016 – Accepted: 5 November 2016 – Published: 22 November 2016

Abstract. Characterization of daytime sources of nitrous acid (HONO) is crucial to understand atmospheric oxidation and radical cycling in the planetary boundary layer. HONO and numerous other atmospheric trace constituents were measured on the Mediterranean island of Cyprus during the CYPHEX (CYprus PHotochemical EXperiment) campaign in summer 2014. Average volume mixing ratios of HONO were 35 pptv (±25 pptv) with a HONO / NO_x ratio of 0.33, which was considerably higher than reported for most other rural and urban regions. Diel profiles of HONO showed peak values in the late morning (60 ± 28 pptv around 09:00 local time) and persistently high mixing ratios during daytime (45 ± 18 pptv), indicating that the photolytic loss of HONO is compensated by a strong daytime source. Budget analyses revealed unidentified sources producing up to 3.4×10^6 molecules cm^{-3} s^{-1} of HONO and up to 2.0×10^7 molecules cm^{-3} s^{-1} NO. Under humid conditions (relative humidity > 70 %), the source strengths of HONO and NO exhibited a close linear correlation ($R^2 = 0.72$), suggesting a common source that may be attributable to emissions from microbial communities on soil surfaces.

1 Introduction

Nitrous acid (HONO) is an important component of the nitrogen cycle, being widespread in the environment. Either in its protonated form (HONO or HNO_2) or as nitrite ions (NO_2^-) it can be found not only in the gas phase, on aerosol particles, in clouds and in dew droplets but also in soil, seawater and sediments (Foster et al., 1990; Rubio et al., 2002; Acker et al., 2005, 2008; Bianchi et al., 1997). It plays a key role in the oxidizing capacity of the atmosphere, as it is an important precursor of the OH radical, which initiates most atmospheric oxidations. OH radicals react with pollutants in the atmosphere to form mostly less toxic compounds (e.g. $CO + OH \rightarrow CO_2 + H_2O$; Levy, 1971). Volatile organic compounds (VOCs) react with OH, contributing to formation of secondary aerosols (SOAs), which can serve as cloud condensation nuclei (CCN; Arey et al., 1990; Duplissy et al., 2008). Furthermore OH oxidizes SO_2 to H_2SO_4, which condense subsequently to form aerosol particles (Zhou et al., 2013). In this way HONO has an indirect effect on the radiative budget and climate. In the first 2–3 h following sunrise, when OH production from other sources (photolysis of O_3

and formaldehyde) is relatively low, photolysis of HONO can be the major source of OH radicals as HONO concentrations may be high after accumulation during nighttime (Lammel and Cape, 1996; Czader et al., 2012; Mao et al., 2010). On average up to 30 % of the daily OH budget in the boundary layer is provided by HONO photolysis (Alicke et al., 2002; Kleffmann et al., 2005; Ren et al., 2006), but it has been reported as high as 56 % (Ren et al., 2003), with ambient HONO mixing ratios ranging from several parts per trillion by volume (pptv) in rural areas up to a few parts per billion by volume (ppbv) in highly polluted regions (Acker et al., 2006a, b; Costabile et al., 2010; Li et al., 2012; Michoud et al., 2014; Spataro et al., 2013; Su et al., 2008a; Zhou et al., 2002a).

In early studies, atmospheric HONO was assumed to be in a photostationary state (PSS) during daytime controlled by the gas-phase reaction of NO and OH (Reaction R1) and two loss reactions, which are the photolysis (Reaction R2) and the reaction with OH (Reaction R3).

$$\mathrm{OH + NO \rightarrow HONO} \quad \text{(R1)}$$

$$\mathrm{HONO} \xrightarrow{h\nu(300-405\,\mathrm{nm})} \mathrm{OH + NO} \quad \text{(R2)}$$

$$\mathrm{HONO + OH \rightarrow NO_2 + H_2O} \quad \text{(R3)}$$

However, field measurements in remote and rural locations as well as urban and polluted regions found several-times-higher daytime HONO concentrations than model predictions, suggesting a large unknown source (Kleffmann et al., 2003, 2005; Su et al., 2008a, 2011; Sörgel et al., 2011a; Michoud et al., 2014; Czader et al., 2012; Wong et al., 2013; Tang et al., 2015; Oswald et al., 2015) even after considering direct emission of HONO from combustion sources (Kessler and Platt, 1984; Kurtenbach et al., 2001). Heterogeneous reactions on aerosols have been proposed as an explanation for the missing source. The hydrolysis (Reaction R4; Finlayson-Pitts et al., 2003) and redox reactions of NO_2 have been intensively investigated on different kinds of surfaces such as fresh soot, aged particles or organic-coated particles (Ammann et al., 1998; Arens et al., 2001; Aubin and Abbatt, 2007; Bröske et al., 2003; Han et al., 2013; Kalberer et al., 1999; Kleffmann et al., 1999; Kleffmann and Wiesen, 2005; Lelievre et al., 2004). Minerals like SiO_2, $CaCO_3$, CaO, Al_2O_3 and Fe_2O_3 showed a catalytic effect on the hydrolysis of NO_2 (Kinugawa et al., 2011; Liu et al., 2015; Wang et al., 2003; Yabushita et al., 2009). Different kinds of surfaces (humic acid and other organic compounds, titanium dioxide, soot) can be photochemically activated, which leads to enhanced NO_2 uptake and HONO production (Reaction R5, George et al., 2005; Langridge et al., 2009; Monge et al., 2010; Ndour et al., 2008; Ramazan et al., 2004; Stemmler et al., 2007; Kebede et al., 2013). The photolysis of particulate nitric acid (HNO_3), nitrate (NO_3^-) and nitro-phenols (R-NO_2) leads to HONO formation as well (Baergen and Donaldson, 2013; Bejan et al., 2006; Ramazan et al., 2004; Scharko et al., 2014; Zhou et al., 2003, 2011). But these reactions cannot account for the HONO levels observed during daytime (Elshorbany et al., 2012).

$$\mathrm{2NO_2 + H_2O \rightarrow HONO + HNO_3} \quad \text{(R4)}$$

$$\text{surface} \xrightarrow{h\nu} e^- \xrightarrow{\mathrm{NO_2}} \mathrm{NO_2^-} \xrightarrow{\mathrm{H_2O}} \mathrm{HONO + OH^-} \quad \text{(R5)}$$

On the other hand, soil nitrite, either biogenic or non-biogenic, has been suggested as an effective source of HONO (Su et al., 2011; Oswald et al., 2013; Mamtimin et al., 2016). Depending on soil properties such as pH and water content and according to Henry's law, HONO can be released (Donaldson et al., 2014b; Su et al., 2011). This is consistent with field flux measurements showing HONO emission from the ground rather than deposition as is the case for HNO_3 (Harrison and Kitto, 1994; Kleffmann et al., 2003; Ren et al., 2011; Stutz et al., 2002; VandenBoer et al., 2013, 2014; Villena et al., 2011; Zhou et al., 2011). In a recent study, Weber et al. (2015) measured large HONO and NO emissions from dryland soils with microbial surface communities (so-called biological soil crusts). Many studies have shown decreasing HONO mixing ratios with altitude in the lowest few hundred meters of the troposphere, due to respective short atmospheric lifetime compared to vertical transport time (Wong et al., 2012, 2013; Vogel et al., 2003; VandenBoer et al., 2013, 2014; Zhang et al., 2009; Young et al., 2012). According to the modeling results of Wong et al. (2013), we estimate that the ground HONO source could be important for up to 200–300 m a.g.l. This indicates that HONO is more relevant for the OH budget close to the surface than in high-altitude air masses.

Several field studies also show a correlation of the unknown HONO source with solar radiation or the photolysis frequency of NO_2 J_{NO_2} (Su et al., 2008a; Soergel et al., 2011a; Wong et al., 2012; Costabile et al., 2010; Michoud et al., 2014; Oswald et al., 2015; Lee et al., 2016). This correlation can be explained either by the aforementioned photosensitized reactions or by temperature-dependent soil–atmosphere exchange (Su et al., 2011). According to Su et al. (2011), the release of HONO from soil surfaces is controlled by both the soil (biogenic and chemical) production of nitrite and the gas–liquid-phase equilibrium. The solubility is strongly temperature-dependent, resulting in higher HONO emissions during noontime and high-radiation J_{NO_2} periods, and lower HONO emissions or even HONO deposition during the nighttime as further confirmed by VandenBoer et al. (2015). This temperature dependence exists not only for equilibrium over soil solution but also for adsorption–desorption equilibrium over dry and humid soil surfaces (Li et al., 2016).

In this study we measured HONO and a suite of other atmospherically relevant trace gases in a coastal area on the Mediterranean island of Cyprus in summer 2014. Due to low local anthropogenic impact and low NO_x levels in aged air masses, but high solar radiation, this is an ideal site at which

to investigate possible HONO sources and to gain a better understanding of HONO chemistry.

2 Instrumentation

HONO was measured with a commercial long-path absorption photometry instrument (effective light path 1.5 m, LOPAP, Quma, Wuppertal, Germany). LOPAP has a collecting efficiency of > 99 % for HONO and a detection limit of 4 pptv at a time resolution of 30 s. To avoid potential interferences induced by long inlet lines and heterogeneous formation or loss of HONO on the inlet walls (Kleffmann et al., 1998; Zhou et al., 2002b; Su et al., 2008b), HONO was collected by a sampling unit installed directly in the outdoor atmosphere, i.e., placed on a mast at a height of 5.8 m above ground installed at the edge of a laboratory container. Furthermore, the LOPAP has two stripping coils placed in series to reduce known interfering signals (Heland et al., 2001). In the first stripping coil HONO is quantitatively collected. Due to the acidic stripping solution, interfering species are collected less efficiently but in both channels. The true concentration of HONO is obtained by subtracting the inferences quantified in the second channel (in this study the average is 1 pptv, at most 5 pptv) from the total signal obtained from the first channel. For a more detailed description of LOPAP, see Heland et al. (2001). This correction of chemical interferences ascertained excellent agreement with the (absolute) differential optical absorption spectroscopy (DOAS) measurements, both in a smog chamber and under urban atmospheric conditions (Kleffmann et al., 2006). A possible interference from peroxynitric acid (HNO_4) has been proposed (Liao et al., 2006; Kerbrat et al., 2012; Legrand et al., 2014), but this will be insignificant at the high temperatures during the CYPHEX (CYprus PHotochemical EXperiment) campaign, at which HNO_4 is unstable. The stripping coils are temperature-controlled by a water-based thermostat, and the whole external sampling unit is shielded from sunlight by a small plastic housing. The reagents were all high-purity-grade chemicals, i.e., hydrochloric acid (37 %, for analysis; Merck), sulfanilamide (for analysis, > 99 %; AppliChem) and N-(1-naphthyl)-ethylenediamine dihydrochloride (for analysis, > 98 %; AppliChem). For calibration Titrisol® 1000 mg NO_2^- ($NaNO_2$ in H_2O; Merck) was diluted to 0.0015 and 0.005 mg L^{-1} NO_2^-. For preparation all solutions were used, and for cleaning of the absorption tubes 18 MΩ H_2O was used. The accuracy of the HONO measurements was 10 %, based on the uncertainties of liquid and gas flow, concentration of calibration standard and regression of calibration.

NO and NO_2 measurements were made with a modified commercial chemiluminescence detector (CLD 790 SR), originally manufactured by ECO Physics (Duernten, Switzerland). The two-channel CLD based on the chemiluminescence of the reaction between NO and O_3 was used for measurements of NO and NO_2. NO_2 was measured as NO using a photolytic converter from Droplet Measurement Technologies (Boulder, USA). In the current study, data were obtained at a time resolution of 5 s. The CLD detection limits (determined by continuously measuring zero air at the measuring site) for NO and NO_2 measurements were 5 and 20 pptv, respectively for an integration period of 5 s. O_3 was measured with a standard UV photometric detector (Model 49, Thermo Environmental Instruments Inc.) with a detection limit of 1 ppb. Data are reported for an integration period of 60 s. The total uncertainties (2σ) for the measurements of NO, NO_2 and O_3 were determined to be 20, 30 and 5 %, respectively, based on the reproducibility of in-field background measurements, calibrations, the uncertainties of the standards and the conversion efficiency of the photolytic converter (Li et al., 2015).

OH and HO_2 radicals were measured using the HydrOxyl Radical measurement Unit based on fluorescence Spectroscopy (HORUS) setup developed at the Max Planck Institute for Chemistry (Mainz, Germany). HORUS is based on laser-induced fluorescence–fluorescence assay by gas expansion (LIF-FAGE) technique, wherein OH radicals are selectively excited at low pressure by pulsed UV light at around 308 nm, and the resulting fluorescence of OH is detected using gated microchannel plate (MCP) detectors (Martinez et al., 2010; Hens et al., 2014). The HORUS instrument had an inlet pre-injector (IPI) (Novelli et al., 2014) which allows the periodic addition of propane to scavenge the atmospheric OH radicals. This procedure allows the removal of potential interference species. HO_2 is estimated by converting atmospheric HO_2 into OH using NO and detecting the additional OH formed. The instrument is calibrated by measuring signals from known amounts of OH and HO_2 generated by photolysis of water vapor in humidified zero air. The accuracy (2σ) of the OH measurements was 29 %, and the precision (1σ) was 4.8×10^5 molecules cm^{-3}.

Photolysis frequencies were determined using a spectroradiometer (Metcon GmbH) with a single monochromator and 512 pixel CCD array as a detector (275–640 nm). The thermostatted monochromator–detector unit was attached via a 10 m optical fiber to a 2-Π integrating hemispheric quartz dome. The spectroradiometer was calibrated prior to the campaign using a 1000 W National Institute of Standards and Technology (NIST) traceable irradiance standard. J values were calculated using molecular parameters recommended by the IUPAC and NASA evaluation panels (Sander et al., 2011; IUPAC, 2015). The J value for HONO was not corrected for upwelling UV radiation and is estimated to have an uncertainty of ∼ 10 % (Bohn et al., 2008).

Aerosol measurements were also performed during the campaign. In this study particulate nitrate and aerosol surface data were used. These were detected by high-resolution time-of-flight aerosol mass spectrometer (HR-ToF-AMS, Aerodyne Research Inc., Billerica, MA USA), and scanning mobility particle sizer (SMPS 3936, TSI, Shoreview, MN USA)

Figure 1. Map of location: the red star shows the location of Ineia and the measuring site. The four red points mark the main cities of Cyprus: Nicosia, Larnaca, Limassol and Paphos (clockwise ordering). Map produced by the Cartographic Research Lab University of Alabama; map of Cyprus: Google Maps.

and aerodynamic particle sizer (APS 3321, TSI), respectively. The mobility- and aerodynamics-based size distributions were combined based on the algorithm proposed by Khlystov et al. (2004).

The VOCs including α-pinene, β-pinene, isoprene, Δ3-carene, limonene and DMS (dimethyl sulfide) were detected by a commercial gas chromatography–mass spectrometry (GC-MS) system (MSD 5973; Agilent Technologies GmbH) coupled with an air sampler and a thermal desorber unit (Markes International GmbH). The VOCs were trapped at 30 °C on a low-dead-volume quartz cold trap (U-T15ATA; Markes International GmbH) filled with two-bed sorbent (Tenax TA and Carbograph I). The cold trap was heated to 320 °C, and the sample was transferred to a 30 m GC column (DB-624, 0.25 mm I.D., 1.4 µm film; J&W Scientific). The temperature of the GC oven was programmed to be stable at 40 °C for 5 min and then rise at a rate of 5 °C min^{-1} up to 140 °C. Thereafter, the rate was increased to 40 °C min^{-1} up to 230 °C, where it was stabilized for 3 min. Each sample was taken every 45 min; calibrations, using a commercial gas standard mixture (National Physical Laboratory, UK), were performed every 8–12 samples.

Carbon monoxide was measured by infrared absorption spectroscopy using a room temperature quantum cascade laser at a time resolution of 1 s. Data are reported as 60 s averages with a total uncertainty of $\sim$ 10 %, mainly determined by the uncertainty of the NIST standard used (Li et al., 2015).

Meteorological parameters (temperature, relative humidity (RH), wind speed and direction, pressure, solar radiation, precipitation) were detected by the weather station Vantage Pro2 from Davis Instruments.

Besides GC-MS all other operating instruments had time resolutions between 20 s and 5 min. For most analyses in this study the data were averaged to 10 min. When GC-MS data were included in the evaluation, 1 h averaged data were used.

3 Site description

Cyprus is a 9251 km^2 island in the southeast Mediterranean Sea (Fig. 1). The measuring site was located on a military compound in Ineia, Cyprus (34.9638° N, 32.3778° E), about 600 m above sea level and approximately 5.5–8 km from the coastline (main wind direction: W–SW). The field site is characterized by light vegetation cover, mainly comprising small shrubs like *Pistacia lentiscus, Sarcopoterium spinosum* and *Nerium oleander*; herbs like *Inula viscosa* and *Foeniculum vulgare*; and few typical Mediterranean trees like *Olea europaea, Pinus* sp. and *Ceratonia siliqua*. The area within a radius of about 15 km around the station is only weakly populated. Paphos (88 266 citizens) is located 20 km south of the field site; Limassol (235 000), Nicosia (325 756) and

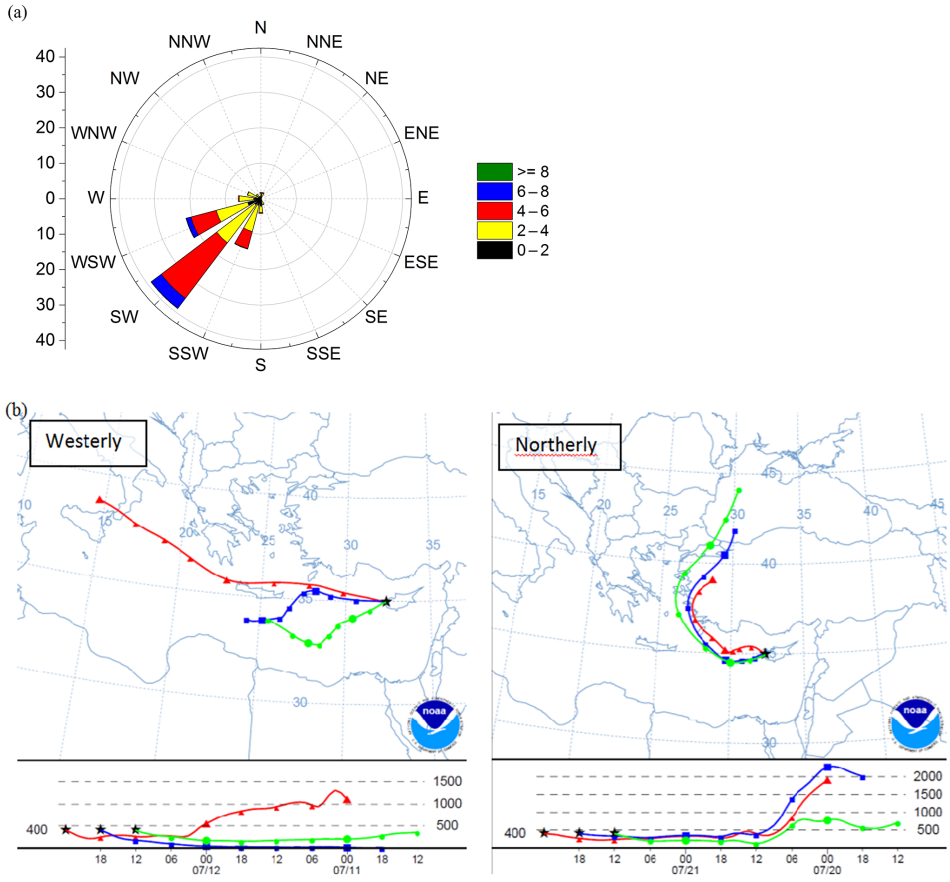

Figure 2. Airflow conditions during the CYPHEX campaign: **(a)** measured local wind direction, **(b)** back trajectories calculated with NOAA Hysplit model showing examples for the two main air mass origins (48 h, UTC = LT − 3 h).

Larnaca (143 367) are 70, 90 and 110 km to the E–SE, respectively (population data according to statistical service of the Republic of Cyprus, http://www.cystat.gov.cy, census of population October 2011). During the campaign (7 July–3 August 2014), clear-sky conditions prevailed and occasionally clouds skimmed the site. No rain was observed, but the elevated field site was impacted by fog during nighttime and early morning due to adiabatic cooling of ascending marine humid air masses. Temperature ranged from 18 to 28 °C. Within the main local wind direction of SW (Fig. 2a) there was no direct anthropogenic influence, resulting in clean humid air from the sea. Analysis of 48 h back trajectories showed mainly two source regions of air mass origin (Fig. 2b). For approximately half (46 %) of the campaign the air masses came from west of Cyprus, spending most of their time over the Mediterranean Sea prior to arriving at the site. During the remaining half of the campaign air masses originated from north of Cyprus, from eastern European countries (Turkey, Bulgaria, Rumania, Ukraine and Russia). Westerly air masses have been shown to exhibit lower concentration of gaseous and aerosol pollutants than the predominant northerly air masses that typically reach the site (Kleanthous et al., 2014). They spent more time over continental terrestrial surface and were likely to be additionally affected by biomass burning events detected in eastern Europe within the measurement periods (FIRMS, MODIS, web fire mapper, Fig. S1 in the Supplement). Previous back-trajectory studies in the eastern Mediterranean support this assumption (Kleanthous et al., 2014; Pikridas et al., 2010).

Most of the time the advected air mass was loaded with high humidity as a result of sea breeze circulation. Two periods of about 4 days with lower relative humidity occurred. These two situations will be contrasted below.

4 Results

The concentrations of HONO and other atmospheric trace gases as well as meteorological conditions observed on Cyprus from 7 July to 3 August 2014 are shown in Fig. 3. In general, low trace gas mixing ratios were indicative of clean marine atmospheric boundary conditions, as pollutants are oxidized by OH during the relatively long air transport time over the Mediterranean Sea (more than 30 h), and without significant impact of direct anthropogenic emissions.

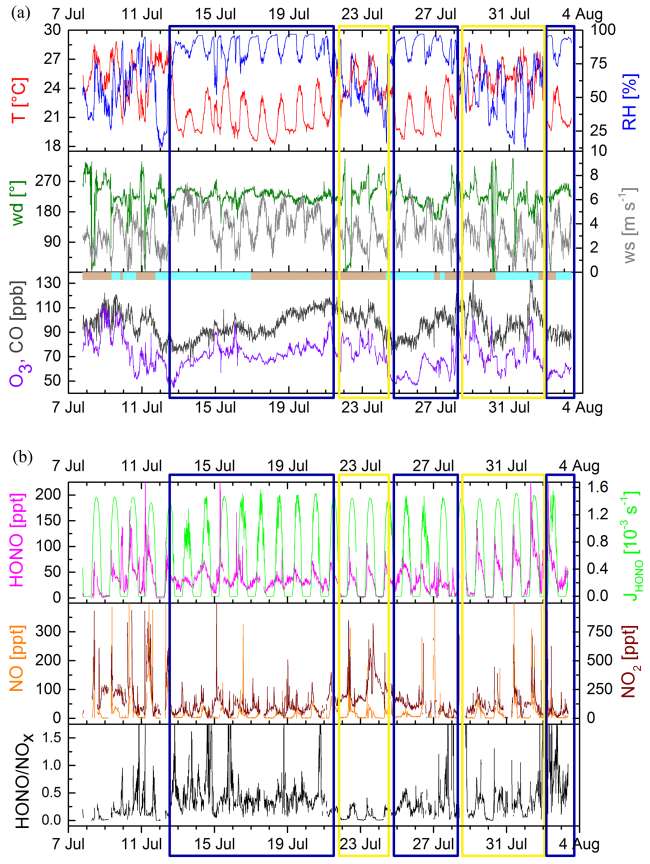

Figure 3. Measured variables during the whole campaign from 7 July to 4 August 2014. **(a)** Meteorological data (temperature, T; relative humidity, RH; wind direction, wd; wind speed, ws), O_3 and CO indicate stable conditions; in the lower panel the bar indicates the air mass origin: bright blue represents westerly, while the brownish color represents northerly. **(b)** Observed mixing ratios of HONO, NO_2 and NO, and the photolysis frequency J_{HONO} and the HONO / NO_x ratio. The yellow and blue boxes reflect the dry and the humid periods, respectively.

Ambient HONO mixing ratios ranged from below detection limit (< 4 pptv) to above 300 pptv. Daily average HONO was 35 pptv (±25 pptv; 1σ standard deviation). The daily average NO_2 and NO mixing ratios were 140 ± 115 and 20 ± 35 pptv, respectively, but showed intermittent peaks up to 50 ppbv when sampling air was streamed from the diesel generator used to power the station, from the access route or the parking lot by local winds (easterly, Fig. S2). These incidents, which account for 4 % of the campaign time, were classified as local air pollution events and were omitted from analysis. Mean O_3 and CO mixing ratios were 72 ± 12 ppb and 98 ± 11 ppbv, respectively. OH radicals ranged from below detection limit (1×10^5 molecules cm^{-3}) during nighttime to 8×10^6 molecules cm^{-3} during daytime (see Fig. S3). Daytime HO_2 / OH ratio ranged from 100 to 150. The mixing ratios of NO_2, O_3 and CO varied in unison and were significantly ($p < 0.05$) higher during periods when air masses originated from eastern Europe (brownish bar in Fig. 3a, lower panel), indicative of air pollution and shorter transport times compared to western Europe (NO_2: northerly: 144 ± 130 pptv, westerly: 127 ± 106 pptv; O_3: northerly: 74 ± 11 ppbv, westerly: 66 ± 12 ppbv; CO: northerly: 101 ± 9 ppbv, westerly: 90 ± 10 ppbv). In contrast, NO and HONO mixing ratios were slightly higher when air masses came from western Europe and over the sea (NO: northerly: 17 ± 35 pptv, westerly: 20 ± 44 pptv; HONO: northerly: 32 ± 26 pptv, westerly: 38 ± 22 pptv).

Besides two different air mass origins, two periods with different behavior of relative humidity were identified, as illustrated by blue and yellow boxes in Fig. 3a and b. In both periods we found northerly and westerly air mass origins. The diel profiles of trace gas mixing ratios and meteorological variables of the humid period (blue box) are shown in Fig. 4a, and the ones of the dry period (yellow box) in Fig. 4b. During the drier period HONO concentrations were stable and low (6 pptv) during nighttime, while mean nighttime HONO mixing ratios during the humid period (Fig. 4a) showed an expected slow increase of about 20 pptv (from 20 to 40 pptv), as anticipated from heterogeneous production and accumulation within a nocturnal boundary layer characterized by a stable stratification and low wind speed (Acker et al., 2005; Su et al., 2008b; Li et al., 2012). During both periods, but more pronounced in the drier period, HONO rapidly increased by a factor of 2 within 2 h after sunrise and then slowly decreased until sunset. Similar profiles were also observed for other trace gases, like isoprene or DMS, which are transported in upslope winds. Strong HONO morning peaks and high daytime mixing ratios suggest a strong daytime source, compensating the short atmospheric lifetime (15 min) caused by fast photolysis.

Mean NO mixing ratios were close to the detection limit (5 pptv) at night and increased after sunrise (06:00 local time, LT) to mean values of 60 pptv (peak 150 pptv) at 09:00 LT, prior to declining for the rest of the day until sunset (20:00 LT). In the absence of local NO sources low nighttime values are a result of the conversion of NO to NO_2 by O_3, which was continuously high (Hosaynali Beygi et al., 2011). The diel profiles of NO mixing ratios followed closely those of HONO mixing ratios. This similarity and their dependency on relative humidity are suggestive of a common source for both reactive nitrogen species.

NO_2 mixing ratios were somewhat lower during nighttime, but in general the diel variability remained in a narrow range between 100 and 200 pptv. Likewise, the diel courses of O_3 and CO mixing ratios revealed relatively low day–night variability in a range of 65–75 and 90–100 ppb, respectively.

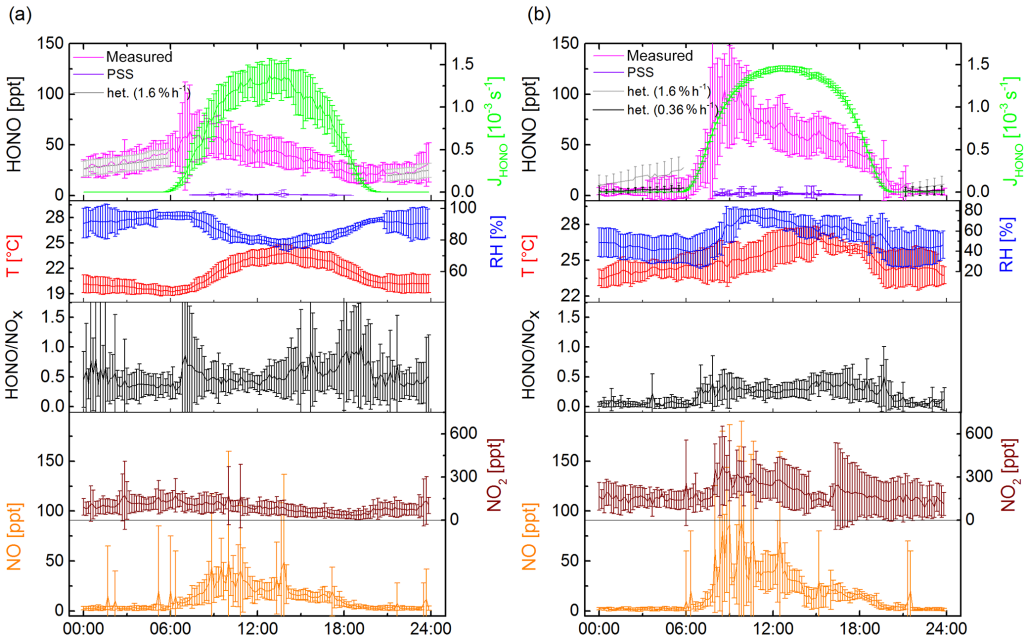

Figure 4. Diel variation of meteorological data (temperature, T; relative humidity, RH), NO and NO_2 mixing ratios, the photolysis rate for HONO J_{HONO} and HONO mixing ratios (pink: measured; violet: daytime photostationary state (PSS); grey: nighttime heterogeneous NO_2 conversion) and HONO / NO_x ratio for **(a)** average for period when RH was above 60 % (blue box in Fig. 3) and **(b)** average for dry period when RH was below 60 % (yellow box in Fig. 3). Error bars represent standard deviation of diel mean.

5 Discussion

Low-NO_x conditions at this remote field site in photochemically aged marine air were found to be an ideal prerequisite to trace as yet undefined local HONO sources. On Cyprus, diel profiles of HONO showed peak values in the late morning and persistently high mixing ratios during daytime, as has been reported for some other remote regions (Acker et al., 2006a; Zhou et al., 2007; Huang et al., 2002). This is not the case for rural and urban sites, where atmospheric HONO mixing ratios are normally observed to continuously build up during nighttime, presumably due to heterogeneous reactions involving NO_x and decline in the morning due to strong photodissociation (e.g., Elshorbany et al., 2012, and references therein).

The diel HONO / NO_x ratio (Fig. 4a, b, third panel) shows consistently high values during the humid period (Fig. 4a) and significant diel variation for the dry case (Fig. 4b) with higher values during daytime. The ratio (average of 0.33 and peak values greater than 2) is higher than that reported for most other regions, suggesting a strong impact of local HONO sources. Elshorbany et al. (2012) investigated data from 15 different urban and rural field measurement campaigns around the globe, and came up with a robust representative mean atmospheric HONO / NO_x ratio as low as 0.02. However, high values were observed at remote mountain sites, with mean values of 0.23 (up to ≈ 0.5 in the late morning; Zhou et al., 2007) or 0.2–0.4 at remote Arctic/polar sites (Li, 1994; Zhou et al., 2001; Beine et al., 2001; Jacobi et al., 2004; Amoroso et al., 2010). Legrand et al. (2014) observed HONO / NO_x ratios between 0.27 and 0.93 during experiments with irradiated Antarctic snow, depending on radiation wavelength, temperature and nitrate content. Elevated HONO / NO_x ratios at low NO_x levels show the importance of HONO formation mechanisms other than heterogeneous NO_x reactions.

5.1 Nighttime HONO accumulation

Between 18:30 and 07:30 LT HONO has an atmospheric lifetime of more than 45 min and [OH] is low, just about 1×10^5 molecules cm^{-3}, so that the calculation of HONO at photostationary state $[HONO]_{pss}$ (Reactions R1–R3) at night is not appropriate. Instead, nighttime HONO concentrations can be estimated due to heterogeneous reaction of NO_2 described in Eq. (1) (Alicke et al., 2002, 2003; Su et al., 2008b; Sörgel et al., 2011b). Three studies in different environments from a rural forest region in eastern Germany (Sörgel et al., 2011b) and a non-urban site in the Pearl River Delta, China (Su et al., 2008b), to an urban, polluted site in Beijing (Spataro et al., 2013) found a conversion rate of about 1.6 % h^{-1} (1.1–1.8 % h^{-1}).

$$[HONO]_{het} = [HONO]_{evening} + 0.016\,h^{-1}[NO_2]\Delta t \quad (1)$$

$[HONO]_{het}$ denotes the accumulation of HONO by heterogeneous conversion of NO_2, $[HONO]_{evening}$ the measured

HONO concentration at 20:30 LT, [NO_2] the measured average NO_2 concentration between 20:30 and 07:30 LT, and Δt time span in hours.

Measured and calculated HONO mixing ratios are compared in Fig. 4 (upper panel). During the humid period, during nighttime the estimated (according Eq. 1; Fig. 4a, upper panel, grey line) and observed HONO mixing ratios are in good agreement ($R^2 = 0.9$). During the drier period the observed HONO mixing ratios were lower than the ones calculated with a NO_2 conversion rate of 1.6 % h^{-1}. Here the approach for the nighttime conversion frequency by, e.g., Alicke et al. (2002, 2003), Su et al. (2008b) or Sörgel et al. (2011b) (rate $= \frac{HONO_{t2} - HONO_{t1}}{\Delta t \cdot \overline{NO_2}}$) was used. The 7-day average conversion rate for the dry nights was 0.36 % h^{-1} (Fig. 4b, upper panel, black line), comparable to results of Kleffmann et al. (2003) reporting a conversion rate of 6×10^{-7} s^{-1} (0.22 % h^{-1}) for rural forested land in Germany.

As already mentioned above, it is apparent that HONO mixing ratios under low-RH conditions during nighttime were much lower than under humid conditions, and HONO morning peaks were most pronounced (compare Fig. 4a and b: humid/dry). HONO (Donaldson et al., 2014a) and NO_2 (Wang et al., 2012; Liu et al., 2015) uptake coefficients have recently been reported to be much stronger for dry soil and at low RH, respectively, which is in line with HONO on Cyprus being close to the detection limit on nights with low relative humidity. On the other hand, it has been shown on glass and on soil proxies that the yield of HONO formation from NO_2 on surfaces is low under dry conditions but sharply increases at RH > 30 % (Liu et al., 2015) or > 60 % (Finlayson-Pitts et al., 2003). On Cyprus the strong morning HONO peaks after dry nights were accompanied by an increase in relative humidity from 40 to 80 %. Deposited and accumulated NO_2 on dry soil surfaces could be released as HONO at high rates under elevated-RH conditions. In contrast, in a humid regime HONO mixing ratios were continuously high during nighttime and showed less pronounced morning peaks, suggesting lower nighttime deposition of NO_2 and lower HONO emissions in the morning, respectively.

As morning HONO peak mixing ratios were most pronounced after dry nights on Cyprus, our observations are to some extent contradictory to earlier results that have proposed that dew formation on the ground surface may be responsible for HONO nighttime accumulation in the aqueous phase, followed by release from this reservoir after dew evaporation the next morning (Zhou et al., 2002a; Rubio et al., 2002; He et al., 2006). We cannot rule out that the latter could have contributed to nighttime accumulation of HONO during humid conditions, as we had no means to measure dew formation at the site, and high daytime HONO mixing ratios were observed under all humidity regimes. However, kinetic models of competitive adsorption of trace gases and water onto particle surfaces predict exchange behavior explicitly distinct from the liquid phase (Donaldson et al., 2014a). The nitrogen composition in thin water films (few water molecular monolayers) is complex, including HONO, NO, HNO_3, water–nitric acid complexes, NO_2^+ and N_2O_4 (Finlayson-Pitts et al., 2003). With only small amounts of surface-bound water, nitric acid is largely undissociated HNO_3 and is assumed to be stabilized upon formation of the HNO_3–H_2O complexes (hydrates), which have unique reactivity compared to nitric acid water aqueous solutions, where it is dissociated H^+ and NO_3^- ions (Finlayson-Pitts et al., 2003). Likewise, HONO formation rates in surface-bound water are about 4 orders of magnitude larger than expected for the aqueous-phase reaction (Pitts et al., 1984).

Diel HONO profiles very similar to those on Cyprus with a late-morning maximum and late-afternoon/early-evening minimum have been observed at the Meteorological Observatory Hohenpeissenberg, a mountain-top site in Germany (Acker et al., 2006a) and by Zhou et al. (2007) at the summit of Whiteface Mountain in New York State. For the latter study, formation of dew could be ruled out as relative humidity was mostly well below saturation. Zhou et al. (2007) argued that the high HONO mixing ratios during morning and late morning can be explained by mountain up-slope flow of polluted air from the cities at the foot of the mountain that results from ground surface heating. On Cyprus the sea breeze, driven by the growing difference between sea and soil surface temperature, brings air to the site which interacted with the soil surface and vegetation and is loaded by respective trace gas emissions. This is endorsed by the simultaneous increase of DMS and isoprene, markers for transportation of marine air and emission by vegetation. In the late afternoon, when the surface cools, down-welling air from aloft would dominate, being less influenced by ground surface processes. Zhou et al. (2007) could show that noontime HONO mixing ratios and average NO_y during the previous 24 h period were strongly correlated, much better than instantaneous HONO / NO_y or HONO / NO_x, which is in line with N accumulation on soil surfaces as discussed above.

5.2 Daytime HONO budget

During daytime (07:30 to 18:00 LT, with HONO lifetime being between 10 and 30 min), $[HONO]_{PSS}$, the photostationary HONO concentration resulting from gas-phase chemistry, can be calculated according to Eq. (2) (Kleffmann et al., 2005):

$$[HONO]_{PSS} = \frac{k_1 [OH][NO]}{k_2[OH] + J_{HONO}}, \quad (2)$$

where k_1 and k_2 are the temperature-dependent rate constants for the gas-phase HONO formation from NO and OH and the loss of HONO by reaction of HONO and OH, respectively (Atkinson et al., 2004; e.g., at 23.0 °C a typical temperature during this study $k_1 \approx 1.36 \times 10^{-11}$ cm^3 s^{-1}; $k_2 \approx 6.01 \times 10^{-12}$ cm^3 s^{-1}). J_{HONO} is the photolysis frequency of

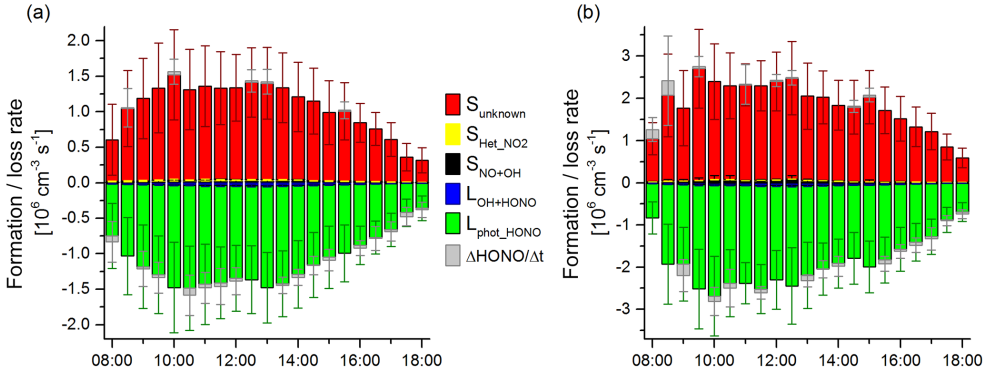

Figure 5. HONO budget analysis for **(a)** the humid and **(b)** the dry period. S_{OH+NO} (black) stands for the formation rate of HONO via the reaction of NO and OH, $S_{Het\_NO_2}$ (yellow) is the formation rate for the heterogeneous reaction of NO_2 (conversion rate $a = 1.6\,\%\,h^{-1}$; $b = 0.36\,\%\,h^{-1}$), L_{phot} (green) and $L_{OH+HONO}$ (blue) are the loss rates via photolysis, and the reaction with OH and $S_{unknown}$ is the unknown source. Error bars indicate standard deviation of diel mean.

HONO, which was measured with a spectroradiometer. [NO] is the observed NO concentration. Since OH data were available only on a few days, diel variations of [OH] were averaged (see Fig. S3).

As has been previously established by many other studies (Su et al., 2008a; Michoud et al., 2014; Sörgel et al., 2011a), homogeneous gas-phase chemistry alone fails to reflect observed HONO mixing ratios. Observed daytime values were up to 30 times higher than calculated based on PSS, indicating strong additional local daytime sources of HONO. Lee et al. (2013) argue that the HONO PSS assumption might overestimate the strength of any unidentified source if the transport time from nearby NO_x emission sources to the measurement site is less than the time required for HONO to reach PSS. In this study, the missing source was calculated according to Su et al. (2008a) (Eq. 3), where PSS was not assumed. Also in our measurements, d[HONO]/dt was not equal to 0, as HONO was not at PSS.

$$S_{HONO} = J_{HONO}[HONO] + k_2[OH][HONO] - k_1[OH][NO] - k_{het}[NO_2] + \frac{\Delta[HONO]}{\Delta t} \quad (3)$$

[HONO] is the measured HONO concentration and k_{het} the heterogeneous conversion rate of NO_2 to HONO, which was discussed above to be $1.6\,\%\,h^{-1}$ during the wet period and $0.36\,\%\,h^{-1}$ during the dry period. $\Delta[HONO] / \Delta t$ is the observed change of HONO concentration unequal to 0. The uncertainty of the calculated missing source S_{HONO} was estimated to be about 16 % based on the Gaussian error propagation of instrument uncertainties of HONO, NO, NO_2, J and OH.

Nevertheless, at the study site of Cyprus, the mean upwind distance between the measurement site and the coastline was about 6 km, and the mean wind velocity was about $3\,m\,s^{-1}$. Accordingly, the respective air mass travel time over land is estimated to be about half an hour, which is somewhat longer than the daytime lifetime of HONO and might provide enough time for the equilibrium processes. Furthermore and in strong contrast to Lee et al. (2013), at the Cyprus site the concentrations of HONO precursors (NO and OH) were extremely low, far too low to explain the observed HONO concentrations. In the late morning (around 10:00 LT) the unknown source was at its maximum, with peak production rates of up to 3.4×10^6 molecules $cm^{-3}\,s^1$ and a daytime average of about $1.3 \times 10^6\,cm^{-3}\,s^{-1}$, which is in good agreement with other studies at rural sites, like a mountain site at Hohenpeissenberg ($(3 \pm 1) \times 10^6\,cm^{-3}\,s^{-1}$, at $NO_x \approx 2$ ppbv; Acker et al., 2006a), a deciduous forest site in Jülich (3.45×10^6 molecules $cm^{-3}\,s^{-1}$, at NO $\approx$ 250 pptv; Kleffmann et al., 2005) and a pine forest site in southwest Spain 0.74×10^6 molecules $cm^{-3}\,s^{-1}$, at $NO_x \approx 1.5$ ppbv; Soergel et al., 2011a) but smaller than at urban sites in Houston ($4–6 \times 10^6\,cm^{-3}\,s^{-1}$, at $NO_x \approx 6$ ppbv; Wong et al., 2012), Beijing ($7 \times 10^6\,cm^{-3}\,s^{-1}$, at $NO_x \approx 15$ ppbv; Yang et al., 2014) and southern China ($5.25 \pm 3.75 \times 10^6\,cm^{-3}\,s^{-1}$, at $NO_x \approx 20$ ppbv (Li et al., 2012), or $1–4 \times 10^7\,cm^{-3}\,s^{-1}$, at $NO_x \approx 35$ ppbv (Su et al., 2008a)).

The contributions of gas-phase reactions and the heterogeneous reaction of NO_2 (conversion rate a $1.6\,\%\,h^{-1}$ and b $0.36\,\%\,h^{-1}$) to the HONO budget are illustrated in Fig. 5 exemplarily. For both periods the contributions are quiet similar; just the absolute values are different. To compensate the strong loss via photolysis, a comparably strong unknown source is necessary as the heterogeneous NO_2 conversion or the gas-phase reaction of OH and NO is insignificant.

In polluted regions with moderate to high NO_x concentrations, HONO sources have often been linked with [NO_2] or [NO_x] (Acker et al., 2005; Li et al., 2012; Levy et al., 2014; Sörgel et al., 2011a; Wentzel et al., 2010). Under the prevailing low-NO_x conditions during CYPHEX (< 250 pptv), correlation analysis (see Table 1) of S_{HONO} with [NO_2] ($R^2 = 0.50$) and [NO_2] · RH ($R^2 = 0.51$) indicate no significant im-

Table 1. Linear correlation factors (Pearson correlation, R^2) of HONO and the unknown source S_{HONO} to meteorological factors and different NO_x parameters.

	During the whole campaign			
			Time-of-day average	
	HONO	S_{HONO}	HONO	S_{HONO}
T	0.006	0.125	0.488	0.214
RH	0.077	0.005[d]	0.092	0.103
Heat flux	0.261	0.300	0.617[c]	0.585[c]
J_{NO_2}	0.263	0.395	*0.718*[b]	*0.672*[b]
NO	0.242	0.154	**0.857**[a]	0.600[c]
NO_2	0.052	0.078	0.620[c]	0.496
$NO_2 \cdot RH$	0.126	0.111	0.638[c]	0.505[c]
$NO_2 \cdot RH \cdot$ aerosol surface	0.095	0.092	0.256	0.579[c]
$NO_2 \cdot J$	0.191	0.164	**0.828**[a]	**0.813**[a]
$NO_2 \cdot RH \cdot J$	0.266	0.221	**0.850**[a]	**0.807**[a]
$NO_2 \cdot RH \cdot J \cdot$ aerosol surface	0.221	0.204	**0.806**[a]	**0.814**[a]
S_{NO}		0.012		−0.015[d]

	During the humid period				During the dry period			
			Time-of-day average				Time-of-day average	
	HONO	S_{HONO}	HONO	S_{HONO}	HONO	S_{HONO}	HONO	S_{HONO}
T	0.006	0.116	0.031	0.123	0.120	0.016	0.453	−0.004
RH	0.000	0.081[d]	0.010[d]	0.146[d]	0.374	0.193	*0.730*[b]	0.603[c]
Heat flux	0.110	0.243	0.184	0.591[c]	0.502[c]	0.335	*0.685*[b]	0.634[c]
J_{NO_2}	0.150	0.465	0.245	*0.669*[b]	*0.678*[b]	0.320	**0.829**[a]	*0.664*[b]
NO	0.168	0.135	0.418	*0.650*[b]	0.487	0.301	*0.730*[b]	0.409
NO_2	0.066	0.065	0.300	0.267	0.037	0.003[d]	0.619[c]	0.174
$NO_2 \cdot RH$	0.084	0.048	0.294	0.171	0.161	0.010	*0.714*[b]	0.456
$NO_2 \cdot RH \cdot$ aerosol surface	0.047	0.072	0.111	0.250	0.241	0.085	0.557[c]	0.551[c]
$NO_2 \cdot J$	0.214	0.261	0.427	**0.845**[a]	0.358	0.016	**0.872**[a]	0.603[c]
$NO_2 \cdot RH \cdot J$	0.231	0.244	0.467	*0.775*[b]	0.434	0.068	**0.820**[a]	*0.703*[b]
$NO_2 \cdot RH \cdot J \cdot$ aerosol surface	0.140	0.152	0.465	*0.795*[b]	0.414	0.130	*0.664*[b]	0.631[c]
S_{NO}		0.294		*0.720*[b]		0.059		0.094

[a] Highly correlated: $R^2 > 0.8$ (in bold font). [b] Moderately correlated: $0.65 < R^2 < 0.8$ (in italic font). [c] Poorly correlated: $0.5 < R^2 < 0.65$ (in normal font).
[d] Anti-correlated.

pact of instantaneous heterogeneous formation of HONO from NO_2. Better correlations of S_{HONO} with J_{NO_2} ($R^2 = 0.67$) and $J_{NO_2} \cdot [NO_2]$ ($R^2 = 0.82$) indicate a photo-induced conversion of NO_2 to HONO as already suggested by George et al. (2005) or Stemmler et al. (2006, 2007). Lee et al. (2016) found even lower correlation with $[NO_2]$ ($R^2 = 0.0001$) but similar good correlation with $J_{NO_2} \cdot [NO_2]$ ($R^2 = 0.70$) at an urban background site in London. Other light-dependent reactions such as the photolysis of nitrate might additionally contribute to high daytime HONO. It is unlikely that aerosol surfaces played an important role in heterogeneous conversion of NO_2 as the mean observed aerosol surface concentration was only about $300\,\mu m^2\,cm^{-3}$. Based on a formula for photo-enhanced conversion of NO_2 on humic acid aerosols which was derived by Stemmler et al. (2007), a HONO formation rate of only 5.1×10^2 molecules $cm^{-3}\,s^{-1}$ can be estimated. Likewise, Sörgel et al. (2015) showed that HONO fluxes from light-activated reactions of NO_2 on humic acid surfaces at low NO_2 levels (< 1 ppb and thus comparable to concentrations observed in this study) saturated at around $0.0125\,nmol\,m^{-2}\,s^{-1}$. Therefore heterogeneous aerosol surface reactions can be neglected as HONO sources at the prevailing low NO_x levels.

Likewise, the nitrate concentrations of highly acidic marine aerosols particulate matter as measured by HR-ToF-AMS (PM1 fraction, mean of $0.075\,\mu g\,m^{-3}$) were too low to account for significant photolytic HONO production (1.7×10^2 molecules $cm^{-3}\,s^{-1}$ or 0.01 % of S_{HONO}) calculated by Eq. (4):

$$S_{photo\_NO_3^-} = \overline{[NO_3^-]} \cdot J_{NO_3^-}, \quad (4)$$

with $S_{photo\_NO_3^-}$ being the source strength of HONO by photolysis of nitrate, $\overline{[NO_3^-]}$ the mean particulate nitrate concentration and $J_{NO_3^-}$ the photolysis frequency of nitrate (aqueous) at noon ($3 \times 10^{-7}\,s^{-1}$; Jankowski et al., 1999).

Recently an enhancement of the photolysis frequency of particulate nitrate relative to gaseous or aqueous nitrate was found (Ye et al., 2016). But even with this enhanced rate of 2×10^{-4} s^{-1} no more than 1.1×10^5 molecules cm^{-3} s^{-1} (8 % of S_{HONO}) HONO would be produced.

5.3 Common daytime source of HONO and NO

During CYPHEX, good correlation was found between [HONO] or S_{HONO} and [NO] ($R^2 = 0.86$ and 0.60, respectively), indicating that both may have a common source. A missing source of NO can be calculated as shown in Eq. (5).

$$S_{NO} = k_1[OH][NO] + k_3[HO_2][NO] + k_4[O_3][NO] + k_5[RO_2][NO] - J_{NO_2}[NO_2] - J_{HONO}[HONO] + \frac{\Delta[NO]}{\Delta t} \quad (5)$$

k_3 and k_4 are the temperature-dependent rate constants for the reaction of NO with HO_2 and O_3, respectively (Atkinson et al., 2004; at 23 °C: $k_3 \approx 8.96 \times 10^{-12}$ cm^3 s^{-1}; $k_4 \approx 1.68 \times 10^{-14}$ cm^3 s^{-1}); k_5 is the rate constant for the reaction of NO and organic peroxy radicals which was assumed to be the same as for the reaction NO + CH_3O_2 (7.7×10^{-12} cm^3 s^{-1} at 298 K; Ren et al., 2010; Sander et al., 2011). Like [OH], [HO_2] was also measured only on a few days, and therefore mean diel data were used (Fig. S3). Total [RO_2] was estimated to be maximum $1.6 \cdot [HO_2]$ (Ren et al., 2010; Hens et al., 2014). Using a RO_2 / HO_2 ratio of 1.2, the absolute values of S_{NO} are reduced by 0.3 to 5.5 %. The budget analysis for NO for both humidity regimes is illustrated in Fig. S4.

For NO_x, an unexpected deviation from the PSS, or Leighton ratio, of clean marine boundary layer air has been observed previously, invoking a hitherto unknown NO sink, or pathway for NO to NO_2 oxidation, other than reactions with OH, HO_2, O_3 and organic peroxides (Hosaynali Beygi et al., 2011). On Cyprus, two different atmospheric humidity regimes can be differentiated. Under dry conditions (RH < 70 %, yellow boxes in Fig. 3) and higher NO_x concentrations (> 150 pptv) S_{NO} is negative, implying a net NO sink of up to 6.4×10^7 molecules cm^{-3} s^{-1} resembling the abovementioned PSS deviations in remote marine air masses (see Figs. 6 and 7). However, during humid conditions (RH > 70, blue boxes in Fig. 3) S_{NO} was positive with values of up to 5.1×10^7 molecules cm^{-3} s^{-1}. Due to low and invariant acetonitrile levels, anthropogenic activity and local biomass burning can be excluded as an NO source at this specific site. A net NO source during humid conditions is assumed to result from (biogenic) NO emission from soil. As shown in Fig. 8, the S_{HONO} and S_{NO} (time-of-day average, excluding 3 days as there are transition days (25 July and 2 August) or the RH changed too quickly (15 July)) were highly correlated ($R^2 = 0.72$), indicative of both reactive N compounds being emitted from the same local source. Both HONO and NO have been reported to be released from soil, with a strong dependency on soil water content (Su et al., 2011; Oswald et al., 2013; Mamtimin et al., 2016). The (dry-state) soil humidification threshold level for NO emission is reported to be somewhat higher than for HONO (Oswald et al., 2013), which might explain why a net NO source was preferentially calculated for higher-relative-humidity conditions, while for HONO a daytime source under all humidity regimes prevailing during the campaign was found. Mamtimin et al. (2016) investigated HONO and NO emissions of natural desert soil and with grapes or cotton cultivation soils in an oasis in the Taklamakan Desert in the Xinjiang region in China. After irrigation they did not find direct emission, but when the soil had almost dried out (gravimetric soil water content: 0.01–0.3) emissions up to 115 ng N m^{-2} s^{-1} were detected. In addition they observed soil-temperature-dependent emission of reactive nitrogen. Analyzing microbial surface communities from drylands, Weber et al. (2015) observed highly correlated NO–N and HONO–N emissions with Spearman rank correlation coefficients ranging between 0.75 and 0.99. In this study, NO and HONO emissions were observed in drying soils with water contents of 20–30 % water holding capacity.

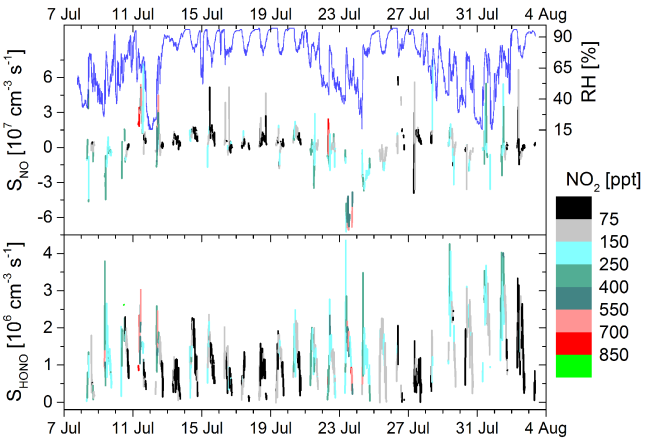

Figure 6. NO_2 (color-coded) and RH dependence of the sources of NO (S_{NO}) and HONO (S_{HONO}).

Even though we cannot make firm conclusions regarding the exact mechanism of HONO formation, the abovementioned correlation analysis (and Table 1) reveal that the instantaneous heterogeneous NO_2 conversion is not a significant HONO source. We propose that HONO is emitted from nitrogen compounds being accumulated on mountain slope soil surfaces produced either biologically by soil microbiota or from previously deposited NO_y. This forms the major daytime HONO source responsible for morning concentration peaks and consistently high daytime mixing ratios at the Cyprus field site. While biological formation is assumed to be more relevant for humid conditions, physical NO_y accumulation can be assumed to be stronger under dry conditions, as uptake coefficients for a variety of trace gases were shown to be significantly higher for dry surfaces, among them NO_2 (Wang et al., 2012; Liu et al., 2015), HONO (Donaldson et

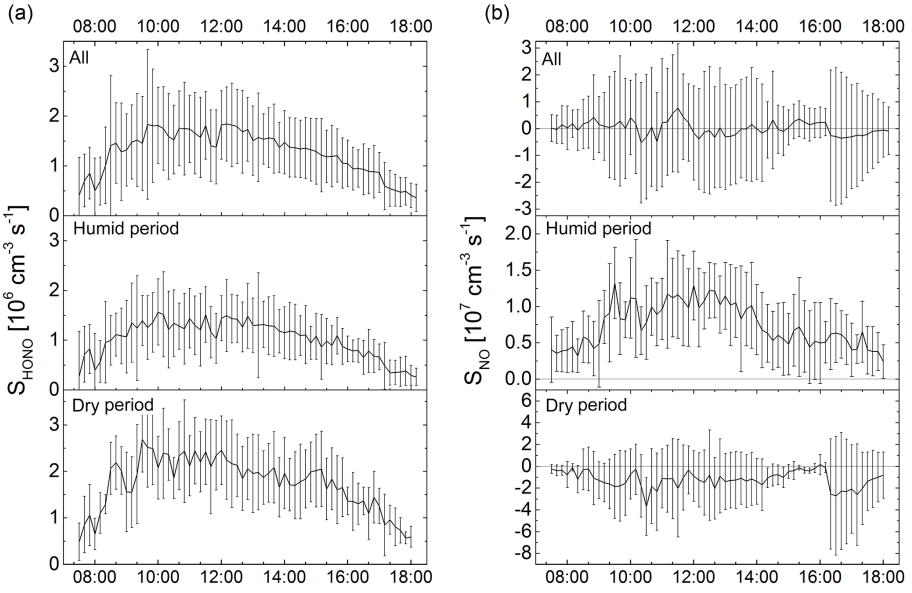

Figure 7. Diel profile of both unknown sources, S_{HONO} **(a)** and S_{NO} **(b)**, for all data, humid (excluding transition days, 25 July and 2 August, and 15 July as RH conditions changed too quickly) and dry periods. Error bars indicate standard deviation of diel average.

al., 2014a) and HCHO (Li et al., 2016). The strongest HONO morning peaks observed after dry nights were accompanied by an increase in relative humidity driven by the sea breeze (Fig. 4b), so we consider HONO as being released preferentially under favorable humid conditions.

5.4 Primary OH production

Many studies showed high contribution of HONO photolysis to the OH budget (up to 30 % on average daily; Alicke et al., 2002; Ren et al., 2006). Here, the primary OH production rates are calculated based on the main OH-forming reactions, which are the photolysis of O_3 and subsequent reaction with water (Reactions R6, R7), the photolysis of HONO (Reaction R2) and the reaction of alkenes with ozone (Reaction R8).

$$O_3 \xrightarrow{h\nu(<340\,\mathrm{nm})} O\left(^1D\right) + O_2 \quad \text{(R6)}$$

$$O\left(^1D\right) + H_2O \rightarrow 2OH \quad \text{(R7)}$$

$$\text{alkene} + O_3 \rightarrow OH + \text{other products} \quad \text{(R8)}$$

Reaction rates were taken from Atkinson et al. (2004) and Atkinson (1997). The water pressure over water was calculated according to Murphy and Koop (2005). Reactions of $O(^1D)$ and HO_2 not forming OH are also considered. OH formation yields of the reactions of alkenes with O_3 were taken from Paulson et al. (1999). Photolysis rates (J values) and concentrations of relevant compounds were as measured on Cyprus. Isoprene, α-pinene, β-pinene, Δ3-carene and limonene (VOC) were taken into account as the most relevant alkenes.

The results of this study are shown in Fig. 9. All three production routes show a clear diel profile with higher production rates during daytime. In the night only the reaction of alkenes with O_3 produced significant amounts of OH (2×10^4 molecules cm^{-3} s^{-1}). With sunrise the other sources become more relevant. During daytime the photolysis of HONO generates about 1.5×10^6 molecules OH cm^{-3} s^{-1}, which is about 10 times higher than the ozonolysis of alkenes at that time. The maximum OH production rate by O_3 photolysis during daytime is about 1.3×10^7 molecules cm^{-3} s^{-1}. In the morning (06:00–08:00 LT) and evening hours (19:00–20:00 LT) the contribution of HONO photolysis to the primary OH production is on average 37 % (see Fig. 9b) with peak values of 65 %, which is much higher than the contribution of O_3 photolysis at that time. During the rest of the day the contribution of HONO decreases to 12 %. At noon the most dominant OH source is the photolysis of O_3 (more than 80 %), while the contribution of the ozonolysis of alkenes is almost negligible (1–2 %). A complete and detailed HO_x budget analysis with CYPHEX data will be published soon.

6 Conclusion

Nitrous acid was found in low concentrations on the east Mediterranean island of Cyprus during summer 2014. Daytime concentrations were much higher than during the night and about 30 times higher than would be expected by budget analysis based on photostationary state. The unknown source was calculated to be about 1.9×10^6 molecules cm^{-3} s^{-1} around noon. Low NO_x concentrations, high HONO / NO_x

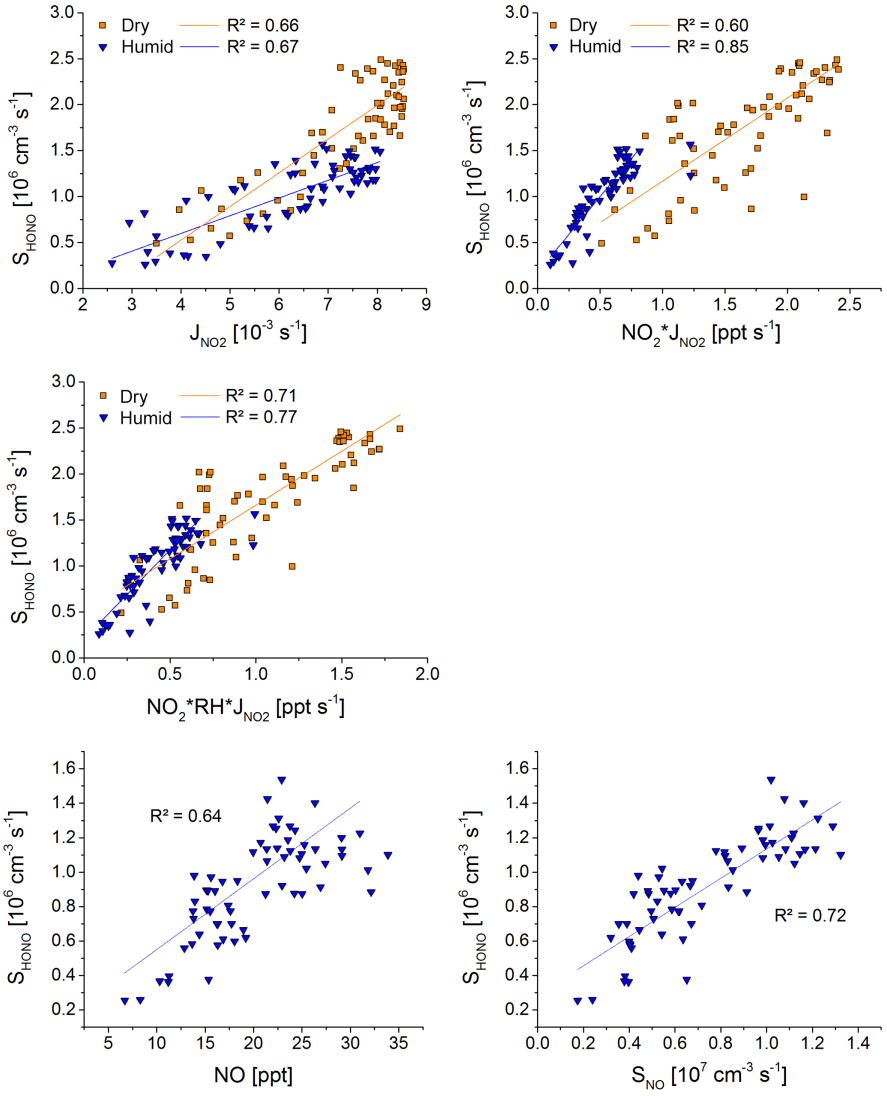

Figure 8. Correlation of S_{HONO} to light-induced NO_2 reaction (for both periods; humid: blue triangle; dry: orange square), to NO and S_{NO} (only for humid period, excluding the transition days – 25 July and 2 August – and the day with quickly changing RH – 15 July); time-of-day-average data were used.

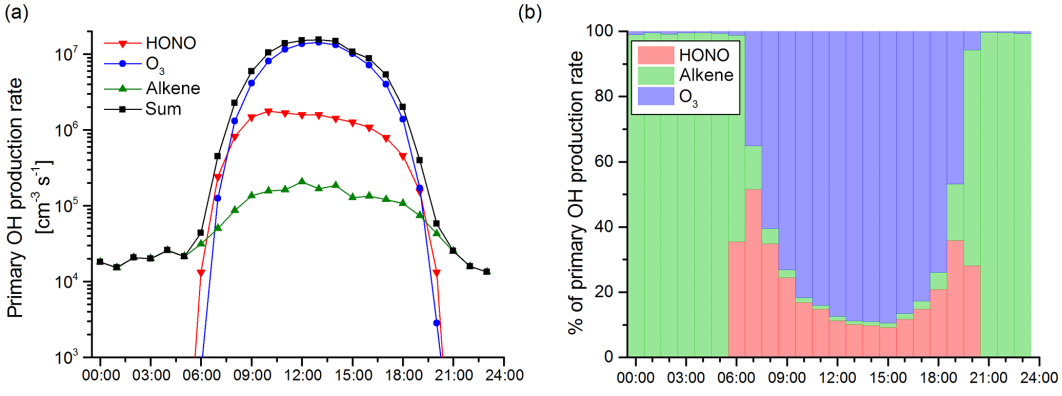

Figure 9. Average diel pattern of primary OH production from HONO, O_3 and VOC, shown as **(a)** production rate and **(b)** percentage contributions to primary OH production.

ratio and low correlation between HONO and NO_2 indicate a local source which is independent of NO_2. Heterogeneous reactions of NO_2 on aerosols play an insignificant role during daytime. Emission from soil, caused either by photolysis of nitrate or gas–soil partitioning of accumulated nitrite/nitrous acid, is supposed to have a higher impact on the HONO concentration during this campaign. Also the NO budget analysis showed a missing source in the humid period, which correlates well with the unknown source of HONO, indicating a common source. The most likely source of HONO and NO is the emission from soil.

Even though the HONO concentration is only in the lower pptv level, it has a high contribution to the primary OH production in the early morning and evening hours.

7 Data availability

Readers who are interested in the data should contact the authors: Hang Su (h.su@mpic.de) or Hannah Meusel (hannah.meusel@mpic.de).

The Supplement related to this article is available online at doi:10.5194/acp-16-14475-2016-supplement.

Acknowledgements. This study was supported by the Max Planck Society (MPG) and the DFG Research Center/Cluster of Excellence "The Ocean in the Earth System-MARUM".

We thank the Cyprus Institute and the Department of Labor Inspection for the logistical support, as well as the military staff at the Lara Naval Observatory in Ineia for the excellent collaboration.

Furthermore we would like to thank Mathias Soergel for his technical support on experimental setup of atmospheric HONO measurements.

The article processing charges for this open-access publication were covered by the Max Planck Society.

Edited by: N. Mihalopoulos
Reviewed by: two anonymous referees

References

Acker, K., Moller, D., Auel, R., Wieprecht, W., and Kalass, D.: Concentrations of nitrous acid, nitric acid, nitrite and nitrate in the gas and aerosol phase at a site in the emission zone during ESCOMPTE 2001 experiment, Atmos. Res., 74, 507–524, 2005.

Acker, K., Moller, D., Wieprecht, W., Meixner, F. X., Bohn, B., Gilge, S., Plass-Dulmer, C., and Berresheim, H.: Strong daytime production of OH from HNO_2 at a rural mountain site, Geophys. Res. Lett., 33, L02809, doi:10.1029/2005gl024643, 2006a.

Acker, K., Febo, A., Trick, S., Perrino, C., Bruno, P., Wiesen, P., Moeller, D., Wieprecht, W., Auel, R., Giusto, M., Geyer, A., Platt, U., and Allegrini, I.: Nitrous acid in the urban area of Rome, Atmos. Environ., 40, 3123–3133, 2006b.

Acker, K., Beysens, D., and Moeller, D.: Nitrite in dew, fog, cloud and rain water: An indicator for heterogeneous processes on surfaces, Atmos. Res., 87, 200–212, 2008.

Alicke, B., Platt, U., and Stutz, J.: Impact of nitrous acid photolysis on the total hydroxyl radical budget during the Limitation of Oxidant Production/Pianura Padana Produzione di Ozono study in Milan, J. Geophys. Res.-Atmos., 107, 8196, doi:10.1029/2000jd000075, 2002.

Alicke, B., Geyer, A., Hofzumahaus, A., Holland, F., Konrad, S., Patz, H. W., Schafer, J., Stutz, J., Volz-Thomas, A., and Platt, U.: OH formation by HONO photolysis during the BERLIOZ experiment, J. Geophys. Res.-Atmos., 108, 8247, doi:10.1029/2001jd000579, 2003.

Ammann, M., Kalberer, M., Jost, D. T., Tobler, L., Rossler, E., Piguet, D., Gaggeler, H. W., and Baltensperger, U.: Heterogeneous production of nitrous acid on soot in polluted air masses, Nature, 395, 157–160, 1998.

Amoroso, A., Domine, F., Esposito, G., Morin, S., Savarino, J., Nardino, M., Montagnoli, M., Bonneville, J. M., Clement, J. C., Ianniello, A., and Beine, H. J.: Microorganisms in Dry Polar Snow Are Involved in the Exchanges of Reactive Nitrogen Species with the Atmosphere, Environ. Sci. Technol., 44, 714–719, 2010.

Arens, F., Gutzwiller, L., Baltensperger, U., Gaggeler, H. W., and Ammann, M.: Heterogeneous reaction of NO_2 on diesel soot particles, Environ. Sci. Technol., 35, 2191–2199, 2001.

Arey, J., Atkinson, R., and Aschmann, S. M.: Product study of the gas-phase reactions of monoterpenes with the OH radical in the presence of NO_x, J. Geophys. Res.-Atmos., 95, 18539–18546, 1990.

Atkinson, R.: Gas-Phase Tropospheric Chemistry of Volatile Organic Compounds: 1. Alkanes and Alkenes, J. Phys. Chem. Ref. Data, 26, 215–290, 1997.

Atkinson, R., Baulch, D. L., Cox, R. A., Crowley, J. N., Hampson, R. F., Hynes, R. G., Jenkin, M. E., Rossi, M. J., and Troe, J.: Evaluated kinetic and photochemical data for atmospheric chemistry: Volume I – gas phase reactions of O_x, HO_x, NO_x and SO_x species, Atmos. Chem. Phys., 4, 1461–1738, doi:10.5194/acp-4-1461-2004, 2004.

Aubin, D. G. and Abbatt, J. P. D.: Interaction of NO_2 with hydrocarbon soot: Focus on HONO yield, surface modification, and mechanism, J. Phys. Chem. A, 111, 6263–6273, 2007.

Baergen, A. M. and Donaldson, D. J.: Photochemical Renoxification of Nitric Acid on Real Urban Grime, Environ. Sci. Technol., 47, 815–820, 2013.

Beine, H. J., Allegrini, I., Sparapani, R., Ianniello, A., and Valentini, F.: Three years of springtime trace gas and particle measurements at Ny-Alesund, Svalbard, Atmos. Environ., 35, 3645–3658, 2001.

Bejan, I., Abd El Aal, Y., Barnes, I., Benter, T., Bohn, B., Wiesen, P., and Kleffmann, J.: The photolysis of ortho-nitrophenols: a new gas phase source of HONO, Phys. Chem. Chem. Phys., 8, 2028–2035, 2006.

Bianchi, M., Feliatra, F., Tréguer, P., Vincendeau, M.-A., and Morvan, J.: Nitrification rates, ammonium and nitrate distribution in upper layers of the water column and in sediments of the Indian

sector of the Southern Ocean, Deep-Sea Res. Pt. II, 44, 1017–1032, 1997.

Bohn, B., Corlett, G. K., Gillmann, M., Sanghavi, S., Stange, G., Tensing, E., Vrekoussis, M., Bloss, W. J., Clapp, L. J., Kortner, M., Dorn, H.-P., Monks, P. S., Platt, U., Plass-Dülmer, C., Mihalopoulos, N., Heard, D. E., Clemitshaw, K. C., Meixner, F. X., Prevot, A. S. H., and Schmitt, R.: Photolysis frequency measurement techniques: results of a comparison within the ACCENT project, Atmos. Chem. Phys., 8, 5373–5391, doi:10.5194/acp-8-5373-2008, 2008.

Bröske, R., Kleffmann, J., and Wiesen, P.: Heterogeneous conversion of NO_2 on secondary organic aerosol surfaces: A possible source of nitrous acid (HONO) in the atmosphere?, Atmos. Chem. Phys., 3, 469–474, doi:10.5194/acp-3-469-2003, 2003.

Costabile, F., Amoroso, A., and Wang, F.: Sub-µm particle size distributions in a suburban Mediterranean area. Aerosol populations and their possible relationship with HONO mixing ratios, Atmos. Environ., 44, 5258–5268, 2010.

Czader, B. H., Rappenglück, B., Percell, P., Byun, D. W., Ngan, F., and Kim, S.: Modeling nitrous acid and its impact on ozone and hydroxyl radical during the Texas Air Quality Study 2006, Atmos. Chem. Phys., 12, 6939–6951, doi:10.5194/acp-12-6939-2012, 2012.

Donaldson, M. A., Berke, A. E., and Raff, J. D.: Uptake of Gas Phase Nitrous Acid onto Boundary Layer Soil Surfaces, Environ. Sci. Technol., 48, 375–383, 2014a.

Donaldson, M. A., Bish, D. L., and Raff, J. D.: Soil surface acidity plays a determining role in the atmospheric-terrestrial exchange of nitrous acid, P. Natl. Acad. Sci. USA, 111, 18472–18477, 2014b.

Duplissy, J., Gysel, M., Alfarra, M. R., Dommen, J., Metzger, A., Prevot, A. S. H., Weingartner, E., Laaksonen, A., Raatikainen, T., Good, N., Turner, S. F., McFiggans, G., and Baltensperger, U.: Cloud forming potential of secondary organic aerosol under near atmospheric conditions, Geophys. Res. Lett., 35, L03818, doi:10.1029/2007gl031075, 2008.

Elshorbany, Y. F., Steil, B., Brühl, C., and Lelieveld, J.: Impact of HONO on global atmospheric chemistry calculated with an empirical parameterization in the EMAC model, Atmos. Chem. Phys., 12, 9977–10000, doi:10.5194/acp-12-9977-2012, 2012.

Finlayson-Pitts, B. J., Wingen, L. M., Sumner, A. L., Syomin, D., and Ramazan, K. A.: The heterogeneous hydrolysis of NO_2 in laboratory systems and in outdoor and indoor atmospheres: An integrated mechanism, Phys. Chem. Chem. Phys., 5, 223–242, 2003.

Foster, J. R., Pribush, R. A., and Carter, B. H.: THE CHEMISTRY OF DEWS AND FROSTS IN INDIANAPOLIS, INDIANA, Atmos. Environ. A-Gen., 24, 2229–2236, 1990.

George, C., Strekowski, R. S., Kleffmann, J., Stemmler, K., and Ammann, M.: Photoenhanced uptake of gaseous NO_2 on solid-organic compounds: a photochemical source of HONO?, Faraday Discuss., 130, 195–210, 2005.

Han, C., Liu, Y., and He, H.: Role of Organic Carbon in Heterogeneous Reaction of NO_2 with Soot, Environ. Sci. Technol., 47, 3174–3181, 2013.

Harrison, R. M. and Kitto, A. M. N.: Evidence for a surface source of atmospheric nitrous-acid, Atmos. Environ., 28, 1089–1094, 1994.

He, Y., Zhou, X. L., Hou, J., Gao, H. L., and Bertman, S. B.: Importance of dew in controlling the air-surface exchange of HONO in rural forested environments, Geophys. Res. Lett., 33, L02813, doi:10.1029/2005gl024348, 2006.

Heland, J., Kleffmann, J., Kurtenbach, R., and Wiesen, P.: A new instrument to measure gaseous nitrous acid (HONO) in the atmosphere, Environ. Sci. Technol., 35, 3207–3212, 2001.

Hens, K., Novelli, A., Martinez, M., Auld, J., Axinte, R., Bohn, B., Fischer, H., Keronen, P., Kubistin, D., Nölscher, A. C., Oswald, R., Paasonen, P., Petäjä, T., Regelin, E., Sander, R., Sinha, V., Sipilä, M., Taraborrelli, D., Tatum Ernest, C., Williams, J., Lelieveld, J., and Harder, H.: Observation and modelling of HO_x radicals in a boreal forest, Atmos. Chem. Phys., 14, 8723–8747, doi:10.5194/acp-14-8723-2014, 2014.

Hosaynali Beygi, Z., Fischer, H., Harder, H. D., Martinez, M., Sander, R., Williams, J., Brookes, D. M., Monks, P. S., and Lelieveld, J.: Oxidation photochemistry in the Southern Atlantic boundary layer: unexpected deviations of photochemical steady state, Atmos. Chem. Phys., 11, 8497–8513, doi:10.5194/acp-11-8497-2011, 2011.

Huang, G., Zhou, X. L., Deng, G. H., Qiao, H. C., and Civerolo, K.: Measurements of atmospheric nitrous acid and nitric acid, Atmos. Environ., 36, 2225–2235, 2002.

IUPAC (Ammann, M., Cox, R. A., Crowley, J. N., Jenkin, M. E., Mellouki, A., Rossi, M. J., Troe, J., and Wallington, T. J.): Task Group on Atmospheric Chemical Kinetic Data Evaluation, available at: http://iupac.pole-ether.fr/index.html, last access: June 2015.

Jacobi, H. W., Bales, R. C., Honrath, R. E., Peterson, M. C., Dibb, J. E., Swanson, A. L., and Albert, M. R.: Reactive trace gases measured in the interstitial air of surface snow at Summit, Greenland, Atmos. Environ., 38, 1687–1697, 2004.

Jankowski, J. J., Kieber, D. J., and Mopper, K.: Nitrate and nitrite ultraviolet actinometers, Photochem. Photobiol., 70, 319–328, 1999.

Kalberer, M., Ammann, M., Arens, F., Gaggeler, H. W., and Baltensperger, U.: Heterogeneous formation of nitrous acid (HONO) on soot aerosol particles, J. Geophys. Res.-Atmos., 104, 13825–13832, 1999.

Kebede, M. A., Scharko, N. K., Appelt, L. E., and Raff, J. D.: Formation of Nitrous Acid during Ammonia Photooxidation on TiO_2 under Atmospherically Relevant Conditions, J. Phys. Chem. Lett., 4, 2618–2623, 2013.

Kerbrat, M., Legrand, M., Preunkert, S., Gallée, H., and Kleffmann, J.: Nitrous acid at Concordia (inland site) and Dumont d'Urville (coastal site), East Antarctica, J. Geophys. Res.-Atmos., 117, D08303, doi:10.1029/2011JD017149, 2012.

Kessler, C. and Platt, U.: Nitrous Acid in Polluted Air Masses – Sources and Formation Pathways, in: Physico-Chemical Behaviour of Atmospheric Pollutants, edited by: Versino, B. and Angeletti, G., Springer, the Netherlands, 412–422, 1984.

Kinugawa, T., Enami, S., Yabushita, A., Kawasaki, M., Hoffmann, M. R., and Colussi, A. J.: Conversion of gaseous nitrogen dioxide to nitrate and nitrite on aqueous surfactants, Phys. Chem. Chem. Phys., 13, 5144–5149, 2011.

Khlystov, A., Stanier, C., and Pandis, S. N.: An algorithm for combining electrical mobility and aerodynamic size distributions data when measuring ambient aerosol, Aerosol Sci. Tech., 38, 229–238, 2004.

Kleanthous, S., Vrekoussis, M., Mihalopoulos, N., Kalabokas, P., and Lelieveld, J.: On the temporal and spatial variation of ozone in Cyprus, Sci. Total Environ., 476–477, 677–687, 2014.

Kleffmann, J. and Wiesen, P.: Heterogeneous conversion of NO_2 and NO on HNO_3 treated soot surfaces: atmospheric implications, Atmos. Chem. Phys., 5, 77–83, doi:10.5194/acp-5-77-2005, 2005.

Kleffmann, J., Becker, K. H., and Wiesen, P.: Heterogeneous NO_2 conversion processes on acid surfaces: possible atmospheric implications, Atmos. Environ., 32, 2721–2729, 1998.

Kleffmann, J., Becker, K. H., Lackhoff, M., and Wiesen, P.: Heterogeneous conversion of NO_2 on carbonaceous surfaces, Phys. Chem. Chem. Phys., 1, 5443–5450, 1999.

Kleffmann, J., Kurtenbach, R., Lorzer, J., Wiesen, P., Kalthoff, N., Vogel, B., and Vogel, H.: Measured and simulated vertical profiles of nitrous acid – Part I: Field measurements, Atmos. Environ., 37, 2949–2955, 2003.

Kleffmann, J., Gavriloaiei, T., Hofzumahaus, A., Holland, F., Koppmann, R., Rupp, L., Schlosser, E., Siese, M., and Wahner, A.: Daytime formation of nitrous acid: A major source of OH radicals in a forest, Geophys. Res. Lett., 32, L05818, doi:10.1029/2005gl022524, 2005.

Kleffmann, J., Lörzer, J. C., Wiesen, P., Kern, C., Trick, S., Volkamer, R., Rodenas, M., and Wirtz, K.: Intercomparison of the DOAS and LOPAP techniques for the detection of nitrous acid (HONO), Atmos. Environ., 40, 3640–3652, doi:10.1016/j.atmosenv.2006.03.027, 2006.

Kurtenbach, R., Becker, K. H., Gomes, J. A. G., Kleffmann, J., Lorzer, J. C., Spittler, M., Wiesen, P., Ackermann, R., Geyer, A., and Platt, U.: Investigations of emissions and heterogeneous formation of HONO in a road traffic tunnel, Atmos. Environ., 35, 3385–3394, 2001.

Lammel, G. and Cape, J. N.: Nitrous acid and nitrite in the atmosphere, Chem. Soc. Rev., 25, 361–369, 1996.

Langridge, J. M., Gustafsson, R. J., Griffiths, P. T., Cox, R. A., Lambert, R. M., and Jones, R. L.: Solar driven nitrous acid formation on building material surfaces containing titanium dioxide: A concern for air quality in urban areas?, Atmos. Environ., 43, 5128–5131, 2009.

Lee, B. H., Wood, E. C., Herndon, S. C., Lefer, B. L., Luke, W. T., Brune, W. H., Nelson, D. D., Zahniser, M. S., and Munger, J. W.: Urban measurements of atmospheric nitrous acid: A caveat on the interpretation of the HONO photostationary state, J. Geophys. Res., 118, 12274–12281, 2013.

Lee, J. D., Whalley, L. K., Heard, D. E., Stone, D., Dunmore, R. E., Hamilton, J. F., Young, D. E., Allan, J. D., Laufs, S., and Kleffmann, J.: Detailed budget analysis of HONO in central London reveals a missing daytime source, Atmos. Chem. Phys., 16, 2747–2764, doi:10.5194/acp-16-2747-2016, 2016.

Legrand, M., Preunkert, S., Frey, M., Bartels-Rausch, Th., Kukui, A., King, M. D., Savarino, J., Kerbrat, M., and Jourdain, B.: Large mixing ratios of atmospheric nitrous acid (HONO) at Concordia (East Antarctic Plateau) in summer: a strong source from surface snow?, Atmos. Chem. Phys., 14, 9963–9976, doi:10.5194/acp-14-9963-2014, 2014.

Lelièvre, S., Bedjanian, Y., Laverdet, G., and Le Bras, G.: Heterogeneous Reaction of NO_2 with Hydrocarbon Flame Soot, J. Phys. Chem. A, 108, 10807–10817, 2004.

Levy, H.: Normal Atmosphere: Large Radical and Formaldehyde Concentrations Predicted, Science, 173, 141–143, 1971.

Levy, M., Zhang, R., Zheng, J., Zhang, A. L., Xu, W., Gomez-Hernandez, M., Wang, Y., and Olaguer, E.: Measurements of nitrous acid (HONO) using ion drift-chemical ionization mass spectrometry during the 2009 SHARP field campaign, Atmos. Environ., 94, 231–240, 2014.

Li, J., Reiffs, A., Parchatka, U., and Fischer, H.: In situ measurements of atmospheric CO and its correlation with NO_x and O_3 at a rural mountain site, Meteorol. Meas. Syst., XXII, 25–38, 2015.

Li, S. M.: Equilibrium of particle nitrite with gas-phase HONO – tropospheric measurements in the high arctic during sunrise, J. Geophys. Res.-Atmos., 99, 25469–25478, 1994.

Li, X., Brauers, T., Häseler, R., Bohn, B., Fuchs, H., Hofzumahaus, A., Holland, F., Lou, S., Lu, K. D., Rohrer, F., Hu, M., Zeng, L. M., Zhang, Y. H., Garland, R. M., Su, H., Nowak, A., Wiedensohler, A., Takegawa, N., Shao, M., and Wahner, A.: Exploring the atmospheric chemistry of nitrous acid (HONO) at a rural site in Southern China, Atmos. Chem. Phys., 12, 1497–1513, doi:10.5194/acp-12-1497-2012, 2012.

Li, G., Su, H., Li, X., Kuhn, U., Meusel, H., Hoffmann, T., Ammann, M., Pöschl, U., Shao, M., and Cheng, Y.: Uptake of gaseous formaldehyde by soil surfaces: a combination of adsorption/desorption equilibrium and chemical reactions, Atmospheric Chemistry and Physics ,16, 10299-10311, 2016.

Liao, W., Case, A. T., Mastromarino, J., Tan, D., and Dibb, J. E.: Observations of HONO by laser-induced fluorescence at the South Pole during ANTCI 2003, Geophys. Res. Lett., 33, L09810, doi:10.1029/2005GL025470, 2006.

Liu, Y., Han, C., Ma, J., Bao, X., and He, H.: Influence of relative humidity on heterogeneous kinetics of NO_2 on kaolin and hematite, Phys. Chem. Chem. Phys., 17, 19424–19431, 2015.

Mamtimin, B., Meixner, F. X., Behrendt, T., Badawy, M., and Wagner, T.: The contribution of soil biogenic NO and HONO emissions from a managed hyperarid ecosystem to the regional NO_x emissions during growing season, Atmos. Chem. Phys., 16, 10175–10194, doi:10.5194/acp-16-10175-2016, 2016.

Mao, J., Ren, X., Chen, S., Brune, W. H., Chen, Z., Martinez, M., Harder, H., Lefer, B., Rappenglück, B., Flynn, J., and Leuchner, M.: Atmospheric oxidation capacity in the summer of Houston 2006: Comparison with summer measurements in other metropolitan studies, Atmos. Environ., 44, 4107–4115, 2010.

Martinez, M., Harder, H., Kubistin, D., Rudolf, M., Bozem, H., Eerdekens, G., Fischer, H., Klüpfel, T., Gurk, C., Königstedt, R., Parchatka, U., Schiller, C. L., Stickler, A., Williams, J., and Lelieveld, J.: Hydroxyl radicals in the tropical troposphere over the Suriname rainforest: airborne measurements, Atmos. Chem. Phys., 10, 3759–3773, doi:10.5194/acp-10-3759-2010, 2010.

Michoud, V., Colomb, A., Borbon, A., Miet, K., Beekmann, M., Camredon, M., Aumont, B., Perrier, S., Zapf, P., Siour, G., Ait-Helal, W., Afif, C., Kukui, A., Furger, M., Dupont, J. C., Haeffelin, M., and Doussin, J. F.: Study of the unknown HONO daytime source at a European suburban site during the MEGAPOLI summer and winter field campaigns, Atmos. Chem. Phys., 14, 2805–2822, doi:10.5194/acp-14-2805-2014, 2014.

Monge, M. E., D'Anna, B., Mazri, L., Giroir-Fendler, A., Ammann, M., Donaldson, D. J., and George, C.: Light changes the atmospheric reactivity of soot, P. Natl. Acad. Sci. USA, 107, 6605–6609, 2010.

Murphy, D. M. and Koop, T.: Review of the vapour pressures of ice and supercooled water for atmospheric applications, Q. J. Roy. Meteor. Soc., 131, 1539–1565, doi:10.1256/qj.04.94, 2005.

Ndour, M., D'Anna, B., George, C., Ka, O., Balkanski, Y., Kleffmann, J., Stemmler, K., and Ammann, M.: Photoenhanced uptake of NO_2 on mineral dust: Laboratory experiments and model simulations, Geophys. Res. Lett., 35, 2008.

Novelli, A., Hens, K., Tatum Ernest, C., Kubistin, D., Regelin, E., Elste, T., Plass-Dülmer, C., Martinez, M., Lelieveld, J., and Harder, H.: Characterisation of an inlet pre-injector laser-induced fluorescence instrument for the measurement of atmospheric hydroxyl radicals, Atmos. Meas. Tech., 7, 3413–3430, doi:10.5194/amt-7-3413-2014, 2014.

Oswald, R., Behrendt, T., Ermel, M., Wu, D., Su, H., Cheng, Y., Breuninger, C., Moravek, A., Mougin, E., Delon, C., Loubet, B., Pommerening-Roeser, A., Soergel, M., Poeschl, U., Hoffmann, T., Andreae, M. O., Meixner, F. X., and Trebs, I.: HONO Emissions from Soil Bacteria as a Major Source of Atmospheric Reactive Nitrogen, Science, 341, 1233–1235, 2013.

Oswald, R., Ermel, M., Hens, K., Novelli, A., Ouwersloot, H. G., Paasonen, P., Petäjä, T., Sipilä, M., Keronen, P., Bäck, J., Königstedt, R., Hosaynali Beygi, Z., Fischer, H., Bohn, B., Kubistin, D., Harder, H., Martinez, M., Williams, J., Hoffmann, T., Trebs, I., and Sörgel, M.: A comparison of HONO budgets for two measurement heights at a field station within the boreal forest in Finland, Atmos. Chem. Phys., 15, 799–813, doi:10.5194/acp-15-799-2015, 2015.

Paulson, S. E., Chung, M. Y., and Hasson, A. S.: OH radical formation from the gas-phase reaction of ozone with terminal alkenes and the relationship between structure and mechanism, J. Phys. Chem. A, 103, 8125–8138, 1999.

Pikridas, M., Bougiatioti, A., Hildebrandt, L., Engelhart, G. J., Kostenidou, E., Mohr, C., Prévôt, A. S. H., Kouvarakis, G., Zarmpas, P., Burkhart, J. F., Lee, B.-H., Psichoudaki, M., Mihalopoulos, N., Pilinis, C., Stohl, A., Baltensperger, U., Kulmala, M., and Pandis, S. N.: The Finokalia Aerosol Measurement Experiment – 2008 (FAME-08): an overview, Atmos. Chem. Phys., 10, 6793–6806, doi:10.5194/acp-10-6793-2010, 2010.

Pitts, J. N., Sanhueza, E., Atkinson, R., Carter, W. P. L., Winer, A. M., Harris, G. W., and Plum, C. N.: An investigation of the dark formation of nitrous acid in environmental chambers, Int. J. Chem. Kinet., 16, 919–939, 1984.

Ramazan, K. A., Syomin, D., and Finlayson-Pitts, B. J.: The photochemical production of HONO during the heterogeneous hydrolysis of NO_2, Phys. Chem. Chem. Phys., 6, 3836–3843, 2004.

Ren, X. R., Harder, H., Martinez, M., Lesher, R. L., Oliger, A., Simpas, J. B., Brune, W. H., Schwab, J. J., Demerjian, K. L., He, Y., Zhou, X. L., and Gao, H. G.: OH and HO_2 chemistry in the urban atmosphere of New York City, Atmos. Environ., 37, 3639–3651, 2003.

Ren, X., Brune, W. H., Oliger, A., Metcalf, A. R., Simpas, J. B., Shirley, T., Schwab, J. J., Bai, C., Roychowdhury, U., Li, Y., Cai, C., Demerjian, K. L., He, Y., Zhou, X., Gao, H., and Hou, J.: OH, HO_2, and OH reactivity during the PMTACS-NY Whiteface Mountain 2002 campaign: Observations and model comparison, J. Geophys. Res.-Atmos., 111, D10S03, doi:10.1029/2005jd006126, 2006.

Ren, X., Gao, H., Zhou, X., Crounse, J. D., Wennberg, P. O., Browne, E. C., LaFranchi, B. W., Cohen, R. C., McKay, M., Goldstein, A. H., and Mao, J.: Measurement of atmospheric nitrous acid at Bodgett Forest during BEARPEX2007, Atmos. Chem. Phys., 10, 6283–6294, doi:10.5194/acp-10-6283-2010, 2010.

Ren, X., Sanders, J. E., Rajendran, A., Weber, R. J., Goldstein, A. H., Pusede, S. E., Browne, E. C., Min, K.-E., and Cohen, R. C.: A relaxed eddy accumulation system for measuring vertical fluxes of nitrous acid, Atmos. Meas. Tech., 4, 2093–2103, doi:10.5194/amt-4-2093-2011, 2011.

Rubio, M. A., Lissi, E., and Villena, G.: Nitrite in rain and dew in Santiago city, Chile. Its possible impact on the early morning start of the photochemical smog, Atmos. Environ., 36, 293–297, 2002.

Sander, S. P., Abbatt, J., Barker, J. R., Burkholder, J. B., Friedl, R. R., Golden, D. M., Huie, R. E., Kolb, C. E., Kurylo, M. J., Moortgat, G. K., Orkin, V. L., and Wine, P. H.: Chemical Kinetics and Photochemical Data for Use in Atmospheric Studies, Evaluation No. 17, JPL Publication 10-6, Jet Propulsion Laboratory, Pasadena, available at: http://jpldataeval.jpl.nasa.gov (last access: January 2016), 2011.

Scharko, N. K., Berke, A. E., and Raff, J. D.: Release of Nitrous Acid and Nitrogen Dioxide from Nitrate Photolysis in Acidic Aqueous Solutions, Environ. Sci. Technol., 48, 11991–12001, 2014.

Sörgel, M., Regelin, E., Bozem, H., Diesch, J.-M., Drewnick, F., Fischer, H., Harder, H., Held, A., Hosaynali-Beygi, Z., Martinez, M., and Zetzsch, C.: Quantification of the unknown HONO daytime source and its relation to NO_2, Atmos. Chem. Phys., 11, 10433–10447, doi:10.5194/acp-11-10433-2011, 2011a.

Sörgel, M., Trebs, I., Serafimovich, A., Moravek, A., Held, A., and Zetzsch, C.: Simultaneous HONO measurements in and above a forest canopy: influence of turbulent exchange on mixing ratio differences, Atmos. Chem. Phys., 11, 841–855, doi:10.5194/acp-11-841-2011, 2011b.

Sörgel, M., Trebs, I., Wu, D., and Held, A.: A comparison of measured HONO uptake and release with calculated source strengths in a heterogeneous forest environment, Atmos. Chem. Phys., 15, 9237–9251, doi:10.5194/acp-15-9237-2015, 2015.

Spataro, F., Ianniello, A., Esposito, G., Allegrini, I., Zhu, T., and Hu, M.: Occurrence of atmospheric nitrous acid in the urban area of Beijing (China), Sci. Total Environ., 447, 210–224, 2013.

Stemmler, K., Ammann, M., Donders, C., Kleffmann, J., and George, C.: Photosensitized reduction of nitrogen dioxide on humic acid as a source of nitrous acid, Nature, 440, 195–198, 2006.

Stemmler, K., Ndour, M., Elshorbany, Y., Kleffmann, J., D'Anna, B., George, C., Bohn, B., and Ammann, M.: Light induced conversion of nitrogen dioxide into nitrous acid on submicron humic acid aerosol, Atmos. Chem. Phys., 7, 4237–4248, doi:10.5194/acp-7-4237-2007, 2007.

Stutz, J., Alicke, B., and Neftel, A.: Nitrous acid formation in the urban atmosphere: Gradient measurements of NO_2 and HONO over grass in Milan, Italy, J. Geophys. Res.-Atmos., 107, 8192, doi:10.1029/2001jd000390, 2002.

Su, H., Cheng, Y. F., Shao, M., Gao, D. F., Yu, Z. Y., Zeng, L. M., Slanina, J., Zhang, Y. H., and Wiedensohler, A.: Nitrous acid (HONO) and its daytime sources at a rural site during the 2004 PRIDE-PRD experiment in China, J. Geophys. Res.-Atmos., 113, D14312, doi:10.1029/2007jd009060, 2008a.

Su, H., Cheng, Y. F., Cheng, P., Zhang, Y. H., Dong, S., Zeng, L. M., Wang, X., Slanina, J., Shao, M., and Wiedensohler, A.: Observation of nighttime nitrous acid (HONO) formation at a non-urban site during PRIDE-PRD2004 in China, Atmos. Environ., 42, 6219–6232, 2008b.

Su, H., Cheng, Y., Oswald, R., Behrendt, T., Trebs, I., Meixner, F. X., Andreae, M. O., Cheng, P., Zhang, Y., and Poeschl, U.: Soil Nitrite as a Source of Atmospheric HONO and OH Radicals, Science, 333, 1616–1618, 2011.

Tang, Y., An, J., Wang, F., Li, Y., Qu, Y., Chen, Y., and Lin, J.: Impacts of an unknown daytime HONO source on the mixing ratio and budget of HONO, and hydroxyl, hydroperoxyl, and organic peroxy radicals, in the coastal regions of China, Atmos. Chem. Phys., 15, 9381–9398, doi:10.5194/acp-15-9381-2015, 2015.

VandenBoer, T. C., Brown, S. S., Murphy, J. G., Keene, W. C., Young, C. J., Pszenny, A. A. P., Kim, S., Warneke, C., de Gouw, J. A., Maben, J. R., Wagner, N. L., Riedel, T. P., Thornton, J. A., Wolfe, D. E., Dubé, W. P., Öztürk, F., Brock, C. A., Grossberg, N., Lefer, B., Lerner, B., Middlebrook, A. M., and Roberts, J. M.: Understanding the role of the ground surface in HONO vertical structure: High resolution vertical profiles during NACHTT-11, J. Geophys. Res.-Atmos., 118, 10155–10171, 2013.

VandenBoer, T. C., Markovic, M. Z., Sanders, J. E., Ren, X., Pusede, S. E., Browne, E. C., Cohen, R. C., Zhang, L., Thomas, J., Brune, W. H., and Murphy, J. G.: Evidence for a nitrous acid (HONO) reservoir at the ground surface in Bakersfield, CA, during CalNex 2010, J. Geophys. Res.-Atmos., 119, 9093–9106, 2014.

VandenBoer, T. C., Young, C. J., Talukdar, R. K., Markovic, M. Z., Brown, S. S., Roberts, J. M., and Murphy, J. G.: Nocturnal loss and daytime source of nitrous acid through reactive uptake and displacement, Nat. Geosci., 8, 55–60, 2015.

Villena, G., Kleffmann, J., Kurtenbach, R., Wiesen, P., Lissi, E., Rubio, M. A., Croxatto, G., and Rappenglueck, B.: Vertical gradients of HONO, NO_x and O-3 in Santiago de Chile, Atmos. Environ., 45, 3867–3873, 2011.

Vogel, B., Vogel, H., Kleffmann, J., and Kurtenbach, R.: Measured and simulated vertical profiles of nitrous acid – Part II. Model simulations and indications for a photolytic source, Atmos. Environ., 37, 2957–2966, 2003.

Wang, L., Wang, W., and Ge, M.: Heterogeneous uptake of NO_2 on soils under variable temperature and relative humidity conditions, J. Environ. Sci., 24, 1759–1766, 2012.

Wang, S. H., Ackermann, R., Spicer, C. W., Fast, J. D., Schmeling, M., and Stutz, J.: Atmospheric observations of enhanced NO_2-HONO conversion on mineral dust particles, Geophys. Res. Lett., 30, 1595, doi:10.1029/2003gl017014, 2003.

Weber, B., Wu, D., Tamm, A., Ruckteschler, N., Rodriguez-Caballero, E., Steinkamp, J., Meusel, H., Elbert, W., Behrendt, T., Soergel, M., Cheng, Y., Crutzen, P. J., Su, H., and Pöschl, U.: Biological soil crusts accelerate the nitrogen cycle through large NO and HONO emissions in drylands, P. Natl. Acad. Sci. USA, 112, 15384–15389, 2015.

Wentzell, J. J. B., Schiller, C. L., and Harris, G. W.: Measurements of HONO during BAQS-Met, Atmos. Chem. Phys., 10, 12285–12293, doi:10.5194/acp-10-12285-2010, 2010.

Wong, K. W., Tsai, C., Lefer, B., Haman, C., Grossberg, N., Brune, W. H., Ren, X., Luke, W., and Stutz, J.: Daytime HONO vertical gradients during SHARP 2009 in Houston, TX, Atmos. Chem. Phys., 12, 635–652, doi:10.5194/acp-12-635-2012, 2012.

Wong, K. W., Tsai, C., Lefer, B., Grossberg, N., and Stutz, J.: Modeling of daytime HONO vertical gradients during SHARP 2009, Atmos. Chem. Phys., 13, 3587–3601, doi:10.5194/acp-13-3587-2013, 2013.

Yabushita, A., Enami, S., Sakamoto, Y., Kawasaki, M., Hoffmann, M. R., and Colussi, A. J.: Anion-Catalyzed Dissolution of NO_2 on Aqueous Microdroplets, J. Phys. Chem. A, 113, 4844–4848, 2009.

Yang, Q., Su, H., Li, X., Cheng, Y., Lu, K., Cheng, P., Gu, J., Guo, S., Hu, M., Zeng, L., Zhu, T., and Zhang, Y.: Daytime HONO formation in the suburban area of the megacity Beijing, China, Sci. China Chem., 57, 1032–1042, 2014.

Ye, C., Zhou, X., Pu, D., Stutz, J., Festa, J., Spolaor, M., Tsai, C., Cantrell, C., Mauldin, R. L., Campos, T., Weinheimer, A., Hornbrook, R. S., Apel, E. C., Guenther, A., Kaser, L., Yuan, B., Karl, T., Haggerty, J., Hall, S., Ullmann, K., Smith, J. N., Ortega, J., and Knote, C.: Rapid cycling of reactive nitrogen in the marine boundary layer, Nature, 532, 489–491, 2016.

Young, C. J., Washenfelder, R. A., Roberts, J. M., Mielke, L. H., Osthoff, H. D., Tsai, C., Pikelnaya, O., Stutz, J., Veres, P. R., Cochran, A. K., VandenBoer, T. C., Flynn, J., Grossberg, N., Haman, C. L., Lefer, B., Stark, H., Graus, M., de Gouw, J., Gilman, J. B., Kuster, W. C., and Brown, S. S.: Vertically Resolved Measurements of Nighttime Radical Reservoirs; in Los Angeles and Their Contribution to the Urban Radical Budget, Environ. Sci. Technol., 46, 10965–10973, 2012.

Zhang, N., Zhou, X. L., Shepson, P. B., Gao, H. L., Alaghmand, M., and Stirm, B.: Aircraft measurement of HONO vertical profiles over a forested region, Geophys. Res. Lett., 36, L15820, doi:10.1029/2009gl038999, 2009.

Zhou, X. L., Beine, H. J., Honrath, R. E., Fuentes, J. D., Simpson, W., Shepson, P. B., and Bottenheim, J. W.: Snowpack photochemical production of HONO: a major source of OH in the Arctic boundary layer in springtime, Geophys. Res. Lett., 28, 4087–4090, 2001.

Zhou, X. L., Civerolo, K., Dai, H. P., Huang, G., Schwab, J., and Demerjian, K.: Summertime nitrous acid chemistry in the atmospheric boundary layer at a rural site in New York State, J. Geophys. Res.-Atmos., 107, 4590, doi:10.1029/2001jd001539, 2002a.

Zhou, X. L., He, Y., Huang, G., Thornberry, T. D., Carroll, M. A., and Bertman, S. B.: Photochemical production of nitrous acid on glass sample manifold surface, Geophys. Res. Lett., 29, 26-1–26-4, doi:10.1029/2002gl015080, 2002b.

Zhou, X. L., Gao, H. L., He, Y., Huang, G., Bertman, S. B., Civerolo, K., and Schwab, J.: Nitric acid photolysis on surfaces in low-NO_x environments: Significant atmospheric implications, Geophys. Res. Lett., 30, 2217, doi:10.1029/2003gl018620, 2003.

Zhou, X., Huang, G., Civerolo, K., Roychowdhury, U., and Demerjian, K. L.: Summertime observations of HONO, HCHO, and O_3 at the summit of Whiteface Mountain, New York, J. Geophys. Res.-Atmos., 112, D08311, doi:10.1029/2006jd007256, 2007.

Zhou, X., Zhang, N., TerAvest, M., Tang, D., Hou, J., Bertman, S., Alaghmand, M., Shepson, P. B., Carroll, M. A., Griffith, S., Dusanter, S., and Stevens, P. S.: Nitric acid photolysis on forest canopy surface as a source for tropospheric nitrous acid, Nat. Geosci., 4, 440–443, 2011.

Zhou, Y., Rosen, E. P., Zhang, H., Rattanavaraha, W., Wang, W., and Kamens, R. M.: SO_2 oxidation and nucleation studies at near-atmospheric conditions in outdoor smog chamber, Environ. Chem., 10, 210–220, 2013.

Supplement of Atmos. Chem. Phys., 16, 14475–14493, 2016
http://www.atmos-chem-phys.net/16/14475/2016/
doi:10.5194/acp-16-14475-2016-supplement

Atmospheric Chemistry and Physics Open Access EGU

Supplement of

Daytime formation of nitrous acid at a coastal remote site in Cyprus indicating a common ground source of atmospheric HONO and NO

Hannah Meusel et al.

Correspondence to: Hang Su (h.su@mpic.de)

Fig. S1: Fires (red dots) detected during the whole measurement campaign from 7.7.2014 to 3.8.2014 (NASA FIRMS Web fire mapper).

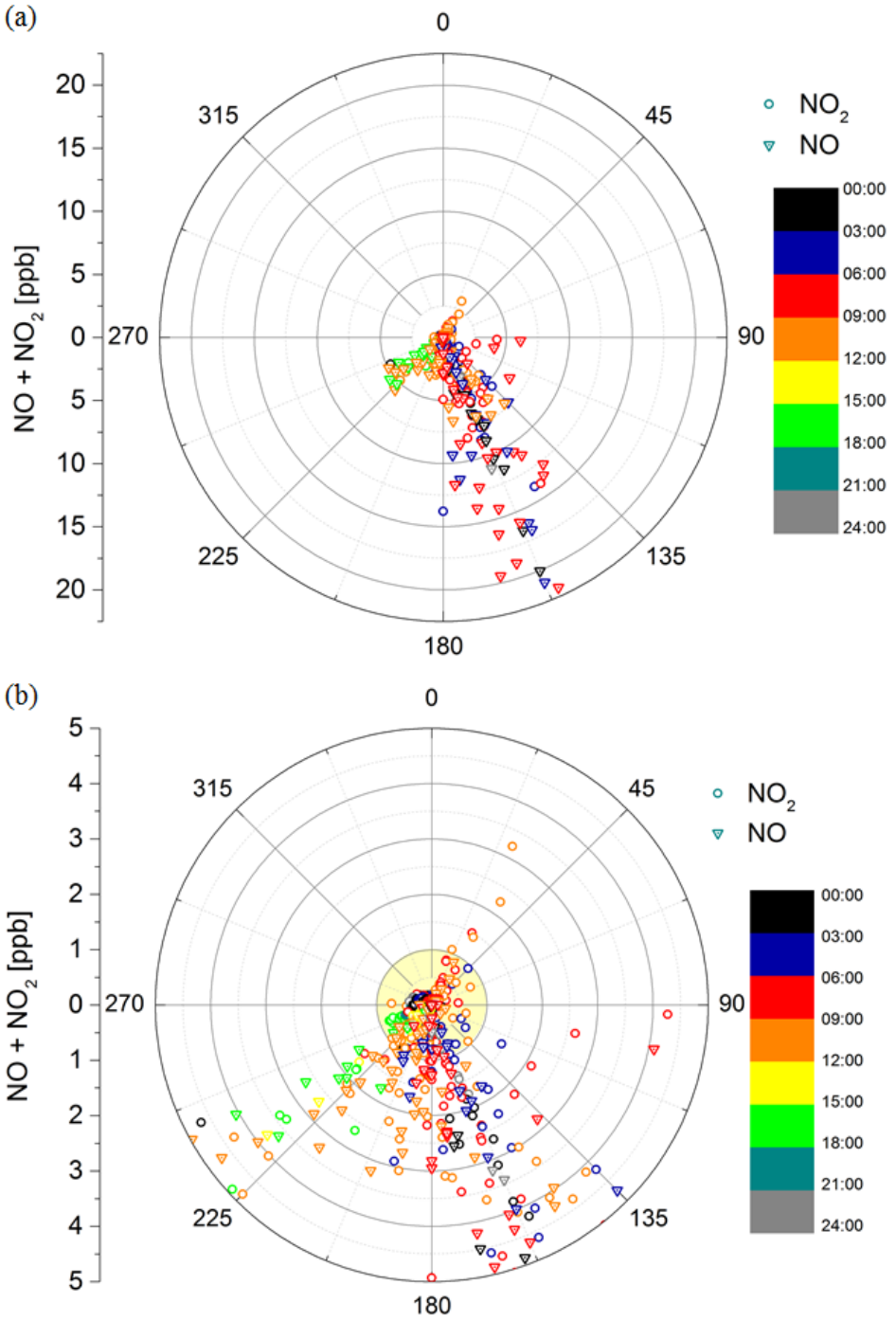

Fig. S2: NOx concentrations in dependence of wind direction and time of day (a) all data, except 5 data points which were between 25 and 50 ppb and b) zoom in to maximum 5 ppb): Strong morning peaks in NO and NO_2 correlate with wind, coming from SSE (Diesel generator), in the afternoon there were also some higher NOx concentrations which correlate with SW-winds (probably indicating some construction or military cars close to the measurement) or NNE to E (street to the base); these high concentrations were not included in further calculations! Only concentrations up to 1 ppb (for NO_2, pale yellow area) and up to 0.5 ppb (for NO) are considered.

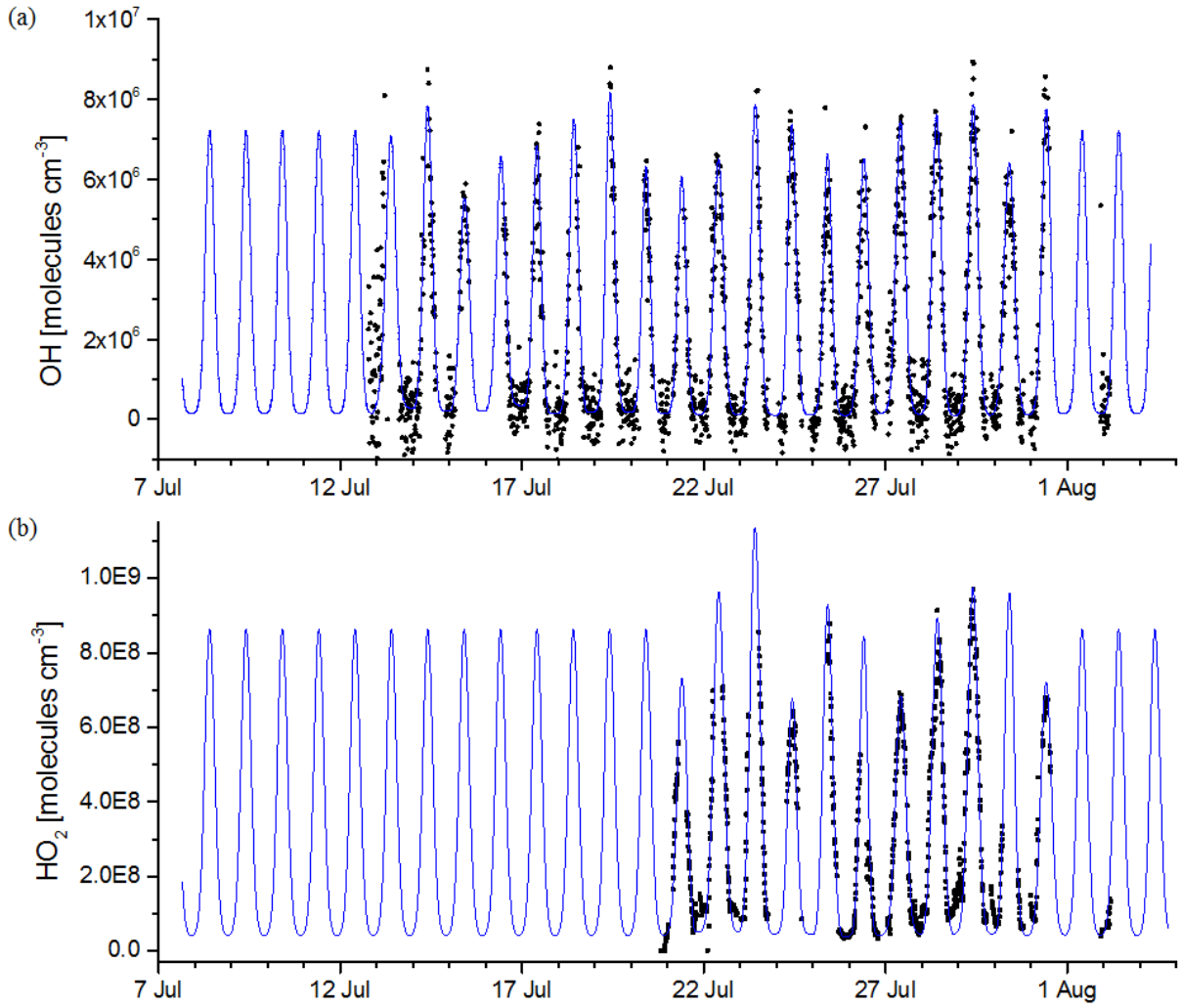

Fig. S3: timeline of OH and HO_2 concentration, black dots indicate real measurement data, blue line is the daily Gauss fit through measurement dots or the average of Gauss fit for those days when no data were available, respectively.

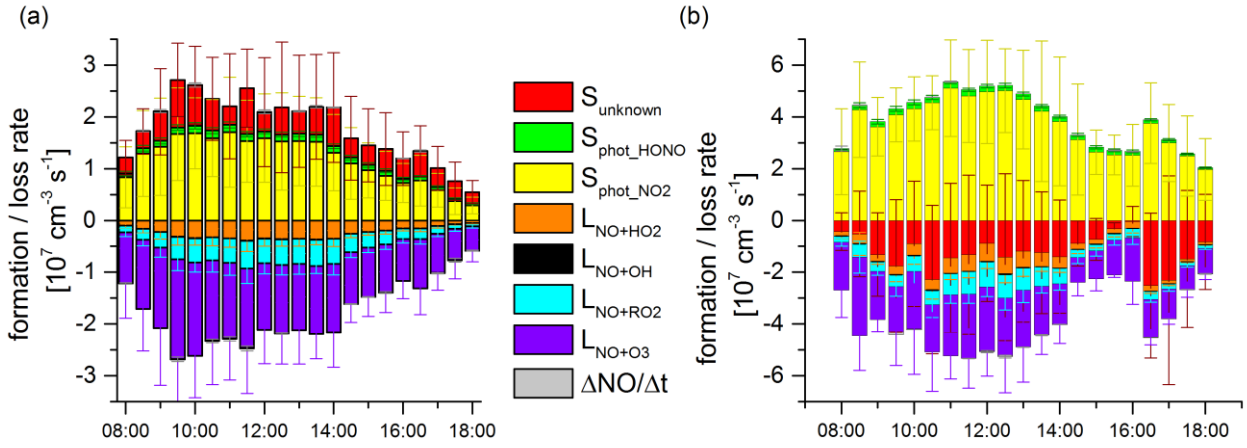

Fig. S4: Contributions of production and loss terms as well as the unknown daytime NO source $S_{unknown}$ for the a) wet and b) dry period. The photolysis of NO_2 has the highest contribution to the NO budget. In the wet period the unknown source of NO is about 40-80% of the photolysis of NO_2. During the dry period there is an unknown sink. The main loss terms are the reaction with O_3 followed by the reaction with RO_2 and HO_2. Error bars indicate standard deviation.

B.2 Meusel et al., ACPD 2017a

Emission of nitrous acid from soil and biological soil crusts represents a dominant source of HONO in the remote atmosphere in Cyprus

Hannah Meusel[1], Alexandra Tamm[1], Uwe Kuhn[1], Dianming Wu[1], Anna Lena Leifke[1], Sabine Fiedler[2], Nina Ruckteschler[1], Petya Yordanova[1], Naama Lang-Yona[1], Jos Lelieveld[3,4], Thorsten Hoffmann[5], Ulrich Pöschl[1], Hang Su[1,6], Bettina Weber[1], Yafang Cheng[1,6]

[1]Max Planck Institute for Chemistry, Multiphase Chemistry Department, Mainz, Germany
[2]Johannes Gutenberg University, Institute for Geography, Mainz, Germany
[3]Max Planck Institute for Chemistry, Atmospheric Chemistry Department, Mainz, Germany
[4]The Cyprus Institute, Nicosia, Cyprus
[5]Johannes Gutenberg University, Institute for Inorganic and Analytical Chemistry, Mainz, Germany
[6]Institute for Environmental and Climate Research, Jinan University, Guangzhou, China

Atmospheric Chemistry and Physics Discussion, 2017, 1-21, (2017a)
DOI: 10.5194/acp-2017-356

Author contributions:

HM, BW, YC designed the research.
HM, AT, DW performed the study.
ALL, SF, PY, NLY, NR provided relevant data.
HM, AT, BW, YC, UK, HS, UPö, TH discussed the results.
HM, AT, UK, BW, HS, JL wrote the paper.

Atmos. Chem. Phys. Discuss., doi:10.5194/acp-2017-356, 2017
Manuscript under review for journal Atmos. Chem. Phys.
Discussion started: 2 May 2017

Atmospheric Chemistry and Physics Discussions

Emission of nitrous acid from soil and biological soil crusts represents a dominant source of HONO in the remote atmosphere in Cyprus

Hannah Meusel[1], Alexandra Tamm[1], Uwe Kuhn[1], Dianming Wu[1], Anna Lena Leifke[1], Sabine Fiedler[2], Nina Ruckteschler[1], Petya Yordanova[1], Naama Lang-Yona[1], Jos Lelieveld[3,4], Thorsten Hoffmann[5], Ulrich Pöschl[1], Hang Su[1,6], Bettina Weber[1], Yafang Cheng[1,6]

[1]Max Planck Institute for Chemistry, Multiphase Chemistry Department, Mainz, Germany
[2]Johannes Gutenberg University, Institute for Geography, Mainz, Germany
[3]Max Planck Institute for Chemistry, Atmospheric Chemistry Department, Mainz, Germany
[4]The Cyprus Institute, Nicosia, Cyprus
[5]Johannes Gutenberg University, Institute for Inorganic and Analytical Chemistry, Mainz, Germany
[6]Institute for Environmental and Climate Research, Jinan University, Guangzhou, China

Corresponding author: Yafang Cheng (yafang.cheng@mpic.de) and Bettina Weber (b.weber@mpic.de)

Abstract. Soil and biological soil crusts can emit nitrous acid (HONO) and nitric oxide (NO). The terrestrial ground surface in arid and semi-arid regions is anticipated to play an important role in the local atmospheric HONO budget, deemed to represent one of the unaccounted HONO sources frequently observed in field studies. In this study HONO and NO emissions from a representative variety of soil and biological soil crust samples from the Mediterranean island Cyprus were investigated under controlled laboratory conditions. A wide range of fluxes was observed, ranging from 0.6 to 264 ng m^{-2} s^{-1} HONO-N at optimal soil water content (20-30% of water holding capacity, WHC). Maximum NO-N at this WHC fluxes were lower (0.8-121 ng m^{-2} s^{-1}). Highest emissions of both reactive nitrogen species were found from bare soil, followed by light and dark cyanobacteria-dominated biological soil crusts (biocrusts), correlating well with the sample nutrient levels (nitrite and nitrate). Extrapolations of lab-based HONO emission studies agree well with the unaccounted HONO source derived previously for the extensive CYPHEX field campaign, i.e., emissions from soil and biocrusts may essentially close the Cyprus HONO budget.

1 Introduction

Nitrous acid (HONO) plays an important role in tropospheric chemistry, as it is one of the major precursors of the hydroxyl (OH) radical which determines the oxidizing capacity of the atmosphere. In the early morning, HONO photolysis has been shown to contribute up to 30% to the local OH budget (Alicke et al., 2002; Kleffmann et al., 2005; Ren et al., 2003 and 2006; Meusel et al., 2016). Currently, the HONO formation processes, especially during daytime, are still not fully understood. Recent ground based field measurements showed unexpected high daytime concentrations of HONO, which could not be explained by atmospheric gas phase reactions (R1-R3) only (Kleffmann et al., 2003 and 2005; Su et al., 2008a; Soergel et al., 2011a; Su et al., 2011; Michoud et al., 2014; Czader et al., 2012; Wong et al., 2013; Tang et al., 2015; Oswald et al., 2015, Meusel et al., 2016).

$$OH + NO \rightarrow HONO \quad (R1)$$

$$HONO \xrightarrow{h\nu\,(300-405\ nm)} OH + NO \quad (R2)$$

Atmos. Chem. Phys. Discuss., doi:10.5194/acp-2017-356, 2017
Manuscript under review for journal Atmos. Chem. Phys.
Discussion started: 2 May 2017

Atmospheric Chemistry and Physics Discussions

$$HONO + OH \rightarrow NO_2 + H_2O \quad \text{(R3)}$$

Several studies have shown that HONO can be heterogeneously formed from NO_2 on a variety of surfaces, e.g., soot, humic acid, minerals, proteins and organically coated particles (Ammann et al., 1998; Arens et al., 2001; Aubin et al., 2007; Bröske et al., 2003; Han et al., 2013; Kalberer et al., 1999; Kleffmann et al., 1999; Kleffmann and Wiesen, 2005; Lelievre et al., 2004; Kinugawa et al., 2011; Liu et al., 2015; Wang et al., 2003; Yabushita et al., 2009; Meusel et al., 2017). Light can activate some of these surfaces (humic acid, proteins and other organic compounds, titanium dioxide, soot), which enhances NO_2 uptake and HONO production (George et al., 2005; Langridge et al., 2009; Monge et al., 2010; Ndour et al., 2008; Ramazan et al., 2004; Stemmler et al., 2007; Kebede et al., 2013; Meusel et al., 2017). But NO_2 uptake coefficients and the ambient aerosol surface areas for heterogeneous reactions of NO_2 were nevertheless frequently found to be too low to account for the observed HONO production rates (Stemmler et al., 2007; Sarwar et al., 2008; Zhang et al., 2016). Besides the heterogeneous NO_2 reaction, Bejan et al. (2006) observed HONO formation during irradiation of nitrophenols. Photolysis of nitrate or nitric acid generates HONO as well (Baergen and Donaldson, 2013; Scharko et al., 2014; Zhou et al., 2003, 2011). Contrary to the detected missing HONO source near the ground, recent airborne measurements (500 – 1200 m above ground level) observed HONO concentrations, which could be explained by gas phase reactions only (Li et al., 2014; Neuman et al., 2016). However, vertical gradient studies show higher HONO concentrations near the ground than in higher altitudes indicating a ground level source (Harrison and Kitto, 1994; Kleffmann et al., 2003; Ren et al., 2011; Stutz et al., 2002; VandenBoer et al., 2013; Villena et al., 2011; Zhou et al., 2011; Wong et al., 2012 and 2013; Vogel et al., 2003; Zhang et al., 2009; Young et al., 2012). This is supported by gas exchange studies showing that HONO and NO can be emitted from (natural) soil and biological soil crusts (biocrusts, BSC), even without applying atmospheric NO_2 (Su et al., 2011; Oswald et al., 2013; Mamtimin et al., 2016; Weber et al., 2015; Meixner and Yang, 2006). HONO and NO can be formed during biological processes (nitrification and denitrification; Pilegaard, 2013), in which NH_3 or NH_4^+ is oxidized stepwise or NO_3^- is reduced (Fig. 1). Depending on soil-pH and according to Henry´s law soil nitrite (NO_2^-) can be converted into gaseous HONO.

Biocrusts grow within the uppermost millimeters to centimeters of soil in arid and semi-arid ecosystems. They are composed of photoautotrophic cyanobacteria, algae, lichens, and bryophytes, growing together with heterotrophic bacteria, fungi and archaea in varying proportions (Belnap et al., 2016). Depending on the dominating photoautotrophs, cyanobacteria-dominated biocrusts with an initial thin light-colored and a well-developed dark type, cyanolichen- and chlorolichen-dominated biocrusts with lichens comprising cyanobacteria or green algae as photobionts, and bryophyte-dominated biocrusts are distinguished (Büdel et al., 2009). Many free living cyanobacteria but also those in symbiosis with fungi (forming lichens) and vascular plants can fix atmospheric nitrogen N_2 and convert it into ammonia (Cleveland et al., 1999; Belnap 2002; Herridge et al., 2008; Barger et al., 2016). Globally it is estimated that 100-290 Tg (N) yr^{-1} is fixed biologically (Cleveland et al., 1999), of which 49 Tg yr^{-1} (17-49%) is fixed by cryptogamic covers, which comprise biocrusts, but also other microbially dominated biomes, like lichen and bryophyte communities occurring on soil, rocks and plants in boreal and tropical regions (Elbert et al., 2012). Studies hav suggested, that nitrogen cycling in soil (N_2 fixation, nitrification, denitrification) and hence reactive nitrogen emission (NO, N_2O, HONO) is often enhanced by well-established biocrusts, especially

by dark cyanobacteria (Cleveland et al., 1999; Elbert et al., 2012; Belnap, 2002; Barger et al., 2013; Johnson et al., 2005; Abed et al., 2013; Strauss et al., 2012; Weber et al., 2015).

In Cyprus, an island in the semi-arid eastern Mediterranean area, biocrusts are ubiquitously covering ground surfaces and hence can be anticipated to play an important role in the local HONO budget. In the CYPHEX campaign 2014 (CYprus PHotochemical EXperiment) the observed diel cycles of HONO ambient air concentrations revealed strong unaccounted sources of HONO and NO, being well correlated with each other (Meusel et al., 2016). With low NO_2 concentrations and high $HONO/NO_x$ ratios, respectively, direct emissions from combustion and heterogeneous reactions of NO_2 could be excluded as significant HONO sources, leaving emissions from soil and the respective surface cover to be the most plausible common source for both nitrogen species (Meusel et al., 2016).

In the present study we measured HONO and NO fluxes from soil and biocrust samples from Cyprus by means of a dynamic chamber system. The aim of this study was to characterize and quantify direct trace gas emissions and demonstrate their impact on the atmospheric chemistry in the remote coastal environment of Cyprus.

2 Methods

2.1 Sampling

Bare soil and biocrust samples were collected on 27th April 2016 on the South/South-East side of the military station in Ineia, Cyprus (34.9638°N, 32.3778°E), where the CYPHEX campaign took place in 2014. It is a rural site about 600 m above sea level, approximately 5-8 km from the coast and is surrounded by typical Mediterranean vegetation (olive and pine trees, small shrubs like *Pistacia lentiscus, Sacopoterium spinosum* and *Inula viscosa).* More details about the site can be found in Meusel et al. (2016).

In an area of about 8580 m² (South/South-East direction of the station) 50 grids (25x25 cm) were placed at randomly selected spots for systematic ground cover assessment. At each grid point occurrence of nine types of surface cover (i.e., light and dark cyanobacteria-, chlorolichen-, cyanolichen-, and moss-dominated biocrust, bare soil, stone, litter, vascular vegetation/shrub) were assigned and quantified. Spatially independent replicate samples were collected of light cyanobacteria-dominated biocrusts (light BSC), dark cyanobacteria-dominated biocrusts with cyanolichens (dark BSC), chlorolichen-dominated biocrusts (chlorolichen BSC I, chlorolichen BSC II), moss-dominated biocrusts (moss BSC) and of bare soil (Fig. S1 of the supplement). Each sample was collected in a plastic petri dish, sealed and stored in the dark at room temperature until further analysis (storage time less than 15 weeks).

In total 43 samples were collected (Table 1) of which 18 samples, i.e., 3 replicates of each HONO emitting surface cover type were used direct (upfront) for nutrient analysis, while all others were first used for trace gas exchange measurements, prior to nutrient and chlorophyll content analysis.

2.2 Meteorological data

During CYPHEX the meteorological parameters were even measured at about 5 m above ground, considered not representative for the micro-habitat of the soil ground surface. Hence we placed three humidity (and temperature) sensors (HOBO Pro v2) just on top of the soil surface about 4 weeks prior to sample collection. Reference meteorological data (air temperature, humidity and precipitation) from Paphos airport (about 20 km south of the

sample area, 12 m asl) and Prodromos (about 40 km east of the sampling area, 1380 m asl) during the sampling period as well as the precipitation data from the last 4 years (2013-2016) were provided by the Department of Meteorology, Cyprus (http://www.moa.gov.cy/moa/ms/ms.nsf/DMLmeteo_reports_en/MLmeteo_reports_en?opendocument; last access: Dec. 2016).

2.3 Soil characteristics: nutrient, chlorophyll and pH

Soil characteristics (nutrient, pH) have an effect on soil emission, e.g., higher nutrient level and lower pH would enhance emission according to Henry law (Su et al., 2011). Nutrient analysis was conducted on samples without gas exchange measurements (n = 3) and on replicate samples after gas exchange measurements in order to analyze potential effects of the applied 'wetting-drying' cycle. Nitrate (NO_3^-), nitrite (NO_2^-) and ammonium (NH_4^+) were analyzed via flow injection analysis with photometric detection (FIAstar 5000, Foss, Denmark). Prior to that, the samples comprised of soil and its biocrust-cover were gently ground and an aliquot of 7 g was solved in 28 mL of 0.0125 M $CaCl_2$. After shaking for 1 hour the mixture was filtered on a N-free filter.

Chlorophyll analysis, as an indicator of biomass of photo-autotrophic organisms, was done according to the dimethyl sulfoxide (DMSO) method (Ronen and Galun, 1984). Ground samples were extracted twice with $CaCO_3$ saturated DMSO (20 mL, 10 mL) at 65°C for 90 min. Both extracts were combined and centrifuged (3000 G) at 15°C for 10 min. The light absorption at 648, 665 and 700 nm was detected with a spectral photometer (Lambda 25 UV/VIS Spectrometer, Perkin Elmer, Rodgau). The amount of chlorophyll a (Chl_a) was calculated according to Arnon et al. (1974). Chlorophyll a+b (Chl_{a+b}) content was calculated according to Lange, Bilger and Pfanz (pers. comm. in Weber et al., 2013):

$$Chl_{a+b}[\mu g] = \left(20.2 \cdot (E_{648} - E_{700}) + 8.02 \cdot (E_{665} - E_{700})\right) \cdot a \quad \text{(eq.1)}$$

$$Chl_a[\mu g] = \left(12.19 \cdot (E_{665} - E_{700})\right) \cdot a \quad \text{(eq.2)}$$

where $Chl_{a+b}[\mu g]$, $Chl_a[\mu g]$ is the chlorophyll content of the sample, E_{648}, E_{665}, E_{700} are light absorption at the given wavelength, and a is the amount of DMSO used in mL.

The pH was determined for each surface cover type (n = 3-4) according to Weber et al. (2015, Suppl.). Here, 1.5 g of the ground sample was mixed with 3.75 mL of pure water and shaken for 15 min. Then the slurry was centrifuged (3000 G, 5 min) to separate the solid phase from the liquid solution. The latter was used for pH determination by means of a pH electrode (Inlab Export Pro-ISM, Mettler Toledo).

2.4 Trace gas exchange measurements

The dynamic chamber method for analyzing NO and HONO emissions from soil samples was already introduced before (Oswald et al., 2013; Weber et al., 2015; Wu et al., 2014). Soil and biocrust samples (25-35 g) were wetted with 8-13 g of pure water (18.2 MΩ) up to water holding capacity and placed into a dynamic Teflon film chamber (≈47 L) flushed with 8 L min^{-1} dry pure air (PAG 03, Ecophysics, Switzerland). Typical drying cycles lasted between 6 and 8 hours. A Teflon coated internal fan ensured complete mixing of the chamber headspace volume. During the experiments the chamber was kept at constant temperature (25°C, the mean daytime air temperature during CYPHEX) and in darkness to avoid photochemical reactions. At the chamber outlet the emitted gases HONO, NO

Atmos. Chem. Phys. Discuss., doi:10.5194/acp-2017-356, 2017
Manuscript under review for journal Atmos. Chem. Phys.
Discussion started: 2 May 2017

Atmospheric Chemistry and Physics Discussions

and water vapor were quantified. HONO was analyzed with a commercial long path absorption photometer (LOPAP, QUMA GmbH; Wuppertal, Germany), with a detection limit of ~4 ppt and 10% uncertainty (based on the uncertainties of liquid and gas flow, concentration of calibration standard and regression of calibration). To avoid any transformation of HONO in the tubing, the sampling unit including the stripping coil from LOPAP was directly connected to the chamber. NO_x ($NO + NO_2$) was detected with a commercial chemiluminescence detector (42i TL, Thermo Scientific; Watham, USA) modified with a photolytic converter with a detection limit of ~50 ppt (NO) and ~200 ppt (NO_2). An infrared CO_2 and H_2O analyzer (Li-840A, LICOR; Lincoln, USA) was used to log the drying and to calculate the soil water content (SWC) of the samples as follows:

$$SWC(WHC) = \frac{m_{H2O,t=n}}{m_{H2O,0}} * 100 \quad \text{(eq. 3)}$$

$$m_{H2O,t=n} = m_{H2O,t=n-1} - \frac{S_{Licor,t=n}}{\sum_{t=0}^{t=N} S_{Licor}} * m_{H2O,0} \quad \text{(eq. 4)}$$

with t=0 denoting the measurement start (wetted sample inserted into chamber), t=n: any time between 0 and N, t=N: time when sample had dried out and measurement was stopped, S_{Licor}: absolute H_2O signal at a given time, $m_{H2O,0}$: mass of water added to sample (water holding capacity, WHC), SWC: soil water content in % WHC.

2.5 Data analysis

Measured data of NO_2^-, NO_3^-, NH_4^+, Chl_{a+b}, Chl_a, NO and HONO optimum flux and NO and HONO integrated flux did not follow a normal distribution. Rather, log-transformed data were normally distributed (Shapiro-Wilk) and therefore used for statistical analysis (Pearson correlation, ANOVA including Tukey Test with significance level of $p = 0.05$) executed with OriginPro (version 9.0; OriginLab coporation, Northampton, Massachusetts, USA).

Precipitation data from the last 4 years (2013-2016) provided by the Department of Meteorology of Cyprus indicate about 30 rain events per year (precipitation > 1 mm with following one or more dry days) were used to estimate annual emissions of total nitrogen by way of HONO and NO.

3 Results and discussion

3.1 Meteorological conditions

One month before sampling, three sensors measuring temperature and relative humidity directly above the soil surface were installed in the field to represent the micro-climate of the ground surface. Reference air temperature, humidity and precipitation measurements at Paphos airport and Prodromos showed one rain event on 11-12 April which is reflected by higher soil humidity (80-100%) and lower temperatures on these days (see Fig. 2). As a consequence, the biological soil crusts were activated and went through one full wetting and drying cycle before sample collection. Temperature above the soil ranged from 10°C in the night to 50°C during the day when solar radiation was most intense. Air temperature was similar during the night but not as hot during the day ranging between 20° and 30°C. Humidity above the ground was low during daytime (<30% rH) and increased during the night up to 80%, while the atmospheric relative humidity (at Paphos airport) ranged between 47 and 73% (without rain event). Thus there were only little variations of humidity with height above the soil surface. Above the ground surface the relative humidity was somewhat lower during the day (mainly caused by higher temperatures) but

somewhat higher during the night, compared to respective weather station data. During and shortly after the main rain event humidity at ground level was higher (80 and 100% rH) compared to ambient air humidity (70-85% rH). Ambient air temperatures were somewhat lower during sample collection of this study as compared to the CYPHEX field campaign in 2014. During CYPHEX, nighttime temperatures (3 m above ground level) did not drop below 18°C. Relative humidity (3 m above ground level) was mostly between 70 and 100% with only two short periods with humidity between 20-60% rH. Hence we can assume that soil surface temperatures were higher and ground rH in the same range during CYPHEX compared to sampling period.

3.2 Cyprus soil and biocrust characteristics

Systematic mapping of surface covers revealed that moss-dominated biocrusts are the most frequent in the investigated Cyprus field site area (21.3%), followed by light (10.4%) and dark BSC (6.5%), whereas chlorolichen- (3.2%) and cyanolichen-dominated BSC (1.8%) only played a minor role (Fig. 3, Fig. S1). The soil surface was partially covered by litter (26.3%), stones (19.5%) and vascular vegetation (8.5%), whereas open soil was rarely found (2.5%). It was previously established that soil and biocrusts emit HONO and NO (Weber et al., 2015; Oswald et al., 2013), jointly accounting for 45.6% of surface area in our studied region. To the best of our knowledge, no data on reactive nitrogen emissions from vascular vegetation and plant litter have been published yet.

Nutrient analysis revealed large variations in concentrations of nitrogen species ranging from 0 to 6.48, 0 to 0.57 and 0 to 22.2 mg (N) kg^{-1} of dry soil/crust mass for NO_3^-, NO_2^-, and NH_4^+, respectively (Fig. 4a, Tab. S1 of the supplement). In general, no significant change in reactive nitrogen contents was found before and after the trace gas exchange experiments (Fig. 4a), indicating no significant impact of one wetting-drying cycle on the nutrient content. Bare soil samples had significantly higher levels of NO_3^- and NO_2^- content compared to dark, chlorolichen and moss BSC. Among the latter three, no significant differences in nutrient levels were observed. Light BSC had NO_2^- contents similar to bare soil. The NH_4^+ content was very similar in all samples, except for one outlier in the group of light BSC with strongly elevated NH_4^+. Higher nitrate and ammonium levels in bare soil compared to crust-covered samples were also reported recently for a warm desert site in South Africa (Weber et al., 2015), indicative of nutrient consumption/integration by the biocrusts. Nitrite, on the other hand, was lower for bare soil samples compared to biocrust samples. While NO_3^- was slightly higher, NH_4^+ and NO_2^- contents (especially of bare soil samples) were lower in the South African arid ecosystem compared to Cyprus.

Chlorophyll was only determined in the samples used for flux measurements. Chl_a ranged from 4.1 (bare soil) to 144.2 mg m^{-2} (moss BSC) and Chl_{a+b} from 9.3 (bare soil) to 211.3 mg m^{-2} (moss BSC), respectively (Fig. 4b, Tab. S1). From bare soil, via light BSC and chlorolichen BSC II, to dark BSC the chlorophyll content increased, but not significantly ($p > 0.2$). Nevertheless, Chl_a and Chl_{a+b} contents of chlorolichen BSC I and moss BSC were significantly higher than these of bare soil, light BSC and chlorolichen BSC II ($p<0.05$, Fig. 4b).. The range of chlorophyll contents is comparable to previous arid ecosystem studies (Weber et al., 2015).

The pH of soil and biocrusts ranged between slightly acidic (6.2) and slightly alkaline (7.6; Fig. 4c). The mean pH of 17 samples was 7.0, i.e., neutral. Only the pH of moss BSC samples was significantly lower than that of bare soil, light BSC and chlorolichen BSC samples ($p=0.05$). Soil and biocrust samples from South Africa were slightly more alkaline (7.1-8.2) with no significant difference among biocrust types (Weber et al., 2015).

Atmos. Chem. Phys. Discuss., doi:10.5194/acp-2017-356, 2017
Manuscript under review for journal Atmos. Chem. Phys.
Discussion started: 2 May 2017

Atmospheric Chemistry and Physics Discussions

3.3 NO and HONO flux measurements

All samples showed HONO and NO emissions during full wetting and drying cycles. Maximum emission rates of HONO were observed at about 17-33% WHC, and of NO at 20-36% with no significant differences between all soil cover types (Fig 5). Emissions declined to zero at 0% WHC and to very small rates >70%. Emission maxima strongly varied between soil cover types, but also between samples of the same cover type (see Fig. 5 and 6, and Table S1). Highest emissions of both HONO-N and NO-N were detected for bare soil (175 ± 87.3 and 92.2 ± 34.7 ng m^{-2} s^{-1}), followed by light (48.6 ± 48.5 and 34.5 ± 42.1 ng m^{-2} s^{-1}) and dark BSC (27.1 ± 35.9 and 16.7 ± 18.3 ng m^{-2} s^{-1}). Both types of chlorolichen- and moss-dominated biocrusts showed very low emission rates of reactive nitrogen (on average < 10 ng m^{-2} s^{-1}). Maximum HONO emissions were somewhat higher than maximum NO emissions, especially for bare soil. Integrating full wetting and drying cycles (6-8 hours), 0.04-1.9 mg m^{-2} HONO-N and 0.06-1.6 mg m^{-2} NO-N were released (Fig. 6, lower panel). While the maximum fluxes of reactive nitrogen emission were higher for HONO than NO, especially from bare soil, the integrated emissions were similar or even larger for NO, which is released over a wider range of SWC.

In general, it is difficult to compare chamber flux measurements of different studies due to different experimental configurations, such as chamber dimension, flow rate, resident time and drying rate etc. Here, we compare our results to studies which applied the same method (with the same or very similar conditions). The emission rates are consistent with these studies where HONO-N or NO-N emissions from soil between 1-3000 ng m^{-2} s^{-1} were found (Su et al., 2011; Oswald et al., 2013; Mamtimin et al., 2016; Wu et al., 2014; Weber et al., 2015). Mamtimin et al. (2016) observed NO-N fluxes at 25°C of 57.5 ng m^{-2} s^{-1}, 18.9 ng m^{-2} s^{-1} and 4.1 ng m^{-2} s^{-1} for soil of grape and cotton fields and desert soil from an oasis in China, respectively. Oswald et al. (2013) found HONO-N and NO-N emissions between 2 and 280 ng m^{-2} s^{-1} (each) from different soil from all over the world covering a wide range of pH, nutrient content and organic matter. Biogenic NO emissions of 44 soil samples from arid and semi-arid regions were reviewed by Meixner and Yang (2006) with N-fluxes ranging from 0 to 142 ng m^{-2} s^{-1}.

In contrast to the results of the present study, where bare soil showed highest emissions, Weber et al. (2015) found lowest emission from bare soil in samples from South Africa. In that study, dark cyanobacteria-dominated biocrusts revealed highest emission rates (each HONO-N and NO-N up to 200 ng m^{-2} s^{-1}), followed by light cyanobacteria-dominated biocrusts (up to 120 ng m^{-2} s^{-1}), whereas in the present study, emissions of dark cyanobacteria-dominated biocrusts tended to be lower. No significant difference of HONO-N and NO-N emissions from light BSC between both sample origins were found. HONO-N and NO-N emissions of moss- and chlorolichen-dominated biocrusts were low in both studies (each <60 ng m^{-2} s^{-1}) but still significantly higher for samples from South Africa than from Cyprus. In the present study HONO maximum emissions were higher than for NO (while integrated emissions being comparable) while in the study of Weber et al. (2015) HONO maximum fluxes were somewhat lower than those of NO. The present results of nitrogen emissions correlate well with the nutrient contents (especially NO_2^- and NO_3^-, Fig. 7). Bare soil, in which highest NO_3^- and NO_2^- levels were found, also showed highest HONO and NO emissions. A very good correlation was found between NO_2^- contents and emission of both nitrogen gas phase species for all samples (R^2 = 0.84 for HONO and 0.85 for NO; $p<0.001$). The level of correlation between NO_3^- and HONO and NO was lower, but still significant (R^2 = 0.68 and 0.67, respectively, $p<0.001$). Only low correlations were found between HONO or NO emissions and NH_4^+-contents (R^2 = 0.165 and 0.232; $p=0.05$). Thus, in the present study it

seems that reactive nitrogen emissions predominantly depend on NO_2^- and NO_3^- contents and not on surface cover types, although biocrusts (especially with cyanobacteria and cyanolichens) are able to fix atmospheric nitrogen (Belnap, 2002; Elbert et al., 2012; Barger et al., 2013; Patova et al., 2016). The results of a two-factorial ANOVA showed that HONO or NO emissions are not significantly related to soil cover type but rather with nitrite content, i.e., its direct aqueous precursor. For nitrate, the two-factorial ANOVA indicated dependencies of both cover type and nutrient content. These results differ from those obtained by Weber et al. (2015) on South African samples, as there HONO and NO emissions were not correlated with bulk concentrations of ammonium, nitrite and nitrate. In their study nitrite content was lowest for bare soil compared to other biocrust types. Ammonium and nitrites levels were also lower than in the present study. Therefore Weber et al. (2015) indicated that biocrusts can enhance N-cycle and emission of reactive nitrogen.

3.4 Comparison of soil emission and observed missing source

To quantify the flux rate of HONO emissions from soil to the local atmosphere and to compare it to the unaccounted source found in Cyprus in 2014 (Meusel et al., 2016), we applied a standard formalism describing the atmosphere-soil exchange of trace gases as a function of the difference between the atmospheric concentration and the equilibrium concentration at the soil solution surface [HONO]* (Su et al., 2011):

$$F^* = v_T ([HONO]^* - [HONO]) \quad \text{(eq.5)}$$

where [HONO] is the ambient HONO concentration measured on Cyprus (mean daytime average 60 ppt) and [HONO]* is the equilibrium concentration at soil surface. [HONO]* can be determined from measurements in a static chamber. In a dynamic chamber system, there is a concentration gradient of HONO between the headspace (where HONO was measured) and the soil surface. Here we use the measurements of water vapor to correct for the soil surface concentration and equilibrium concentration of HONO by assuming a similar gradient for the two species. A correction coefficient of 3.8 was determined, which is the ratio of the equilibrium rH of 100% over wet soil surface to the initial headspace rH of 25-30% after inserting the wet sample into the chamber. The transfer velocity, v_t, depends primarily on meteorological and soil conditions, and is typically on the order of ~1 cm s^{-1}. The flux rate of NO was calculated accordingly with mean daytime NO concentrations of 38 ppt. The calculated flux F* is about (67±3) % of the flux measured in the chamber.

The distribution of nine different surface cover types was mapped (Fig. 2), including stones, vascular vegetation and litter not being attributed to emit significant amounts of HONO and NO to the atmosphere. The residual HONO emitting surface covers comprised 45.6% of total surface in the investigated area. Combining the information on soil/biocrust population and the calculated flux F*, a site-specific community emission F_{comm} of HONO and NO can be estimated via following equation (eq. 6).

$$F_{comm,max} = \sum_i^{type} F^*_{max,i} * p_i/100 \quad \text{or} \quad F_{comm,int} = \sum_i^{type} F^*_{int,i} * p_i/100 \quad \text{(eq. 6)}$$

where F_{comm} denotes the estimated community flux, $F^*_{max,i\ or\ int,i}$ the maximum or integrated emission rates of each individual surface cover type i [ng N m^{-2} s^{-1} or µg N m^{-2}] and p_i the fraction of population type i [%].

Under optimum soil water conditions (20-30% WHC) and constant temperatures of about 25°C, between 2.2 and 18.8 ng m^{-2} s^{-1} of total HONO-N and 1.6-16.2 ng m^{-2} s^{-1} of total NO-N are emitted from the different crust/soil population combinations derived from the vegetation cover assessment. In the lower range of total emissions the

contribution from bare soil dominated with up to 69% (HONO) and 55% (NO), respectively, followed by moss BSC (HONO: 23%; NO: 32%). At high levels of total emission, the contribution from light BSC dominated (HONO: 43%, NO: 49%), decreasing the contribution of bare soil down to about 25% (HONO) and 13% (NO). Emissions from dark BSC contribute about 20% or 24% to the total HONO or NO flux while the contribution from moss BSC decreased to 10% or 12%, respectively. Emissions from chlorolichen BSC didn´t play a significant role (< 2.4%) in general (see Fig. 8).

After heavy rainfalls moistening the soil to full water-holding capacity, 11-113 µg m^{-2} of HONO-N and 10-131 µg m^{-2} of NO-N can be calculated for one complete wetting-and-drying period. Assuming 30 rain events per year (based on the statistic of 4 years precipitation data), a wetting-drying cycle time of 7 days, and constant emissions in between them (at 10% WHC) up to 160 mg m^{-2} yr^{-1} of nitrogen can be emitted directly by the sum of HONO-N and NO-N from Cyprus natural ground surfaces, i.e., excluding heterogeneous conversion of NO_2 on ground surface.

The release of HONO from the ground surface to the atmosphere can be related to the atmospheric HONO production rate via eq. 7 (adapted from Su et al., 2011) and then compared to the missing source.

$$S_{ground} = \frac{0.35 * F_{comm,max}}{BLH} * a \quad \text{(eq.7)}$$

with S_{ground}: HONO or NO emitted from ground surface; BLH: boundary layer height (mixed layer height) and a: factor to convert ng N in number of molecules (10^{-9}*6.022x10^{23}/14).

Based on the studies by Likos (2008) and Leelamanie (2010) and the meteorological conditions during CYPHEX (no rain event, but high rH, usually > 75%) a soil water content, slightly lower than the optimal water content for HONO and NO emissions, of 10% WHC was estimated, at which emissions of about 35% of the maximum was found.

In Cyprus during the summer of 2014 a mean boundary layer height of 300 m was observed by means of a ceilometer.. The mean air temperature during the campaign was comparable to the lab based chamber studies (25°C) but soil temperatures at the Cyprus field site could largely vary during daytime and reach maximum temperatures of up to 50°C (Fig. 4). At these high temperatures 6-10 fold higher emissions can be expected in general (Mamtimin et al., 2016), but also a quicker drying of the soil and biocrusts. At 25°C HONO emissions from the ground would equal a source strength of 1.1x10^5-9.8x10^5 cm^{-3} s^{-1} and would cover up to 75% of the missing mean source of 1.3x10^6 cm^{-3} s^{-1} (Meusel et al., 2016). In some mornings of the campaign dew formation was expected causing an increase in soil humidity. Combined with rising temperatures after sun-rise these optimized meteorological conditions may have led to enhanced soil emissions and would confer a reasonable explanation for the strong HONO morning peaks observed during the campaign. Similarly, the NO source strength from ground emission at 25°C is in the range from 8.3x10^4 to 8.0x10^5 cm^{-3} s^{-1}. As the observed unaccounted source of NO in Cyprus was of the order of 10^7 cm^{-3} s^{-1} soil emissions can only contribute up to 8% indicating other NO sources. Note that during CYPHEX there were two periods with lower rH, in which even a NO sink was detected.

4 Conclusions

HONO and NO emission rates from soil and biological soil crusts were derived by means of lab-based enclosure trace gas exchange measurements, and revealed quite similar ranges of reactive nitrogen source strengths. Emissions of both compounds strongly correlated with NO_2^- and NO_3^- content of the samples. Emissions from bare soil were

highest, but bare soil surface spots were rarely found at the investigated CYPHEX field study site. The estimated total ground surface HONO flux in the natural habitat is consistent with the previously unaccounted source estimated for Cyprus, i.e., the unaccounted HONO source can essentially be explained by emissions from soil/biocrusts. For NO, the measured and simulated fluxes cannot account for the unaccounted NO source (during the humid periods of the CYPHEX campaign 2014), indicating that emission from soil was not the only missing source of NO.

References

Abed, R. M. M., Lam, P., de Beer, D., and Stief, P.: High rates of denitrification and nitrous oxide emission in arid biological soil crusts from the Sultanate of Oman, Isme Journal, 7, 1862-1875, 10.1038/ismej.2013.55, 2013.

Alicke, B., Platt, U., and Stutz, J.: Impact of nitrous acid photolysis on the total hydroxyl radical budget during the Limitation of Oxidant Production/Pianura Padana Produzione di Ozono study in Milan, Journal of Geophysical Research-Atmospheres, 107, 10.1029/2000jd000075, 2002.

Ammann, M., Kalberer, M., Jost, D. T., Tobler, L., Rossler, E., Piguet, D., Gaggeler, H. W., and Baltensperger, U.: Heterogeneous production of nitrous acid on soot in polluted air masses, Nature, 395, 157-160, 10.1038/25965, 1998.

Arens, F., Gutzwiller, L., Baltensperger, U., Gaggeler, H. W., and Ammann, M.: Heterogeneous reaction of NO2 on diesel soot particles, Environmental Science & Technology, 35, 2191-2199, 10.1021/es000207s, 2001.

Aubin, D. G., and Abbatt, J. P. D.: Interaction of NO_2 with hydrocarbon soot: Focus on HONO yield, surface modification, and mechanism, Journal of Physical Chemistry A, 111, 6263-6273, 10.1021/jp068884h, 2007.

Baergen, A. M., and Donaldson, D. J.: Photochemical renoxification of nitric acid on real urban grime, Environmental Science & Technology, 47, 815-820, 10.1021/es3037862, 2013.

Barger, N. N., Castle, S. C., and Dean, G. N.: Denitrification from nitrogen-fixing biologically crusted soils in a cool desert environment, southeast Utah, USA, Ecological Processes, 2, 16, 10.1186/2192-1709-2-16, 2013.

Barger, N. N., Weber, B., Garcia-Pichel, F., Zaady, E., Belnap, J.: Patterns and controls on nitrogen cycling of biological soil crusts. In: Weber, B., Büdel, B., Belnap, J. (eds) Biological soil crusts: An organizing principle in drylands, Ecological Studies 226, Springer International Publishing Switzerland, pp 257-285, 2016.

Bejan, I., Abd El Aal, Y., Barnes, I., Benter, T., Bohn, B., Wiesen, P., and Kleffmann, J.: The photolysis of ortho-nitrophenols: a new gas phase source of HONO, Physical Chemistry Chemical Physics, 8, 2028-2035, 10.1039/b516590c, 2006.

Belnap, J.: Nitrogen fixation in biological soil crusts from southeast Utah, USA, Biology and Fertility of Soils, 35, 128-135, 10.1007/s00374-002-0452-x, 2002.

Belnap, J., Weber, B., Büdel, B.: Biological soil crusts as an organizing principle in drylands. In: Weber, B., Büdel, B., Belnap, J. (eds) Biological soil crusts: An organizing principle in drylands, Ecological Studies 226, Springer International Publishing Switzerland, pp 3-13, 2016.

Broske, R., Kleffmann, J., and Wiesen, P.: Heterogeneous conversion of NO_2 on secondary organic aerosol surfaces: A possible source of nitrous acid (HONO) in the atmosphere?, Atmospheric Chemistry and Physics, 3, 469-474, 2003.

Büdel, B., Darienko, T., Deutschewitz, K., Dojani, S., Friedl, T., Mohr, K., Salisch, M., Reisser, W. and Weber, B.: Southern African biological soil crusts are ubiquitous and highly diverse in drylands, being restricted by rainfall frequency. Microbial Ecology 57(2): 229-47, 2009.

Cleveland, C. C., Townsend, A. R., Schimel, D. S., Fisher, H., Howarth, R. W., Hedin, L. O., Perakis, S. S., Latty, E. F., Von Fischer, J. C., Elseroad, A., and Wasson, M. F.: Global patterns of terrestrial biological nitrogen (N_2) fixation in natural ecosystems, Global Biogeochemical Cycles, 13, 623-645, 10.1029/1999gb900014, 1999.

Czader, B. H., Rappenglueck, B., Percell, P., Byun, D. W., Ngan, F., and Kim, S.: Modeling nitrous acid and its impact on ozone and hydroxyl radical during the Texas Air Quality Study 2006, Atmospheric Chemistry and Physics, 12, 6939-6951, 10.5194/acp-12-6939-2012, 2012.

Darby, B. J., Neher, D. A.: Microfauna within biological soil crusts. In: Weber, B., Büdel, B., Belnap, J. (eds) Biological soil crusts: An organizing principle in drylands, Ecological Studies 226, Springer International Publishing Switzerland, pp 139-157, 2016.

Dumack, K., Koller, R., Weber, B. and Bonkowski, M.: Estimated heterotrophic protist abundances and their diversity in South African biological soil crusts. South African Journal of Science 112(7/8). Art. #2015-0302, 5 pages. http://dx.doi.org/10.17159/sajs.2016/20150302, 2016

Elbert, W., Weber, B., Burrows, S., Steinkamp, J., Budel, B., Andreae, M. O., and Poschl, U.: Contribution of cryptogamic covers to the global cycles of carbon and nitrogen, Nature Geosci, 5, 459-462, http://www.nature.com/ngeo/journal/v5/n7/abs/ngeo1486.html#supplementary-information, 2012.

George, C., Strekowski, R. S., Kleffmann, J., Stemmler, K., and Ammann, M.: Photoenhanced uptake of gaseous NO_2 on solid-organic compounds: a photochemical source of HONO?, Faraday Discussions, 130, 195-210, 10.1039/b417888m, 2005.

Han, C., Yang, W. J., Wu, Q. Q., Yang, H., and Xue, X. X.: Heterogeneous photochemical conversion of NO_2 to HONO on the humic acid surface under simulated sunlight, Environmental Science & Technology, 50, 5017-5023, 10.1021/acs.est.5b05101, 2016.

Harrison, R. M., and Kitto, A. M. N.: Evidence for a surface source of atmospheric nitrous acid, Atmospheric Environment, 28, 1089-1094, 10.1016/1352-2310(94)90286-0, 1994.

Herridge, D. F., Peoples, M. B., and Boddey, R. M.: Global inputs of biological nitrogen fixation in agricultural systems, Plant and Soil, 311, 1-18, 10.1007/s11104-008-9668-3, 2008.

Johnson, S. L., Budinoff, C. R., Belnap, J., and Garcia-Pichel, F.: Relevance of ammonium oxidation within biological soil crust communities, Environmental Microbiology, 7, 1-12, 10.1111/j.1462-2920.2004.00649.x, 2005.

Kalberer, M., Ammann, M., Arens, F., Gaggeler, H. W., and Baltensperger, U.: Heterogeneous formation of nitrous acid (HONO) on soot aerosol particles, Journal of Geophysical Research-Atmospheres, 104, 13825-13832, 10.1029/1999jd900141, 1999.

Kebede, M. A., Scharko, N. K., Appelt, L. E., and Raff, J. D.: Formation of nitrous acid during ammonia photooxidation on TiO_2 under atmospherically relevant conditions, Journal of Physical Chemistry Letters, 4, 2618-2623, 10.1021/jz401250k, 2013.

Kinugawa, T., Enami, S., Yabushita, A., Kawasaki, M., Hoffmann, M. R., and Colussi, A. J.: Conversion of gaseous nitrogen dioxide to nitrate and nitrite on aqueous surfactants, Physical Chemistry Chemical Physics, 13, 5144-5149, 10.1039/C0CP01497D, 2011.

Kleffmann, J., H. Becker, K., Lackhoff, M., and Wiesen, P.: Heterogeneous conversion of NO_2 on carbonaceous surfaces, Physical Chemistry Chemical Physics, 1, 5443-5450, 10.1039/A905545B, 1999.

Kleffmann, J., Kurtenbach, R., Lorzer, J., Wiesen, P., Kalthoff, N., Vogel, B., and Vogel, H.: Measured and simulated vertical profiles of nitrous acid - Part I: Field measurements, Atmospheric Environment, 37, 2949-2955, 10.1016/s1352-2310(03)00242-5, 2003.

Kleffmann, J., Gavriloaiei, T., Hofzumahaus, A., Holland, F., Koppmann, R., Rupp, L., Schlosser, E., Siese, M., and Wahner, A.: Daytime formation of nitrous acid: A major source of OH radicals in a forest, Geophysical Research Letters, 32, 10.1029/2005gl022524, 2005.

Kleffmann, J., and Wiesen, P.: Heterogeneous conversion of NO_2 and NO on HNO_3 treated soot surfaces: atmospheric implications, Atmospheric Chemistry and Physics, 5, 77-83, 2005.

Langridge, J. M., Gustafsson, R. J., Griffiths, P. T., Cox, R. A., Lambert, R. M., and Jones, R. L.: Solar driven nitrous acid formation on building material surfaces containing titanium dioxide: A concern for air quality in urban areas?, Atmospheric Environment, 43, 5128-5131, http://dx.doi.org/10.1016/j.atmosenv.2009.06.046, 2009.

Lelièvre, S., Bedjanian, Y., Laverdet, G., and Le Bras, G.: Heterogeneous reaction of NO_2 with hydrocarbon flame soot, The Journal of Physical Chemistry A, 108, 10807-10817, 10.1021/jp0469970, 2004.

Li, X., Rohrer, F., Hofzumahaus, A., Brauers, T., Häseler, R., Bohn, B., Broch, S., Fuchs, H., Gomm, S., Holland, F., Jäger, J., Kaiser, J., Keutsch, F. N., Lohse, I., Lu, K., Tillmann, R., Wegener, R., Wolfe, G. M., Mentel, T. F., Kiendler-Scharr, A., and Wahner, A.: Missing gas-phase source of HONO inferred from Zeppelin measurements in the troposphere, Science, 344, 292-296, 10.1126/science.1248999, 2014.

Liu, Y., Han, C., Ma, J., Bao, X., and He, H.: Influence of relative humidity on heterogeneous kinetics of NO_2 on kaolin and hematite, Physical Chemistry Chemical Physics, 17, 19424-19431, 10.1039/c5cp02223a, 2015.

Mamtimin, B., Meixner, F. X., Behrendt, T., Badawy, M., and Wagner, T.: The contribution of soil biogenic NO and HONO emissions from a managed hyperarid ecosystem to the regional NOx emissions during growing season, Atmos. Chem. Phys., 16, 10175-10194, 10.5194/acp-16-10175-2016, 2016.

Meixner, F. X., and Yang, W. X.: Biogenic emissions of nitric oxide and nitrous oxide from arid and semi-arid land, in: Dryland Ecohydrology, edited by: D'Odorico, P., and Porporato, A., Springer Netherlands, Dordrecht, 233-255, 2006.

Meusel, H., Kuhn, U., Reiffs, A., Mallik, C., Harder, H., Martinez, M., Schuladen, J., Bohn, B., Parchatka, U., Crowley, J. N., Fischer, H., Tomsche, L., Novelli, A., Hoffmann, T., Janssen, R. H. H., Hartogensis, O., Pikridas, M., Vrekoussis, M., Bourtsoukidis, E., Weber, B., Lelieveld, J., Williams, J., Pöschl, U., Cheng, Y., and Su, H.: Daytime formation of nitrous acid at a coastal remote site in Cyprus indicating a common ground source of atmospheric HONO and NO, Atmos. Chem. Phys., 16, 14475-14493, 10.5194/acp-16-14475-2016, 2016.

Meusel, H., Elshorbany, Y., Kuhn, U., Bartels-Rausch, T., Reinmuth-Selzle, K., Kampf, C. J., Li, G., Wang, X., Lelieveld, J., Pöschl, U., Hoffmann, T., Su, H., Ammann, M., and Cheng, Y.: Light-induced protein nitration and degradation with HONO emission, Atmos. Chem. Phys. Discuss., 2017, 1-22, 10.5194/acp-2017-277, 2017.

Michoud, V., Colomb, A., Borbon, A., Miet, K., Beekmann, M., Camredon, M., Aumont, B., Perrier, S., Zapf, P., Siour, G., Ait-Helal, W., Afif, C., Kukui, A., Furger, M., Dupont, J. C., Haeffelin, M., and Doussin, J. F.: Study of the unknown HONO daytime source at a European suburban site during the MEGAPOLI summer and winter field campaigns, Atmospheric Chemistry and Physics, 14, 2805-2822, 10.5194/acp-14-2805-2014, 2014.

Monge, M. E., D'Anna, B., Mazri, L., Giroir-Fendler, A., Ammann, M., Donaldson, D. J., and George, C.: Light changes the atmospheric reactivity of soot, Proceedings of the National Academy of Sciences of the United States of America, 107, 6605-6609, 10.1073/pnas.0908341107, 2010.

Ndour, M., D'Anna, B., George, C., Ka, O., Balkanski, Y., Kleffmann, J., Stemmler, K., and Ammann, M.: Photoenhanced uptake of NO_2 on mineral dust: Laboratory experiments and model simulations, Geophysical Research Letters, 35, 10.1029/2007gl032006, 2008.

Neuman, J. A., Trainer, M., Brown, S. S., Min, K. E., Nowak, J. B., Parrish, D. D., Peischl, J., Pollack, I. B., Roberts, J. M., Ryerson, T. B., and Veres, P. R.: HONO emission and production determined from airborne measurements over the Southeast U.S, Journal of Geophysical Research: Atmospheres, 121, 9237-9250, 10.1002/2016JD025197, 2016.

Oswald, R., Behrendt, T., Ermel, M., Wu, D., Su, H., Cheng, Y., Breuninger, C., Moravek, A., Mougin, E., Delon, C., Loubet, B., Pommerening-Roeser, A., Soergel, M., Poeschl, U., Hoffmann, T., Andreae, M. O., Meixner, F. X., and Trebs, I.: HONO emissions from soil bacteria as a major source of atmospheric reactive nitrogen, Science, 341, 1233-1235, 10.1126/science.1242266, 2013.

Oswald, R., Ermel, M., Hens, K., Novelli, A., Ouwersloot, H. G., Paasonen, P., Petaja, T., Sipila, M., Keronen, P., Back, J., Konigstedt, R., Beygi, Z. H., Fischer, H., Bohn, B., Kubistin, D., Harder, H., Martinez, M., Williams, J., Hoffmann, T., Trebs, I., and Soergel, M.: A comparison of HONO budgets for two measurement heights at a field station within the boreal forest in Finland, Atmospheric Chemistry and Physics, 15, 799-813, 10.5194/acp-15-799-2015, 2015.

Patova, E., Sivkov, M., and Patova, A.: Nitrogen fixation activity in biological soil crusts dominated by cyanobacteria in the Subpolar Urals (European North-East Russia), FEMS Microbiology Ecology, 92, 10.1093/femsec/fiw131, 2016.

Pilegaard, K.: Processes regulating nitric oxide emissions from soils, Philosophical Transactions of the Royal Society B: Biological Sciences, 368, 10.1098/rstb.2013.0126, 2013.

Ramazan, K. A., Syomin, D., and Finlayson-Pitts, B. J.: The photochemical production of HONO during the heterogeneous hydrolysis of NO_2, Physical Chemistry Chemical Physics, 6, 3836-3843, 10.1039/b402195a, 2004.

Ren, X. R., Harder, H., Martinez, M., Lesher, R. L., Oliger, A., Simpas, J. B., Brune, W. H., Schwab, J. J., Demerjian, K. L., He, Y., Zhou, X. L., and Gao, H. G.: OH and HO_2 chemistry in the urban atmosphere of New York City, Atmospheric Environment, 37, 3639-3651, 10.1016/s1352-2310(03)00459-x, 2003.

Ren, X., Brune, W. H., Oliger, A., Metcalf, A. R., Simpas, J. B., Shirley, T., Schwab, J. J., Bai, C., Roychowdhury, U., Li, Y., Cai, C., Demerjian, K. L., He, Y., Zhou, X., Gao, H., and Hou, J.: OH, HO_2, and OH reactivity during

the PMTACS-NY Whiteface Mountain 2002 campaign: Observations and model comparison, Journal of Geophysical Research-Atmospheres, 111, 10.1029/2005jd006126, 2006.

Ren, X., Sanders, J. E., Rajendran, A., Weber, R. J., Goldstein, A. H., Pusede, S. E., Browne, E. C., Min, K. E., and Cohen, R. C.: A relaxed eddy accumulation system for measuring vertical fluxes of nitrous acid, Atmospheric Measurement Techniques, 4, 2093-2103, 10.5194/amt-4-2093-2011, 2011.

Ronen, R., and Galun, M.: Pigment extraction from lichens with dimethylsufoxide (DMSO) and estimation of chlorophyll degradation, Environmental and Experimental Botany, 24, 239-245, 10.1016/0098-8472(84)90004-2, 1984.

Sarwar, G., Roselle, S. J., Mathur, R., Appel, W., Dennis, R. L., and Vogel, B.: A comparison of CMAQ HONO predictions with observations from the Northeast Oxidant and Particle Study, Atmospheric Environment, 42, 5760-5770, http://dx.doi.org/10.1016/j.atmosenv.2007.12.065, 2008.

Scharko, N. K., Berke, A. E., and Raff, J. D.: Release of nitrous acid and nitrogen dioxide from nitrate photolysis in acidic aqueous solutions, Environmental Science & Technology, 48, 11991-12001, 10.1021/es503088x, 2014.

Soergel, M., Regelin, E., Bozem, H., Diesch, J. M., Drewnick, F., Fischer, H., Harder, H., Held, A., Hosaynali-Beygi, Z., Martinez, M., and Zetzsch, C.: Quantification of the unknown HONO daytime source and its relation to NO2, Atmospheric Chemistry and Physics, 11, 10433-10447, 10.5194/acp-11-10433-2011, 2011a.

Stemmler, K., Ammann, M., Donders, C., Kleffmann, J., and George, C.: Photosensitized reduction of nitrogen dioxide on humic acid as a source of nitrous acid, Nature, 440, 195-198, 10.1038/nature04603, 2006.

Stemmler, K., Ndour, M., Elshorbany, Y., Kleffmann, J., D'Anna, B., George, C., Bohn, B., and Ammann, M.: Light induced conversion of nitrogen dioxide into nitrous acid on submicron humic acid aerosol, Atmospheric Chemistry and Physics, 7, 4237-4248, 2007.

Strauss, S. L., Day, T. A., and Garcia-Pichel, F.: Nitrogen cycling in desert biological soil crusts across biogeographic regions in the Southwestern United States, Biogeochemistry, 108, 171-182, 10.1007/s10533-011-9587-x, 2012.

Stutz, J., Alicke, B., and Neftel, A.: Nitrous acid formation in the urban atmosphere: Gradient measurements of NO_2 and HONO over grass in Milan, Italy, Journal of Geophysical Research-Atmospheres, 107, 10.1029/2001jd000390, 2002.

Su, H., Cheng, Y. F., Cheng, P., Zhang, Y. H., Dong, S., Zeng, L. M., Wang, X., Slanina, J., Shao, M., and Wiedensohler, A.: Observation of nighttime nitrous acid (HONO) formation at a non-urban site during PRIDE-PRD2004 in China, Atmospheric Environment, 42, 6219-6232, 10.1016/j.atmosenv.2008.04.006, 2008a.

Su, H., Cheng, Y. F., Shao, M., Gao, D. F., Yu, Z. Y., Zeng, L. M., Slanina, J., Zhang, Y. H., and Wiedensohler, A.: Nitrous acid (HONO) and its daytime sources at a rural site during the 2004 PRIDE-PRD experiment in China, Journal of Geophysical Research-Atmospheres, 113, 10.1029/2007jd009060, 2008b.

Su, H., Cheng, Y., Oswald, R., Behrendt, T., Trebs, I., Meixner, F. X., Andreae, M. O., Cheng, P., Zhang, Y., and Poeschl, U.: Soil nitrite as a source of atmospheric HONO and OH radicals, Science, 333, 1616-1618, 10.1126/science.1207687, 2011.

Tang, Y., An, J., Wang, F., Li, Y., Qu, Y., Chen, Y., and Lin, J.: Impacts of an unknown daytime HONO source on the mixing ratio and budget of HONO, and hydroxyl, hydroperoxyl, and organic peroxy radicals, in the coastal regions of China, Atmospheric Chemistry and Physics, 15, 9381-9398, 10.5194/acp-15-9381-2015, 2015.

VandenBoer, T. C., Brown, S. S., Murphy, J. G., Keene, W. C., Young, C. J., Pszenny, A. A. P., Kim, S., Warneke, C., de Gouw, J. A., Maben, J. R., Wagner, N. L., Riedel, T. P., Thornton, J. A., Wolfe, D. E., Dubé, W. P., Öztürk, F., Brock, C. A., Grossberg, N., Lefer, B., Lerner, B., Middlebrook, A. M., and Roberts, J. M.: Understanding the role of the ground surface in HONO vertical structure: High resolution vertical profiles during NACHTT-11, Journal of Geophysical Research: Atmospheres, 118, 10,155-110,171, 10.1002/jgrd.50721, 2013.

Villena, G., Kleffmann, J., Kurtenbach, R., Wiesen, P., Lissi, E., Rubio, M. A., Croxatto, G., and Rappenglueck, B.: Vertical gradients of HONO, NOx and O_3 in Santiago de Chile, Atmospheric Environment, 45, 3867-3873, 10.1016/j.atmosenv.2011.01.073, 2011.

Vogel, B., Vogel, H., Kleffmann, J., and Kurtenbach, R.: Measured and simulated vertical profiles of nitrous acid - Part II. Model simulations and indications for a photolytic source, Atmospheric Environment, 37, 2957-2966, 10.1016/s1352-2310(03)00243-7, 2003.

Wang, S. H., Ackermann, R., Spicer, C. W., Fast, J. D., Schmeling, M., and Stutz, J.: Atmospheric observations of enhanced NO_2-HONO conversion on mineral dust particles, Geophysical Research Letters, 30, 10.1029/2003gl017014, 2003.

Weber, B., Wessels, D. C., Deutschewitz, K., Dojani, S., Reichenberger, H., and Büdel, B.: Ecological characterization of soil-inhabiting and hypolithic soil crusts within the Knersvlakte, South Africa, Ecological Processes, 2, 8, 10.1186/2192-1709-2-8, 2013.

Weber, B., Wu, D., Tamm, A., Ruckteschler, N., Rodriguez-Caballero, E., Steinkamp, J., Meusel, H., Elbert, W., Behrendt, T., Soergel, M., Cheng, Y., Crutzen, P. J., Su, H., and Poeschi, U.: Biological soil crusts accelerate the nitrogen cycle through large NO and HONO emissions in drylands, Proceedings of the National Academy of Sciences of the United States of America, 112, 15384-15389, 10.1073/pnas.1515818112, 2015.

Wong, K. W., Tsai, C., Lefer, B., Haman, C., Grossberg, N., Brune, W. H., Ren, X., Luke, W., and Stutz, J.: Daytime HONO vertical gradients during SHARP 2009 in Houston, TX, Atmospheric Chemistry and Physics, 12, 635-652, 10.5194/acp-12-635-2012, 2012.

Wong, K. W., Tsai, C., Lefer, B., Grossberg, N., and Stutz, J.: Modeling of daytime HONO vertical gradients during SHARP 2009, Atmospheric Chemistry and Physics, 13, 3587-3601, 10.5194/acp-13-3587-2013, 2013.

Wu, D., Kampf, C. J., Pöschl, U., Oswald, R., Cui, J., Ermel, M., Hu, C., Trebs, I., and Sörgel, M.: Novel tracer method to measure isotopic labeled gas-phase nitrous acid ($HO^{15}NO$) in Biogeochemical Studies, Environmental Science & Technology, 48, 8021-8027, 10.1021/es501353x, 2014.

Yabushita, A., Enami, S., Sakamoto, Y., Kawasaki, M., Hoffmann, M. R., and Colussi, A. J.: Anion-catalyzed dissolution of NO_2 on aqueous microdroplets, The Journal of Physical Chemistry A, 113, 4844-4848, 10.1021/jp900685f, 2009.

Young, C. J., Washenfelder, R. A., Roberts, J. M., Mielke, L. H., Osthoff, H. D., Tsai, C., Pikelnaya, O., Stutz, J., Veres, P. R., Cochran, A. K., VandenBoer, T. C., Flynn, J., Grossberg, N., Haman, C. L., Lefer, B., Stark, H., Graus, M., de Gouw, J., Gilman, J. B., Kuster, W. C., and Brown, S. S.: Vertically resolved measurements of

nighttime radical reservoirs; in Los Angeles and their contribution to the urban uadical budget, Environmental Science & Technology, 46, 10965-10973, 10.1021/es302206a, 2012.

Zhang, N., Zhou, X. L., Shepson, P. B., Gao, H. L., Alaghmand, M., and Stirm, B.: Aircraft measurement of HONO vertical profiles over a forested region, Geophysical Research Letters, 36, 10.1029/2009gl038999, 2009.

Zhang, L., Wang, T., Zhang, Q., Zheng, J., Xu, Z., and Lv, M.: Potential sources of nitrous acid (HONO) and their impacts on ozone: A WRF-Chem study in a polluted subtropical region, Journal of Geophysical Research: Atmospheres, 121, 3645-3662, 10.1002/2015JD024468, 2016.

Zhou, X. L., Gao, H. L., He, Y., Huang, G., Bertman, S. B., Civerolo, K., and Schwab, J.: Nitric acid photolysis on surfaces in low-NOx environments: Significant atmospheric implications, Geophysical Research Letters, 30, 10.1029/2003gl018620, 2003.

Zhou, X., Zhang, N., TerAvest, M., Tang, D., Hou, J., Bertman, S., Alaghmand, M., Shepson, P. B., Carroll, M. A., Griffith, S., Dusanter, S., and Stevens, P. S.: Nitric acid photolysis on forest canopy surface as a source for tropospheric nitrous acid, Nature Geoscience, 4, 440-443, 10.1038/ngeo1164, 2011.

Table 1: Overview on the samples, distribution of replicates of soil/biocrust type and the different analysis:

Type	Only nutrient analysis	Flux measurements, followed by nutrient and chlorophyll analysis	Sum
Bare soil	3	3	6
Dark BSC	3	5	8
Light BSC	3	4	10
Light BSC + cyanolichen	3		
Chlorolichen BSC I	3	3	12
Chlorolichen BSC II		6	
Moss BSC	3	4	7
sum	18	25	43

Atmos. Chem. Phys. Discuss., doi:10.5194/acp-2017-356, 2017
Manuscript under review for journal Atmos. Chem. Phys.
Discussion started: 2 May 2017

Atmospheric Chemistry and Physics Discussions

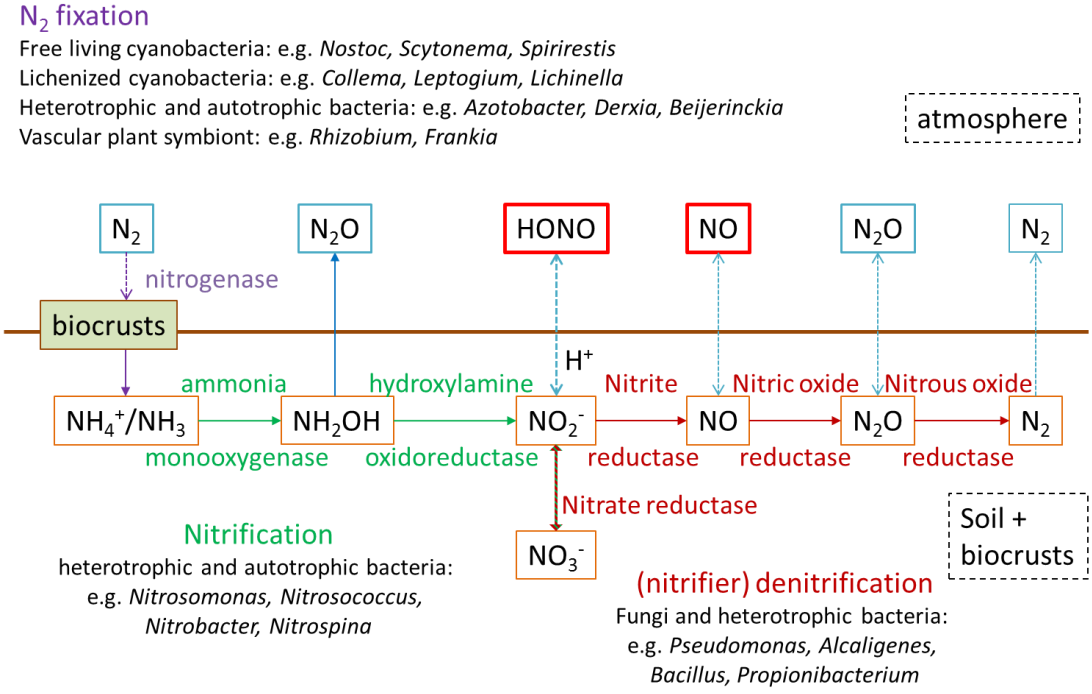

Fig. 1: Nitrogen cycle at the atmosphere and pedosphere/biosphere interface including nitrogen fixation, nitrification, denitrification and emission. Involved enzymes and organisms are specified.

Atmos. Chem. Phys. Discuss., doi:10.5194/acp-2017-356, 2017
Manuscript under review for journal Atmos. Chem. Phys.
Discussion started: 2 May 2017

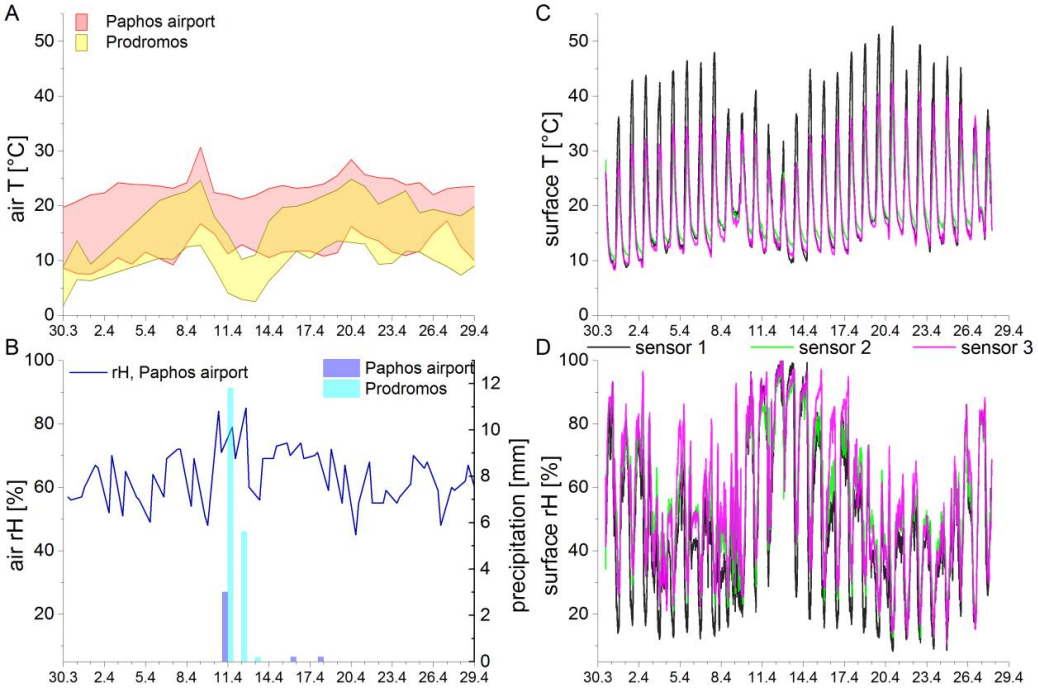

Fig. 2: Climatic conditions of air and soil during April 2016, about one month before samples were taken. Atmospheric data was adopted from the Department of Meteorology, Cyprus. Minimum and maximum air temperatures (A) of one day at both sites are presented by red and yellow shaded areas. Air-rH data (B; dark blue line, left axis) were only available for Paphos airport, representing values at 8:00 and 13:00 local time. Precipitation data at Paphos airport and Prodromos (B; blue bars, right axis) show the daily rainfall. Surface temperature and rH are shown on the right side (C, D). The time resolution is 5 min. The variations between sensors arise from 3 different locations/surface (bare soil, next to rock, under shrubs). (http://www.moa.gov.cy/moa/ms/ms.nsf/DMLmeteo_reports_en/DMLmeteo_reports_en?OpenDocument)

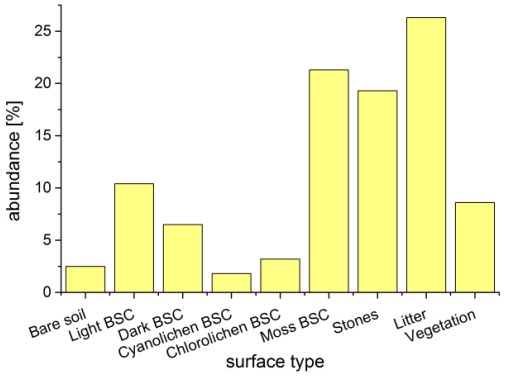

Fig. 3: Distribution of different types of ground surfaces in the studied area. Information derived from 50 grids.

Atmos. Chem. Phys. Discuss., doi:10.5194/acp-2017-356, 2017
Manuscript under review for journal Atmos. Chem. Phys.
Discussion started: 2 May 2017

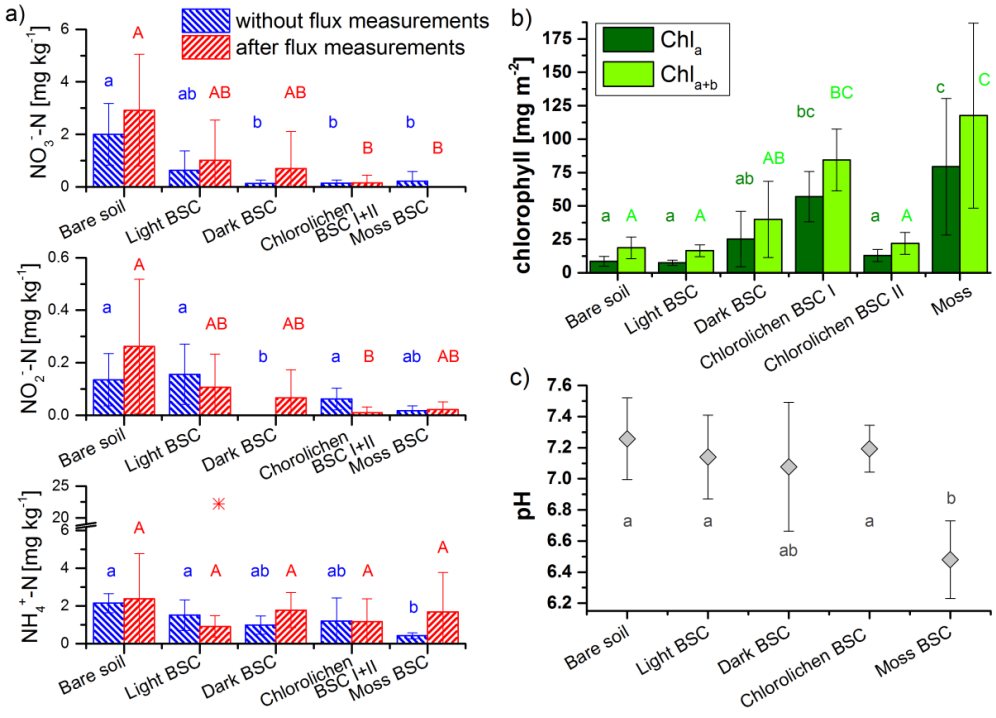

Fig. 4: Nutrient- and chlorophyll contents as well as pH values of bare soil and biocrust samples of different types. a) Nitrate, nitrite and ammonium contents without and after flux measurements. The red star indicates an outlier, b) Chlorophyll a and chlorophyll a+b contents of samples after flux measurements c) pH values of samples without and after flux measurements (bare soil and moss BSC: n = 4; light, dark and chlorolichen BSC: n = 3). Number of replicates for a and b see table 1. In all 3 plots error bars indicate standard deviation and different letters indicate significant differences (of log-transformed data; p=0.05).

Atmos. Chem. Phys. Discuss., doi:10.5194/acp-2017-356, 2017
Manuscript under review for journal Atmos. Chem. Phys.
Discussion started: 2 May 2017

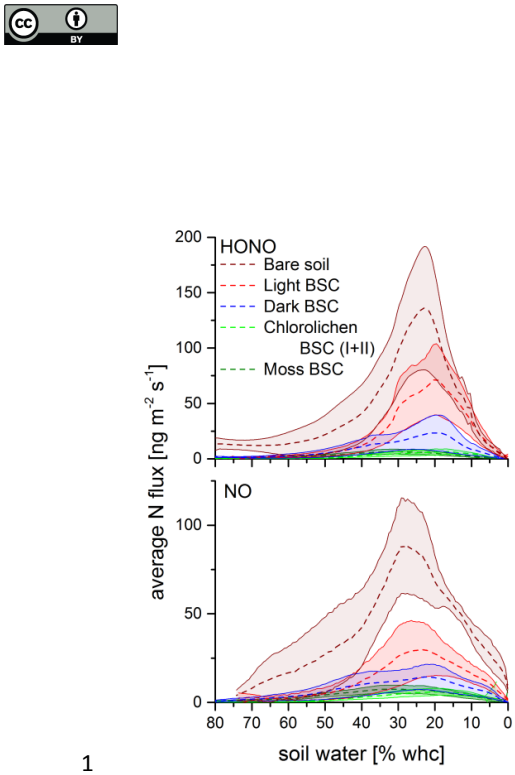

Fig. 5: HONO and NO emission fluxes as a function of soil water content. Dotted lines are the mean fluxes. Shaded areas indicate the standard deviation.

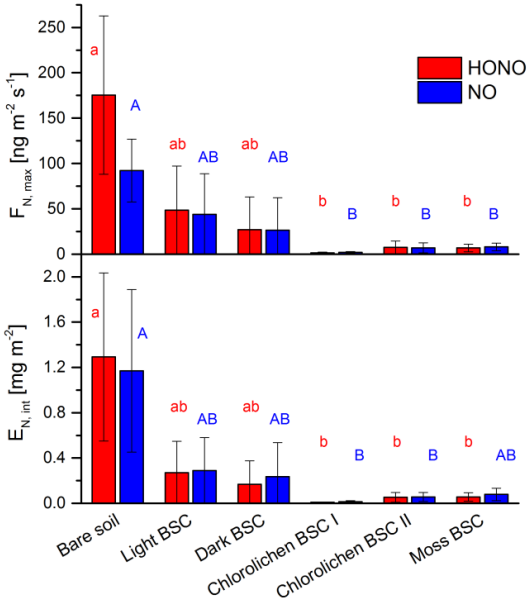

Fig. 6: Emission of HONO and NO from bare soil and biocrusts. Upper panel: Maximum HONO-N and NO-N fluxes in ng m^{-2} s^{-1} at optimum water conditions; Lower panel: Emissions integrated over a whole wetting-and-drying cycle in mg (N) m^{-2}; letters show significant difference (p=0.05,of log-transformed data); error bars indicate standard deviation of replicates (bare soil n=3; light BSC n=4; dark BSC n=5; chlorolichen BSC I n=3; chlorolichen BSC II n=6; moss BSC n=4).

Atmos. Chem. Phys. Discuss., doi:10.5194/acp-2017-356, 2017
Manuscript under review for journal Atmos. Chem. Phys.
Discussion started: 2 May 2017

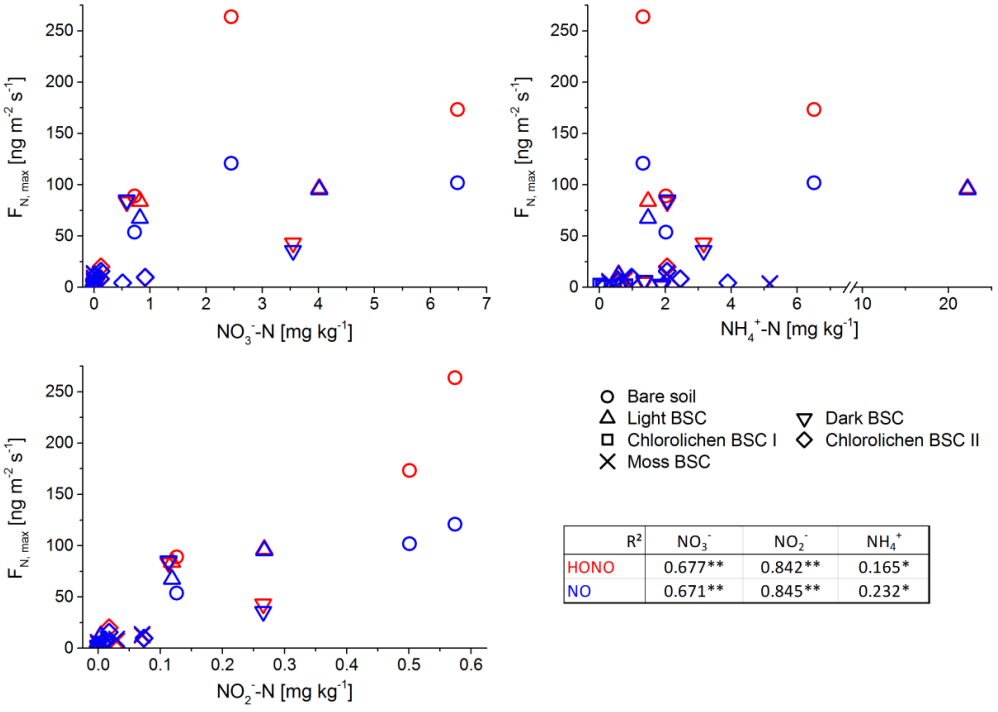

R^2	NO_3^-	NO_2^-	NH_4^+
HONO	0.677**	0.842**	0.165*
NO	0.671**	0.845**	0.232*

Fig. 7: Correlation between maximum flux of HONO and NO and nutrient content of all Cyprus soil and biocrust samples with Pearson correlation factors (of log transformed data; **: p < 0.001; *: p < 0.05).

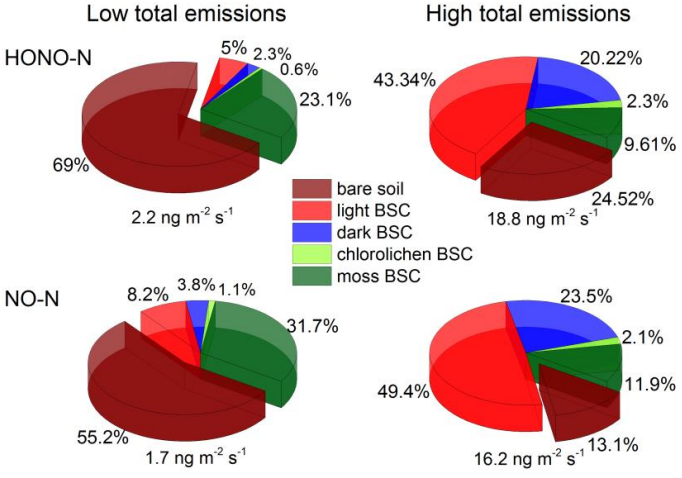

Fig. 8: Contributions of different ground surfaces to the total F*.

Supplement for

Emission of nitrous acid from soil and biological soil crusts represents a dominant source of HONO in the remote atmosphere in Cyprus

Hannah Meusel[1], Alexandra Tamm[1], Uwe Kuhn[1], Dianming Wu[1], Anna Lena Leifke[1], Sabine Fiedler[2], Nina Ruckteschler[1], Petya Yordanova[1], Naama Lang-Yona[1], Jos Lelieveld[3,4], Thorsten Hoffmann[5], Ulrich Pöschl[1], Hang Su[1,6], Bettina Weber[1], Yafang Cheng[1,6]

[1]Max Planck Institute for Chemistry, Multiphase Chemistry Department, Mainz, Germany
[2]Johannes Gutenberg University, Institute for Geography, Mainz, Germany
[3]Max Planck Institute for Chemistry, Atmospheric Chemistry Department, Mainz, Germany
[4]The Cyprus Institute, Nicosia, Cyprus
[5]Johannes Gutenberg University, Institute for Inorganic and Analytical Chemistry, Mainz, Germany
[6]Institute for Environmental and Climate Research, Jinan University, Guangzhou, China

Corresponding author: Yafang Cheng (yafang.cheng@mpic.de) and Bettina Weber (b.weber@mpic.de)

Table S1: Overview over soil and biocrust samples including nutrient and chlorophyll analyses and HONO and NO emission fluxes.

sample type		NO_2^--N	NO_3^--N	NH_4^+-N	chl_{a-b}	chl_a	$HONO_{max}$	NO_{max}	$HONO_{int}$	NO_{int}	HONO/NO	
		mg kg^{-1}			mg m^{-2}		ng (N) m^{-2} s^{-1}		µg (N) m^{-2}		(max)	(int)
Bare soil	1	0.126	0.723	2.017	17.45	8.61	89.12	53.70	465.49	341.45	1.66	1.36
Bare soil	2	0.574	2.450	1.325	18.66	6.84	263.80	120.99	1899.9	1544.8	2.18	1.23
Bare soil	3	0.501	6.478	6.509	31.71	13.93	173.32	101.83	1510.4	1621.3	1.70	0.93
Dark BSC	1	0.0	0.0	1.906	40.80	27.48	1.29	1.73	9.45	17.1	0.74	0.55
Dark BSC	2	0.0	0.0	1.873	32.13	18.61	3.08	2.90	16.42	25.49	1.06	0.64
Dark BSC	3	0.004	0.050	1.365	30.42	15.52	4.69	6.64	36.28	63.53	0.71	0.57
Dark BSC	4	0.265	3.549	3.159	95.66	66.01	43.15	35.86	337.45	359.56	1.20	0.94
Dark BSC	5	0.113	0.582	2.061	21.65	11.26	83.43	85.1	443.86	712.1	0.98	0.62
Light BSC	1	0.0	0.0	0.626	12.71	6.05	1.28	1.74	8.61	14.84	0.73	0.58
Light BSC	2	0.004	0.0	0.587	16.34	7.72	12.35	11.44	61.48	66.07	1.08	0.93
Light BSC	3	0.267	4.015	22.209	24.60	11.00	96.53	95.22	540.77	592.28	1.01	0.91
Light BSC	4	0.119	0.819	1.478	18.09	8.31	83.89	67.5	475.72	481.0	1.24	0.99
Chlorolichen BSC I	1	0.0	0.0	0.085	61.39	37.48	0.63	0.83	3.73	6.03	0.76	0.62
Chlorolichen BSC I	2	0.0	0.0	0.0	84.12	58.64	2.45	2.62	12.02	15.73	0.93	0.76
Chlorolichen BSC I	3	0.0	0.0	0.829	107.59	74.85	1.24	2.03	10.50	24.54	0.61	0.43
Chlorolichen BSC II	1	0.0	0.0	0.187	24.75	14.18	1.69	1.88	15.23	15.32	0.90	0.99
Chlorolichen BSC II	2	0.011	0.116	2.460	10.58	10.58	7.98	8.40	54.53	63.25	0.95	0.86
Chlorolichen BSC II	3	0.074	0.916	0.982	21.73	12.29	9.65	9.88	94.72	103.62	0.98	0.91
Chlorolichen BSC II	4	0.017	0.128	2.062	17.97	9.50	19.97	15.83	110.68	95.15	1.26	1.16
Chlorolichen BSC II	5	0.007	0.513	3.894	37.46	22.65	4.27	4.43	35.14	49.83	0.96	0.71
Chlorolichen BSC II	6	0.0	0.0	0.585	17.43	9.71	1.52	1.54	7.87	11.60	0.98	0.68
Moss BSC	1	0.071	0.0	2.048	48.93	27.82	12.68	13.44	104.08	148.62	0.94	0.70
Moss BSC	2	0.0	0.0	0.306	83.63	54.53	4.34	5.79	40.07	57.66	0.75	0.69
Moss BSC	3	0.030	0.0	0.763	211.31	144.21	6.78	8.87	62.54	89.10	0.77	0.70
Moss BSC	4	0.005	0.029	5.164	169.64	123.26	3.49	3.65	16.61	19.58	0.96	0.85

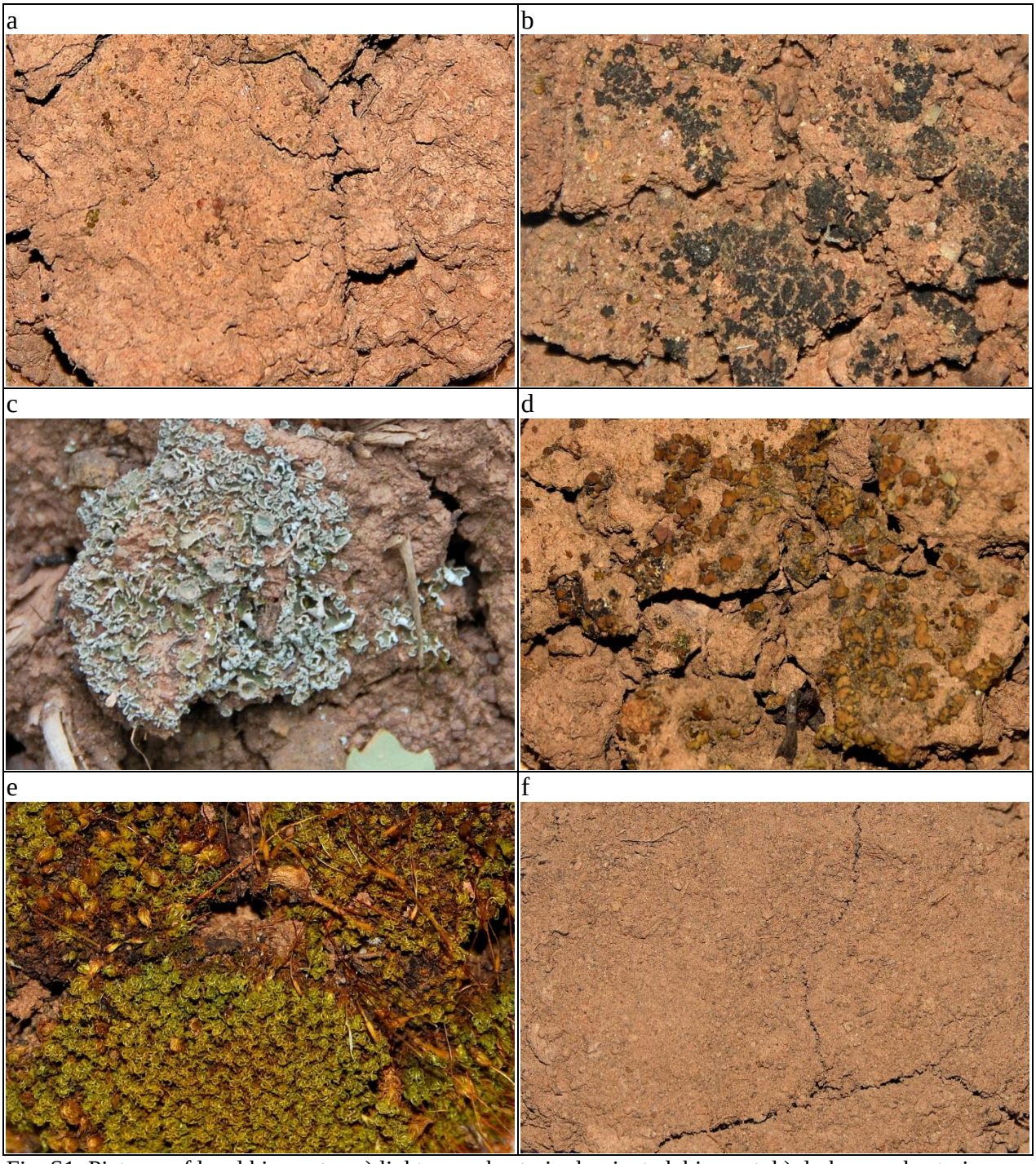

Fig. S1: Pictures of local biocrusts: a) light cyanobacteria-dominated biocrust, b) dark cyanobacteria-dominated biocrust with *Collema* sp. as dominating cyanolichen species, c) chlorolichen-dominated biocrust with *Cladonia* sp. as dominating lichen species, type I, d) chlorolichen-dominated biocrust with *Placidium* sp. as dominating lichen species, type II, e) moss-dominated biocrust with *Trichostomum crispulum* as dominating moss species, f) bare soil.

B.3 Meusel et al., ACPD 2017b

Light-induced protein nitration and degradation with HONO emission

Hannah Meusel[1], Yasin Elshorbany[2], Uwe Kuhn[1], Thorsten Bartels-Rausch[3], Kathrin Reinmuth-Selzle[1], Christopher J. Kampf[4], Guo Li[1], Xiaoxiang Wang[1], Jos Lelieveld[5], Ulrich Pöschl[1], Thorsten Hoffmann[6], Hang Su[1,7*], Markus Ammann[3], Yafang Cheng[1,7*]

[1] Max Planck Institute for Chemistry, Multiphase Chemistry Department, Mainz, Germany
[2] NASA Goddard Space Flight Center, Greenbelt, Maryland, USA & Earth System Science, Interdisciplinary Center, University of Maryland, College Park, Maryland, USA
[3] Paul Scherer Institute, Villigen, Switzerland
[4] Johannes Gutenberg University, Institute for Organic Chemistry, Mainz, Germany
[5] Max Planck Institute for Chemistry, Atmospheric Chemistry Department, Mainz, Germany
[6] Johannes Gutenberg University, Institute for Inorganic and Analytical Chemistry, Mainz, Germany
[7] Institute for Environmental and Climate Research, Jinan University, Guangzhou, China

Atmospheric Chemistry and Physics Discussion, 2017, 1-22, (2017b)
DOI: 10.5194/acp-2017-277

Author contributions:

HS, YE, YC designed the research.
HM, YC, HS, TBR performed the study.
KRS, GL, XW provided relevant data.
HM, YC, HS, UK, UPö, CJK, TH, MA discussed the results.
HM, YC, UK, JL wrote the paper.

Atmos. Chem. Phys. Discuss., doi:10.5194/acp-2017-277, 2017
Manuscript under review for journal Atmos. Chem. Phys.
Discussion started: 28 March 2017

Atmospheric Chemistry and Physics Discussions

Light-induced protein nitration and degradation with HONO emission

Hannah Meusel[1], Yasin Elshorbany[2], Uwe Kuhn[1], Thorsten Bartels-Rausch[3], Kathrin Reinmuth-Selzle[1], Christopher J. Kampf[4], Guo Li[1], Xiaoxiang Wang[1], Jos Lelieveld[5], Ulrich Pöschl[1], Thorsten Hoffmann[6], Hang Su[1,7*], Markus Ammann[3], Yafang Cheng[1,7*]

[1] Max Planck Institute for Chemistry, Multiphase Chemistry Department, Mainz, Germany
[2] NASA Goddard Space Flight Center, Greenbelt, Maryland, USA & Earth System Science Interdisciplinary Center, University of Maryland, College Park, Maryland, USA
[3] Paul Scherer Institute, Villigen, Switzerland
[4] Johannes Gutenberg University, Institute for Organic Chemistry, Mainz, Germany
[5] Max Planck Institute for Chemistry, Atmospheric Chemistry Department, Mainz, Germany
[6] Johannes Gutenberg University, Institute for Inorganic and Analytical Chemistry, Mainz, Germany
[7] Institute for Environmental and Climate Research, Jinan University, Guangzhou, China

* Correspondence to: Y. Cheng (yafang.cheng@mpic.de) or H. Su (h.su@mpic.de)

Abstract. Proteins can be nitrated by air pollutants (NO_2), enhancing their allergenic potential. This work provides insight into protein nitration and subsequent decomposition in the present of solar radiation. We also investigated light-induced formation of nitrous acid (HONO) from protein surfaces that were nitrated either online with instantaneous gas phase exposure to NO_2 or offline by an efficient nitration agent (tetranitromethane, TNM). Bovine serum albumin (BSA) and ovalbumin (OVA) were used as model substances for proteins. Nitration degrees of about 1% were derived applying NO_2 concentrations of 100 ppb under VIS/UV illuminated condition, while simultaneous decomposition of (nitrated) proteins was also found during long-term (20h) irradiation exposure. Gas exchange measurements of TNM- nitrated proteins revealed that HONO can be formed and released even without contribution of instantaneous heterogeneous NO_2 conversion. However, fumigation with NO_2 was found to increase HONO emissions substantially. In particular, a strong dependence of HONO emissions on light intensity, relative humidity (RH), NO_2 concentrations and the applied coating thickness were found. The 20 hours long-term studies revealed sustained HONO formation, even if concentrations of the intact (nitrated) proteins were too low to be detected after the gas exchange measurements. A reaction mechanism for the NO_2 conversion based on the Langmuir-Hinshelwood kinetics is proposed.

1 Introduction

Primary biological aerosols (PBA), or bioaerosols, including proteins, from different sources and with distinct properties, are known to influence atmospheric cloud microphysics and public health (Lang-Yona et al., 2016; D'Amato et al., 2007; Pummer et al., 2015). Bioaerosols represent a diverse subset of atmospheric particulate matter that is directly emitted in form of active or dead organisms, or fragments, like bacteria, fungal spores, pollens, viruses, and plant debris. Proteins are found ubiquitously in the atmosphere as part of these airborne, typically coarse-size biological particles (diameter > 2.5 µm), but also in fine particulate matter (diameter < 2.5 µm) associated with a host of different constituents such as polymers derived from biomaterials and proteins dissolved in

Atmos. Chem. Phys. Discuss., doi:10.5194/acp-2017-277, 2017
Manuscript under review for journal Atmos. Chem. Phys.
Discussion started: 28 March 2017

Atmospheric Chemistry and Physics Discussions

hydrometeors, mixed with fine dust and other particles (Miguel et al. 1999; Riediker et al., 2000; Zhang and Anastasio, 2003). Proteins contribute up to 5% of particle mass in airborne particles (Franze et al., 2003a; Staton et al., 2015; Menetrez et al., 2007) and are also found at surfaces of soils and plants. Proteins can be nitrated and are then likely to enhance allergic responses (Gruijthuijsen et al., 2006). Nitrogen dioxide ($\bullet NO_2$) has emerged as an important biological reactant and has been shown to be capable of electron (or H atom) abstraction from the amino acid tyrosine (Tyr) to form TyrO• in aqueous solutions (tyrosine phenoxyl radical, also called tyrosyl radical; Prütz et al. 1984 and 1985; Alfassi 1987; Houée-Lévin et al., 2015), which subsequently can be nitrated by a second NO_2 molecule. Shiraiwa et al. (2012) observed nitration of protein aerosol, but not solely with NO_2 in the gasphase, and demonstrated that simultaneous O_3 exposure of airborne proteins in dark conditions can significantly enhance NO_2 uptake and consequent protein nitration (3-nitrotyrosine formation) by way of direct O_3-mediated formation of the TyrO• intermediate. A connection between increased allergic diseases and elevated environmental pollution, especially traffic-related air pollution has been proposed (Ring et al., 2001). Tyrosine is one of the photosensitive amino acids and it is subject of direct and indirect photo-degradation under solar-simulated conditions (Boreen, et al., 2008), especially mediated by both UV-B (λ 280−320 nm) and UV-A (λ 320 –400 nm) radiation (Houee-Levin et al., 2015; Bensasson et al., 1993). Direct light absorption or absorption by adjacent endogenous or exogenous chromophores and subsequent energy transfer results in an electronically-excited state of tyrosine (for details see Houée-Lévin et al. 2015 and references therein). If the triplet state of tyrosine is generated, it can undergo electron transfer reactions and deprotonation to yield TyrO• (Fig.1, Bensasson 1993; Davies 1991; Berto et al., 2016). Regardless of how the tyrosyl radical is generated, it can be nitrated by reaction with NO_2, but also hydroxylated or dimerized (Shiraiwa et al., 2012; Reinmuth-Selzle et al., 2014; Kampf et al., 2015).

With respect to atmospheric chemistry, Bejan et al. (2006) have shown that photolysis of ortho-nitrophenols (as is the case for 3-nitrotyrosine) can generate nitrous acid (HONO). HONO is of great interest for atmospheric composition, as its photolysis forms OH radicals, being the key oxidant for degradation of most air pollutants in the troposphere (Levy, 1971). In the lower atmosphere, up to 30% of the primary OH radical production can be attributed to photolysis of HONO, especially during the early morning when other photochemical OH sources are still small (R1, Kleffmann et al., 2005; Alicke et al., 2002; Ren et al., 2006; Su et al., 2008; Meusel et al. 2016).

$$HONO \xrightarrow{h\nu} OH + NO \qquad (h\nu = 300 - 405\ \text{nm}) \tag{R1}$$

HONO can be directly emitted by combustion of fossil fuel (Kurtenbach et al., 2001) or formed by gas phase reactions of NO and OH (the backwards reaction of R1) and heterogeneous reactions of NO_2 on wet surfaces according to R2. On carbonaceous surfaces (soot, phenolic compounds) HONO is formed via electron or H transfer reactions (R3 and R4-R6; Kalberer et al., 1999; Kleffmann et al., 1999; Gutzwiller et al., 2002; Aubin and Abbatt 2007; Han et al., 2013; Arens et al., 2001, 2002; Ammann et al., 1998, 2005).

$$2NO_2 + H_2O \rightarrow HONO + HNO_3 \tag{R2}$$

$$NO_2 + \{C - H\}_{red} \rightarrow HONO + \{C\}_{ox} \tag{R3}$$

$$ArOH + NO_2 \rightarrow ArO\cdot + HONO \tag{R4}$$

$$ArOH + H_2O \rightarrow ArO^- + H_3O^+ \tag{R5}$$

$$ArO^- + NO_2 \rightarrow NO_2^- + ArO\cdot \xrightarrow{H_3O^+} HONO + H_2O \tag{R6}$$

Atmos. Chem. Phys. Discuss., doi:10.5194/acp-2017-277, 2017
Manuscript under review for journal Atmos. Chem. Phys.
Discussion started: 28 March 2017

Atmospheric Chemistry and Physics Discussions

Previous atmospheric measurements and modeling studies have shown unexpected high HONO concentrations during daytime, which can also contribute to aerosol formation through enhanced oxidation of precursor gases (Elshorbany et al., 2014). Measured mixing ratios are typically about one order of magnitude higher than simulated ones, and an additional source of 200-800 ppt h^{-1} would be required to explain observed mixing ratios (Kleffmann et al., 2005; Acker et al., 2006; Sörgel et al., 2011; Li et al., 2012; Su et al., 2008; Elshorbany et al., 2012; Meusel et al., 2016) indicating that estimates of daytime HONO sources are still under debate. It was suggested that HONO arises from the photolysis of nitric acid and nitrate or by heterogeneous photochemistry of NO_2 on organic substrates and soot (Zhou et al., 2001; 2002 and 2003; Villena et al., 2011; Ramazan et al., 2004; George et al., 2005; Sosedova et al., 2011; Monge et al., 2010; Han et al., 2016). Stemmler et al. (2006, 2007) found HONO formation on light-activated humic acid, and field studies showed that HONO formation correlates with aerosol surface area, NO_2 and solar radiation (Su et al., 2008; Reisinger, 2000; Costabile et al., 2010; Wong et al., 2012; Sörgel et al., 2015) and is increased during foggy periods (Notholt et al., 1992). Another proposed source of HONO is the soil, where it has been found to be co-emitted with NO by soil biological activities (Oswald et al., 2013; Su et al., 2011; Weber et al., 2015).

In view of light-induced nitration of proteins and HONO formation by photolysis of nitro-phenols, light-enhanced production of HONO on protein surfaces can be anticipated, which, to the best of our knowledge, has not been studied before.

This work aims at providing insight into protein nitration, the atmospheric stability of the nitrated protein, and respective formation of HONO from protein surfaces that were nitrated either offline in liquid phase prior to the gas exchange measurements, or online with instantaneous gas phase exposure to NO_2, with particular emphasis on environmental parameters like light intensity, relative humidity (RH) und NO_2 concentrations. Bovine serum albumin (BSA), a globular protein with a molecular mass of 66.5 kDa and 21 tyrosine residues per molecule, was chosen as a well-defined model substance for proteins. Nitrated ovalbumin (OVA) was used to study the light-induced degradation of proteins that were nitrated prior to gas exchange measurements. This well-studied protein has a molecular mass of 45 kDa and 10 tyrosine residues per molecule.

2 Materials and methods

2.1 Protein preparation and analysis

BSA (albumin from bovine serum, Cohn V fraction, lyophilized powder, ≥ 96%; Sigma Aldrich, St. Louis, Missouri, USA) or nitrated OVA (ovalbumin) was solved in pure water (18.2MΩ cm) and coated onto the glass tube.

The nitration of ovalbumin (OVA) was described previously (Yang et al., 2010; Zhang et al., 2011). Briefly, OVA (Grade V, A5503-5G, Sigma Aldrich, Germany) was dissolved in phosphate buffered saline PBS (P4417-50TAB, Sigma Aldrich, Germany) to a concentration of 10 mg/ml. 50 µl tetranitromethane TNM (T25003-5G, Sigma Aldrich, Germany) dissolved in methanol 4% (v/v) were added to a 2.5 ml aliquot of the OVA solution and stirred for 180 min at room temperature. Size exclusion chromatography columns (PD-10 Sephadex G-25 M, 17-0851-01, GE Healthcare, Germany) were used for clean-up. The eluate was dried in a freeze dryer and stored in a refrigerator at 4°C.

Atmos. Chem. Phys. Discuss., doi:10.5194/acp-2017-277, 2017
Manuscript under review for journal Atmos. Chem. Phys.
Discussion started: 28 March 2017

Atmospheric Chemistry and Physics Discussions

After the flow-tube-experiments (see below) the proteins were extracted with water from the tube and analyzed with liquid chromatography (HPLC-DAD; Agilent Technologies 1200 series) according to Selzle et al. (2013). This method provides a straightforward and efficient way to determine the nitration of proteins. Briefly, a monomerically bound C18 column (Vydac 238TP, 250 mm×2.1 mm inner diameter, 5 µm particle size; Grace Vydac, Alltech) was used for chromatographic separation. Eluents were 0.1 % (v/v) trifluoroacetic acid in water (LiChrosolv) (eluent A) and acetonitrile (ROTISOLV HPLC Gradient Grade, Carl Roth GmbH + Co. KG, Germany) (eluent B). Gradient elution was performed at a flow rate of 200 µL/min. ChemStation software (Rev. B.03.01, Agilent) was used for system control and data analysis. For each chromatographic run, the solvent gradient started at 3% B followed by a linear gradient to 90% B within 15 min, flushing back to 3% B within 0.2 min, and maintaining 3% B for additional 2.8 min. Column re-equilibration time was 5 min before the next run. Absorbance was monitored at wavelengths of 280 and 357 nm. The sample injection volume was 10-30 µL. Each chromatographic run was repeated three times. The protein nitration degree was determined by the method of Selzle et al. (2013). Native and un-treated BSA did not show any degree of nitration.

2.2 Coated-wall flow tube system

Figure 2 shows a flowchart of the set-up of the experiment. NO_2 was provided in a gas bottle (1 ppm in N_2, Carbagas AG, Grümligen, Switzerland). NO_2 was further diluted (mass flow controller, MFC3) with humidified pure nitrogen to achieve NO_2 mixing ratios between 20 and 100 ppb. Impurities of HONO in the NO_2-gas cylinder were removed by means of a HONO scrubber. The Na_2CO_3 trap was prepared by soaking 4mm firebrick in a saturated Na_2CO_3 in 50% ethanol / water solution and drying for 24 hours. The impregnated firebrick granules were put into a 0.8 cm inner diameter and 15 cm long glass tube, which was closed by quartz wool plugs on both sides. A constant total flow was provided by means of another N_2 mass flow controller (MFC2) that compensated for changes in NO_2 addition. Different fractions of total surface areas (50, 70 and 100%) of the reaction tube (50 cm x 0.81 cm i.d.) were coated with 2 mg BSA or nitrated OVA, respectively. Therefore 2 mg protein was dissolved in 600 µL pure water, injected into the tube and then gently dried in a low humidity N_2 flow (RH ~ 30-40%) with continuous rotation of the tube. The coated reaction tube was exposed to the generated gas mixture and irradiated with either (i) 1, 3 or 7 VIS lights (400-700 nm; L 15 W/954, lumilux de luxe daylight, Osram, Augsburg, Germany) which is 0, 23, 69 or 161 W m^{-2} respectively or (ii) 4 VIS and 3 UV lights (340-400 nm; UV-A, TL-D 15 W/10, Philips, Hamburg, Germany).
An overview of the experiments performed during this study is shown in table 1. Light induced decomposition of nitrated proteins was studied on OVA. Instantaneous NO_2 transformation and its light- and RH- dependence on heterogeneous HONO formation were studied on BSA in short-term experiments. Extended studies on BSA were performed to explore the persistence of the surface reactivity and respective catalytic effects.
A commercial long path absorption photometry instrument (LOPAP, QUMA) was used for HONO analysis. The measurement technique was introduced by Heland et al. (2001). This wet chemical analytical method has an unmatched low detection limit of 3-5 ppt with high HONO collection efficiency (≥ 99%). HONO is continuously trapped in a stripping coil flushed with an acidic solution of sulfanilamide. In a second reaction with n-(1-naphthyl)ethylenediamine-dihydrochloride an azo dye is formed, whose concentration is determined by absorption photometry in a long Teflon tubing. LOPAP has two stripping coils in series to reduce known interferences. In the

first stripping coil HONO is quantitatively collected. Due to the acidic stripping solution, interfering species are collected less efficiently but in both channels. The true concentration of HONO is obtained by subtracting the interferences quantified in the second channel from the total signal obtained in the first channel. The accuracy of the HONO measurements was 10%, based on the uncertainties of liquid and gas flow, concentration of calibration standard and regression of calibration.

The reagents were all high-purity-grade chemicals, i.e., hydrochloric acid (37 %, ACS reagent, Sigma Aldrich, St. Louis, Missouri, USA), sulfanilamide (for analysis, >99 %; Sigma Aldrich) and N-(1-naphthyl)-ethylenediamine dihydrochloride (>98%; ACS reagent, Fluka by Sigma Aldrich). For calibration Titrisol® 1000 mg NO_2^- ($NaNO_2$ in H_2O; Merck) was diluted to 0.001 mg/L NO_2^-. For preparation of all solutions and for cleaning of the absorption tubes 18MΩ H_2O was used.

NO_x concentrations were analyzed by means of a commercial chemiluminescence detector from EcoPhysics (CLD 77 AM, Duernten, Switzerland).

3 Results and discussion

3.1 BSA nitration and degradation

Nitrated proteins can lead to a stronger allergic response. Nitration of proteins can be enhanced by O_3 activation (in the dark). In the environment, about half a day light is present. What happens with irradiated proteins when exposed to NO_2. Can they be nitrated efficiently? To investigate the degree of protein nitration under illuminated conditions, BSA coated on the reaction tube (17.5 µg cm^{-2}) was exposed to 7 VIS lamps (40% of a clear sky irradiance for a solar zenith of 48°; Stemmler et al., 2006) and 100 ppb NO_2 at 70% RH. After 20 hours the BSA nitration degree (ND, concentration of nitrated tyrosine residues divided by the total concentration of tyrosine residues) investigated by means of the HPLC-DAD method was (1.0 ± 0.1)%. Introducing UV radiation (4 VIS plus 3 UV lamps) resulted in a slightly higher ND of (1.1 ± 0.1)%. Note that no intact protein could be detected by HPLC-DAD after another 20 hours of irradiation without NO_2, indicating light induced decomposition of proteins. However, the applied HPLC-DAD technique only detects (nitro-)tyrosine residues in proteins, and does not provide information about protein fragments or single nitrated or non-nitrated tyrosine residues. Hence, proteins might have been decomposed while tyrosine remains in its nitrated form, not detectable by our analysis method. Similarly, proteins (here: OVA) that were nitrated with TNM in aqueous phase prior to coating (21.5 µg cm^{-2}) to an extent of 12.5% also decomposed when illuminated about 6 hours (1-7 VIS lights; with and without 20 ppb NO_2). Thus the nitration of proteins by light and NO_2 was confirmed, but with simultaneous gradual decomposition of the proteins. Effects of UV irradiation (240-340 nm) on proteins containing aromatic amino acids were reviewed previously (Neves-Peterson et al., 2012). It was shown that triplet state tryptophan and tyrosine can transfer electron to a nearby disulfide bridge to form the tryptophan and tyrosine radical. The disulfide bridge could break leading to conformational changes in the protein but not necessarily resulting in inactivation of the protein. In strong UV light (≈200 nm) the peptide bond could also break (Nikogosyan and Görner, 1999).

Franze et al. (2005) analyzed a variety of natural samples (road dust, window dust and particulate matter PM 2.5) collected in the metropolitan area of Munich, containing 0.08-21 g/kg proteins, and revealed equivalent degrees of

nitration (EDN, concentration of nitrated protein divided by concentration of all proteins) between 0.01 and 0.1% only. Such low nitration degree is in line with light induced decomposition of (nitrated) proteins. On the other hand, an EDN up to 10% (average 5%) was found for BSA and birch pollen extract (BPE) exposed to Munich ambient air for two weeks under dark conditions, with daily mean NO_2 (O_3) concentration of 17 to 50 ppb (7 to 43 ppb) in the same study, suggesting the deficiency of decomposition without being irradiated. BSA and OVA loaded on syringe-filters and exposed to 200 ppb NO_2/O_3 for 6 days under dark conditions were nitrated to 6 and 8%, respectively (Yang et al., 2010). Reinmuth-Selzle et al. (2014) found similar ND for major birch pollen allergen Bet v 1 loaded on syringe-filters exposed to 80-470 ppb NO_2 and O_3. When exposed for 3-72 hours to NO_2/O_3 at RH < 92% the ND was 2-4%, while at condensing conditions (RH > 98%) the ND increased to 6% after less than one day (19 hours). The ND of Bet v 1 was considerably increased to 22% for proteins solved in the aqueous phase (0.16 mg mL^{-1}) when bubbling with a 120 ppb NO_2/O_3 gas mixture for a similar period of time (17 hours). Other nitration methods, investigated by Reinmuth-Selzle et al. (2014), e.g., nitration of Bet v 1 with peroxynitrite ($ONOO^-$, formed by reaction of NO with O_2^-) or TNM lead to ND between 10 and 72% depending on reaction time, reagent concentration and temperature. Similarly high NDs of 45-50% were obtained by aqueous phase TNM nitration of BSA and OVA by Yang et al. (2010).

3.2 HONO formation

3.2.1 HONO formation from nitrated proteins

Strong HONO emissions were found for OVA nitrated in the liquid phase prior to gas exchange measurements (ND = 12.5%). A strong correlation between HONO emission and light intensity was observed (50% RH; Fig. 3). Initially, we did not apply NO_2. Thus the observed HONO formation (up to 950 ppt) originated from decomposing nitrated proteins rather than from heterogeneous conversion of NO_2. However, when exposed to 20 ppb of NO_2 in dark conditions, HONO formation increased 4-fold (50 to 200 ppt), and about 2-fold with 7 VIS lamps turned on (950 to 1800 ppt). After 7 hours of flow tube experiments (4.5 h irradiation with varying light intensities (0-1-3-7 lights) + 2.5 h irradiation/20 ppb NO_2 (7-3-0- lights)), no intact protein was found according to the analysis of HPLC-DAD.

3.2.2 Light dependency

To investigate HONO formation on unmodified BSA coating (31.4 µg cm^{-2}) in dependence on light conditions, the radiation intensity (number of VIS lamps) was changed under otherwise constant conditions of exposure at 20 ppb NO_2 and 50% RH. Decreasing light intensity revealed a linearly decreasing trend in HONO formation from about 1000 ppt to 140 ppt (red symbols in Fig. 4). After re-illumination to the initial high light intensity the HONO formation was reduced by 32% (blue symbol in Fig. 4). Stemmler et al. (2006) and Sosedova et al. (2011) also observed a similar saturation of HONO formation on humic acid, tannic and gentisic acid at higher light intensities. Stemmler et al. (2006) argued that surface sites activated for NO_2 heterogeneous conversion by light (R3) would become de-activated by competition with photo-induced oxidants (X^*, R7-8), e.g., primary chromophores or electron donors are oxidized by surface*, which is in line with the observed decomposition of the native protein presented above.

Atmos. Chem. Phys. Discuss., doi:10.5194/acp-2017-277, 2017
Manuscript under review for journal Atmos. Chem. Phys.
Discussion started: 28 March 2017

Atmospheric Chemistry and Physics Discussions

$$surface \xrightarrow{hv} surface^* \xrightarrow{NO_2} HONO + surface_{ox} \quad \text{(R7)}$$

$$X \xrightarrow{hv} X^* \xrightarrow{surface^*} surface - X \quad \text{(R8)}$$

In other studies the NO_2 uptake coefficient on soot, mineral dust, humic acid and other solid organic compounds similarly increased at increasing light intensities (George et al., 2005; Stemmler et al., 2007; Ndour et al., 2008; Monge et al., 2010; Han et al., 2016). Note that the HONO yield (ratio of HONO formed to NO_2 lost) was found to be constant at light intensities in the range of 60-200 W m^{-2} in the work of Han et al. (2016), but have shown a linear dependence on light for nitrated phenols (Bejan et al., 2006).

3.2.3 NO_2 dependency

At about 50% relative humidity and high illumination intensities (7 VIS lamps, ~161 W m^{-2}), heterogeneous formation of HONO strongly correlated with the applied NO_2 concentration (Fig. 5). On a BSA surface of about 16.1 µg cm^{-2} (Tab. 1) the produced HONO concentration increased from 56 ppt at 20 ppb NO_2 to 160 ppt at 100 ppb NO_2. Only at a threshold NO_2 level well above those typically observed in natural environments (>>150 ppb) this increasing trend slowed down to some extent, indicative of saturation of active surface sites. A similar pattern of NO_2 dependence was also observed for light-induced HONO formation from humic acid (Stemmler et al., 2006) and phenolic compounds like gentisic and tannic acid (Sosedova et al., 2011), and for heterogeneous NO_2 conversion on soot under dark conditions (Stadler and Rossi, 2000; Salgado and Rossi, 2002; Arens et al., 2001).

For better comparison of the different studies the HONO concentration measured at different NO_2 concentrations was normalized to the HONO concentration at 20 ppb NO_2 ($[HONO]_{NO2}/[HONO]_{NO2=20ppb}$) in Fig. 5, as variable absolute amounts of HONO were found in different studies and matrices. A cease of the NO_2 dependency on heterogeneous HONO formation can be assessed for most of the studies at NO_2 concentrations ≥ 200 ppb. A very similar correlation (up to 40 ppb NO_2) was observed when NO_2 was applied additionally during the gas phase photolysis of nitrophenols (fig. 5; Bejan et al., 2006). Even though the matrix (nitrophenols) and conditions (illuminated) of the latter is comparable to the experiment presented here, for BSA no clear indication of saturation was found up to 160 ppb of NO_2, pointing to a highly reactive surface of BSA for NO_2 under illuminated conditions. As shown with R7 and R8, the concentration dependence depends on the competing channel R8, therefore, this is strongly matrix dependent, both in terms of chemical and physical properties.

3.2.4 Impact of coating thickness

Strong differences in HONO concentrations were found for experiments with different coating thicknesses applying otherwise similar conditions (20 ppb of NO_2, 7 VIS lamps and 50% RH). While only 55 ppt of HONO concentration was observed for a shallow homogeneous coating of 16.1 µg cm^{-2} (217.6 nm thickness, see below) applied on the whole length of the tube, up to 2 ppb were found for a thick (more uneven) coating of 31.44 µg cm^{-2} (435.2 nm thickness) covering only 50% of the tube (Fig. 6). Potential explanations are that thicker coating leads to (1) more bulk reactions producing HONO, or (2) different morphologies, e.g., higher effective reaction surfaces.

A strong increase in NO_2 uptake coefficients with increasing coating thickness was also observed for humic acid coatings (Han et al., 2016). However, they found an upper threshold value of 2 µg cm^{-2} of cover load (20 nm

absolute thickness, assuming a humic acid density of 1 g cm^{-3}), above which uptake coefficients were found to be constant. The authors also proposed that NO_2 can diffuse deeper into the coating and below 2 µg cm^{-2} the full cover depth would react with NO_2, respectively.

For proteins the number of molecules per monolayer depends on their orientation and respective layer thickness can vary accordingly. One (dry, crystalline) BSA molecule has a volume of about 154 nm^3 (Bujacz, 2012). In a flat orientation (4.4 nm layer height, and a projecting area of 35 nm² per molecule) $3.64x10^{14}$ molecules (40.5 µg; 0.32 µg cm^{-2}) of BSA are needed to form one complete monolayer in the flow tube (i.d. of 0.81 cm, 50 cm length, 100% surface coating). Hence, the thinnest BSA coating applied in the experiment (16.1 µg cm^{-2}) would consist of 50 monolayers revealing a total coating thickness of 217.6 nm, and the thickest BSA coating (31 µg cm^{-2}) would have 99 monolayers and an absolute thickness of 435.1 nm. At the other extreme (non-flat) orientation, more BSA molecules are needed to sustain one monolayer. With 21.7 nm² of projected area of one molecule and 7.1 nm monolayer height, $5.86x10^{14}$ molecules of BSA are needed to form one complete monolayer in the flow tube. The coatings would consist of between 31 (thinnest) and 61 (thickest) monolayers of BSA. With a flat orientation 1-2% (number or weight) of BSA molecules would build the uppermost surface monolayer, whereas in an upright molecule orientation 1.6-3.3% would be in direct contact with surface ambient air.

In the crystalline form several molecules of water stick tightly to BSA. As BSA is highly hygroscopic, more water molecules are adsorbed at higher relative humidity. At 35% RH BSA is deliquesced (Mikhailov et al., 2004). Therefore the above described number of monolayers and the absolute layer thickness are a lower bound estimate.

Conclusively, the thickness dependence on HONO formation is extremely complex. Activation and photolysis of nitrated Tyr occurs throughout the BSA layer. The heterogeneous reaction of NO_2 may or may be not limited to the surface depending on solubility and diffusivity of NO_2. Also the release of HONO may be limited by diffusion.

3.2.5 RH dependency

The dependence of HONO emission on relative humidity is shown in Fig. 7. Here about 25 ppb of NO_2 was applied to a (not nitrated) BSA coated flow tube (17.5 µg cm^{-2}) both in dark and illuminated conditions (7 VIS lights). HONO formation scaled with relative humidity. Kleffmann et al. (1999) proposed that higher humidity inhibits the self-reaction of HONO ($2\ HONO_{(s,\ g)} \rightarrow NO_2 + NO + H_2O$), which leads to higher HONO yield from heterogeneous NO_2 conversion.

The RH dependence of HONO formation on proteins is different to other surfaces. For example, no influence of RH has been observed for dark heterogeneous HONO formation on soot particles sampled on filters (Arens et al., 2001). For HONO formation on tannic acid coatings (both at dark and irradiated conditions) a linear but relatively weak dependence has been reported between 10 and 60% RH, while below 10% and above 60% RH the correlation between HONO formation and RH was much stronger (Sosedova et al., 2011). Similar results were observed for anthrarobin coatings by Arens et al. (2002). This type of dependence of HONO formation on phenolic surfaces on RH equals the HONO formation on glass, following the BET water uptake isotherm of water on polar surfaces (Finnlayson-Pitts et al., 2003; Summer et al., 2004). For humic acid surfaces the NO_2 uptake coefficients also weakly increased below 20% RH and were found to be constant between 20 and 60% (Stemmler et al., 2007).

Atmos. Chem. Phys. Discuss., doi:10.5194/acp-2017-277, 2017
Manuscript under review for journal Atmos. Chem. Phys.
Discussion started: 28 March 2017

Atmospheric Chemistry and Physics Discussions

While on solid matter chemical reactions are essentially confined to the surface rather than in the bulk, proteins can adopt an amorphous solid or semisolid state, influencing the rate of heterogeneous reactions and multiphase processes. Molecular diffusion in the non-solid phase affects the gas uptake and respective chemical transformation. Shiraiwa et al. (2011) could show that the ozonolysis of amorphous protein is kinetically limited by bulk diffusion. The reactive gas uptake exhibits a pronounced increase with relative humidity, which can be explained by a decrease of viscosity and increase of diffusivity, as the uptake of water transforms the amorphous organic matrix from a glassy to a semisolid state (moisture-induced phase transition). The viscosity and diffusivity of proteins depend strongly on the ambient relative humidity because water can act as a plasticizer and increase the mobility of the protein matrix (for details see Shiraiwa et al. 2011 and references therein). Shiraiwa et al. (2011) further showed that the BSA phase changes from solid through semisolid to viscous liquid as RH increases, while trace gas diffusion coefficients increased about 10 orders of magnitude. This way, characteristic times for heterogeneous reaction rates can decrease from seconds to days as the rate of diffusion in semisolid phases can decrease by multiple orders of magnitude in response to both low temperature (not investigated in here) and/or low relative humidity. Accordingly, we propose that HONO formation rate depends on the condensed phase diffusion coefficients of NO_2 diffusing into the protein bulk, HONO released from the bulk and mobility of excited intermediates.

3.2.6 Long term exposure with NO_2 under irradiated conditions

To study long-term effects of irradiation on HONO formation from proteins, flow tubes were coated with 2 mg BSA (17.5 ± 0.4 µg cm^{-2}; 90% of total length) and exposed to 100 ppb NO_2, at 80% RH at illuminated conditions for a time period of up to 20 hours (Fig. 8). Samples illuminated with VIS light only (red and orange colored lines in Fig. 8) showed persistent HONO emissions over the whole measurement period. For reasons unknown, and even though the observed HONO concentrations were within the expected range with regard to the applied NO_2 concentrations, RH and cover characteristics, one sample (orange in Fig. 8) showed a sharp short-term increase in the initial phase followed by respective decrease, not in line with all other samples (compare Fig. 6). However, after 4 hours both VIS irradiated samples showed virtually constant HONO emissions (-3.8 and +1.6 ppt h^{-1}, respectively). The sample illuminated with UV/VIS light (3 UV and 4 VIS lamps) showed a sustained sharp increase in the first 4 hours, followed by persistent and very stable (decay rate as low as -0.5 ppt h^{-1}) HONO emissions at an about 3-fold higher level compared to samples irradiated with VIS only.

Integrating the 20 hour experiments, 9.23×10^{15} (4.6 ppb*h, VISa), 1.53×10^{16} (7.7 ppb*h, VISb) and 4.01×10^{16} (20 ppb*h, UV/VIS) molecules of HONO were produced. This means between 7.7×10^{13} and 3.3×10^{14} molecules of HONO per cm^2 of BSA geometric surface were formed. With respect to the different experimental conditions concerning cover thickness, RH, and NO_2 concentrations, this is in a similar order of magnitude as found for humic acid (2×10^{15} molecules cm^{-2} in 13 hours) by Stemmler et al. (2006).

If BSA acts like a catalytic converter as in a Langmuir-Hinshelwood reaction each BSA molecule can react several times with NO_2 to heterogeneously form HONO. As described in 3.1, BSA nitration is in competition with NO_2 surface reactions and only a limited number of NO_2 molecules could react with BSA forming HONO via nitration of proteins and subsequent decomposition of nitrated proteins. A BSA molecule contains 21 tyrosine residues, which could react with NO_2. But even a strong nitration agent such as TNM is not capable of nitrating all tyrosine residues

Atmos. Chem. Phys. Discuss., doi:10.5194/acp-2017-277, 2017
Manuscript under review for journal Atmos. Chem. Phys.
Discussion started: 28 March 2017

Atmospheric Chemistry and Physics Discussions

and a mean nitration degree of 19% was found (Peterson et al., 2001; Yang et al., 2010), i.e., 4 tyrosine residues of one BSA molecule can be nitrated to form HONO. As 2 mg of BSA was applied for each flow tube coating, a total of $1.8x10^{16}$ protein molecules can be inferred. In 20 hours of irradiating with VIS light 13-22% of the accessible Tyr residues (4 each BSA molecule) would have been reacted. Irradiating with additional UV lights at least 56% of the tyrosine residues would have been nitrated and decomposed, respectively. But as NO_2 is a much weaker nitrating agent and nitration of only one tyrosine residue is probable (ND of BSA with O_3/NO_2 6%; Yang et al., 2010) up to 85% BSA molecules would have been reacted when irradiated with VIS lights, and even more HONO molecules as coated BSA molecules would have been generated under UV/VIS light conditions. Other amino-acids of the protein like tryptophan or phenylalanine might also be nitrated but without formation of HONO (Goeschen et al., 2011). Hence, a contribution of heterogeneous conversion of NO_2 can be anticipated.

3.3 Kinetic studies

The experimental results (especially the stability over a long time) indicate that the formation of HONO from NO_2 on protein surfaces likely underlies the Langmuir-Hinshelwood mechanism in which the protein would act as a catalytic converter (Fig. 9). The first step is the fast reversible physical adsorption of NO_2 (k_1) and water followed by the slow conversion into HONO (eq.1 and eq.2). In our experiments and in the atmosphere there is always sufficient water and for simplification we assume that the reaction rate only depends on NO_2.

$$\frac{d[NO_2]_s}{dt} = k_1 * [NO_2]_g \quad \text{(eq.1)}$$

$$\frac{d[HONO]_s^1}{dt} = k_2 * [NO_2]_s \quad \text{(eq.2)}$$

where index s and g indicate sorbed and gaseous state, respectively.

From the experiments in which higher HONO concentrations were detected with higher light intensities we conclude that the heterogeneous conversion of NO_2 to HONO is light induced or a photochemical reaction. It was observed that the nitration of proteins is a competitive (side) reaction of the direct HONO formation (eq.2) but light induced decomposition of nitrated protein also produces HONO (eq.3).

$$\frac{d[HONO]_s^2}{dt} = k_4 * k_5 * [NO_2]_s \quad \text{(eq.3)}$$

As these two processes cannot be discriminated by the observations presented here, we combine both reactions to formulate an overall formation equation (eq.4) with $k' = k_2 + k_4 * k_5$

$$\frac{d[HONO]_s}{dt} = [HONO]_s^1 + [HONO]_s^2 = k' * [NO_2]_s \quad \text{(eq.4)}$$

The final step of the mechanism is the release of the generated HONO into the air. Since proteins are in general slightly acidic, the desorption of HONO (k_3) should be fairly fast (eq.5).

$$\frac{d[HONO]_g}{dt} = k_3 * [HONO]_s \quad \text{(eq.5)}$$

An effective formation rate of gaseous NO_2 to gaseous HONO k_{eff} was calculated according to eq.6.

$$\frac{d[HONO]_g}{dt} = k_{eff} * [NO_2]_g \quad \text{(eq.6)}$$

with $k_{eff} = k_1 * k' * k_3$

In the first 5-10 min of the long-term experiments HONO increased (Fig. 8 – zoomed in range). This slope was taken as $d[HONO]_g/dt$ in eq.6. Effective rate constants between $1.48x10^{-6}$ s^{-1} (VIS a) and $7.40x10^{-6}$ s^{-1} (VIS b) were

calculated. When irradiating with VIS light only, the concentration of HONO was either constant or decreased for 2 h after this first 10 min. When irradiating with additional UV light, the HONO signal showed an enhancement in two steps. In the first 10 min it was strongly increasing (1327 ppt h^{-1}) and then in the next hour it increased less with 170 ppt h^{-1} prior to stabilization. Therefore two rate constants of 4.10×10^{-6} s^{-1} and 5.2×10^{-7} s^{-1} were obtained, respectively. Reactive uptake coefficients for NO_2 were calculated according to Li et al. (2016). For both irradiation types the uptake coefficient γ was in the range of 7×10^{-6} at the very beginning of each experiment. After a few minutes they decreased to a mean of 1×10^{-7}. The calculated k_{eff} values and uptake coefficient are in the same range and match the NO_2 uptake coefficients on irradiated humic acid surfaces (coatings) and aerosols obtained by Stemmler et al. (2006 and 2007) which were in between 2×10^{-6} and 2×10^{-5} (coatings) and 1×10^{-6} and 6×10^{-6} (aerosols), depending on NO_2 concentrations and light intensities. Similar NO_2 uptake coefficients on humic acid were observed by Han et al. (2016). George et al., (2005) reported about a two-fold increased NO_2 uptake coefficients for irradiated organic substrates (benzophenone, catechol, anthracene) compared to dark conditions, in the order of $(0.6\text{-}5) \times 10^{-6}$. NO_2 uptake coefficients on gentisic acid and tannic acid were in between $(3.3\text{-}4.8) \times 10^{-7}$ (Sosedova et al., 2011), still being higher than on fresh soot or dust (about 1×10^{-7}; Monge et al., 2010; Ndour et al., 2008). The NO_2 uptake coefficients on BSA in presence of O_3 (1×10^{-5}, for 26 ppb NO_2 and 20 ppb O_3) published by Shiraiwa et al. (2012) were somewhat higher than the values calculated here without O_3 but with light.

As proteins can efficiently be nitrated by O_3 and NO_2 in polluted air (Franze et al., 2005, Shiraiwa et al., 2012; Reinmuth-Selzle et al. 2014), the emission of HONO from light-induced decomposing nitrated proteins could play an important role in the HONO budget. As proteins are nitrated at their tyrosine residues (at the ortho position to the OH group on the aromatic ring) the underlying mechanism of this HONO formation should be very similar to the HONO formation by photolysis of ortho-nitrophenols described by Bejan et al. (2006). This starts with a photo-induced hydrogen transfer from the OH group to the vicinal NO_2 group (Fig. 1), which leads to an excited intermediate from which HONO is eliminated subsequently.

4. Summary and Conclusion

Photochemical nitration of proteins accompanied by formation of HONO by (i) heterogeneous conversion of NO_2 and (ii) by decomposition of nitrated proteins was studied under relevant atmospheric conditions. NO_2 concentrations ranged from 20 ppb (typical for urban regions in Europe and USA) up to 100 ppb (representative for highly polluted industrial regions). The applied relative humidity of up to 80% and light intensities of up to 161 W/m^2 are common on cloudy days. Under illuminated conditions very low nitration of proteins or even no native protein was observed, indicating a light-induced decomposition of nitrated proteins to shorter peptides. These might still include nitrated residues of which potential health effects are not yet known. An average effective rate constant of the total NO_2-HONO conversion of 3.3×10^{-6} s^{-1} (for about 120 cm^2 of protein surface and a layer volume of 0.003 cm^3; surface/volume ratio ~ 40000 cm^{-1}) was obtained. At 20 ppb NO_2 238 ppt h^{-1} HONO would be formed. Projecting this to $1 m^2$ of pure BSA surface a formation of 19.8 ppb HONO h^{-1} m^{-2} could be estimated. No data about representative protein surface areas on atmospheric aerosol particles are available. However, the number and mass concentration of primary biological aerosol particles such as pollen, fungal spores and bacteria, containing proteins,

are in the range of 10-10^4 m^{-3} and 10^{-3}-1 µg m^{-3}, respectively (Shiraiwa et al., 2012). Therefore it is difficult to estimate the importance of HONO formation on protein surface and its contribution to the HONO budget. In many studies the calculated un-known source strength of daytime HONO formation is with a range of about 200-800 ppt h^{-1} (Kleffmann et al., 2005; Acker et al., 2006; Li et al., 2012).

Acknowledgment

This study was supported by the Max Planck Society (MPG).

References

Acker, K., Moller, D., Wieprecht, W., Meixner, F. X., Bohn, B., Gilge, S., Plass-Dulmer, C., and Berresheim, H.: Strong daytime production of OH from HNO2 at a rural mountain site, Geophysical Research Letters, 33, 2006.

Alfassi, Z. B.: Selective Oxidation of Tyrosine Oxidation by NO2 and ClO2 at basic pH, Radiation Physics and Chemistry, 29, 405-406, 1987.

Alicke, B., Platt, U., and Stutz, J.: Impact of nitrous acid photolysis on the total hydroxyl radical budget during the Limitation of Oxidant Production/Pianura Padana Produzione di Ozono study in Milan, Journal of Geophysical Research-Atmospheres, 107, 2002.

Ammann, M., Kalberer, M., Jost, D. T., Tobler, L., Rossler, E., Piguet, D., Gaggeler, H. W., and Baltensperger, U.: Heterogeneous production of nitrous acid on soot in polluted air masses, Nature, 395, 157-160, 1998.

Arens, F., Gutzwiller, L., Baltensperger, U., Gaggeler, H. W., and Ammann, M.: Heterogeneous reaction of NO2 on diesel soot particles, Environmental Science & Technology, 35, 2191-2199, 10.1021/es000207s, 2001.

Aubin, D. G., and Abbatt, J. P. D.: Interaction of NO2 with hydrocarbon soot: Focus on HONO yield, surface modification, and mechanism, Journal of Physical Chemistry A, 111, 6263-6273, 2007.

Bensasson RV, Land EJ, Truscott TG. Excited states and free radicals in biology and medicine. Oxford: Oxford University Press; 1993.

Bejan, I., Abd El Aal, Y., Barnes, I., Benter, T., Bohn, B., Wiesen, P., and Kleffmann, J.: The photolysis of ortho-nitrophenols: a new gas phase source of HONO, Physical Chemistry Chemical Physics, 8, 2028-2035, 2006.

Bujacz, A.: Structures of bovine, equine and leporine serum albumin, Acta Crystallographica Section D, 68, 1278-1289, doi:10.1107/S0907444912027047, 2012.

Costabile, F., Amoroso, A., and Wang, F.: Sub-mu m particle size distributions in a suburban Mediterranean area. Aerosol populations and their possible relationship with HONO mixing ratios, Atmospheric Environment, 44, 5258-5268, 2010.

D'Amato, G., Cecchi, L., Bonini, S., Nunes, C., Annesi-Maesano, I., Behrendt, H., Liccardi, G., Popov, T., and Van Cauwenberge, P.: Allergenic pollen and pollen allergy in Europe, Allergy, 62, 976-990, 10.1111/j.1398-9995.2007.01393.x, 2007.

Elshorbany, Y. F., Steil, B., Brühl, C., and Lelieveld, J.: Impact of HONO on global atmospheric chemistry calculated with an empirical parameterization in the EMAC model, Atmos. Chem. Phys., 12, 9977-10000, doi:10.5194/acp-12-9977-2012, 2012.

Elshorbany, Y.F., P. Crutzen, B. Steil, A. Pozzer, and J. Lelieveld, Global and regional impacts of HONO on the chemical composition of clouds and aerosols, Atmos. Chem. Phys., 14, 1167-1184, 2014.

Finlayson-Pitts, B. J., Wingen, L. M., Sumner, A. L., Syomin, D., and Ramazan, K. A.: The heterogeneous hydrolysis of NO2 in laboratory systems and in outdoor and indoor atmospheres: An integrated mechanism, Physical Chemistry Chemical Physics, 5, 223-242, 10.1039/b208564j, 2003.

Franze, T., Krause, K., Niessner, R., and Poeschl, U.: Proteins and amino acids in air particulate matter, Journal of Aerosol Science, 34, S777-S778, 2003.

Franze, T., Weller, M. G., Niessner, R., and Poschl, U.: Protein nitration by polluted air, Environmental Science & Technology, 39, 2005.

George, C., Strekowski, R. S., Kleffmann, J., Stemmler, K., and Ammann, M.: Photoenhanced uptake of gaseous NO2 on solid-organic compounds: a photochemical source of HONO?, Faraday Discussions, 130, 195-210, 2005.

Goeschen, C., Wibowo, N., White, J. M., and Wille, U.: Damage of aromatic amino acids by the atmospheric free radical oxidant NO3[radical dot] in the presence of NO2[radical dot], N2O4, O3 and O2, Organic & Biomolecular Chemistry, 9, 3380-3385, 10.1039/C0OB01186J, 2011.

Gruijthuijsen, Y. K., Grieshuber, I., Stoecklinger, A., Tischler, U., Fehrenbach, T., Weller, M. G., Vogel, L., Vieths, S., Poeschl, U., and Duschl, A.: Nitration enhances the allergenic potential of proteins, International Archives of Allergy and Immunology, 141, 265-275, 2006.

Han, C., Yang, W. J., Wu, Q. Q., Yang, H., and Xue, X. X.: Heterogeneous Photochemical Conversion of NO2 to HONO on the Humic Acid Surface under Simulated Sunlight, Environmental Science & Technology, 50, 5017-5023, 2016.

Heland, J., Kleffmann, J., Kurtenbach, R., and Wiesen, P.: A new instrument to measure gaseous nitrous acid (HONO) in the atmosphere, Environmental Science & Technology, 35, 3207-3212, 2001.

Houee-Levin, C., Bobrowski, K., Horakova, L., Karademir, B., Schoneich, C., Davies, M. J., and Spickett, C. M.: Exploring oxidative modifications of tyrosine: An update on mechanisms of formation, advances in analysis and biological consequences, Free Radical Research, 49, 347-373, 10.3109/10715762.2015.1007968, 2015.

Kalberer, M., Ammann, M., Arens, F., Gaggeler, H. W., and Baltensperger, U.: Heterogeneous formation of nitrous acid (HONO) on soot aerosol particles, Journal of Geophysical Research-Atmospheres, 104, 13825-13832, 1999.

Kampf, C. J., Liu, F., Reinmuth-Selzle, K., Berkemeier, T., Meusel, H., Shiraiwa, M., and Pöschl, U.: Protein Cross-Linking and Oligomerization through Dityrosine Formation upon Exposure to Ozone, Environmental Science & Technology, 49, 10859-10866, 10.1021/acs.est.5b02902, 2015.

Kleffmann, J., H. Becker, K., Lackhoff, M., and Wiesen, P.: Heterogeneous conversion of NO2 on carbonaceous surfaces, Physical Chemistry Chemical Physics, 1, 5443-5450, 1999.

Kleffmann, J., Kurtenbach, R., Lorzer, J., Wiesen, P., Kalthoff, N., Vogel, B., and Vogel, H.: Measured and simulated vertical profiles of nitrous acid - Part I: Field measurements, Atmospheric Environment, 37, 2949-2955, 2003.

Kleffmann, J., Gavriloaiei, T., Hofzumahaus, A., Holland, F., Koppmann, R., Rupp, L., Schlosser, E., Siese, M., and Wahner, A.: Daytime formation of nitrous acid: A major source of OH radicals in a forest, Geophysical Research Letters, 32, 2005.

Kurtenbach, R., Becker, K. H., Gomes, J. A. G., Kleffmann, J., Lorzer, J. C., Spittler, M., Wiesen, P., Ackermann, R., Geyer, A., and Platt, U.: Investigations of emissions and heterogeneous formation of HONO in a road traffic tunnel, Atmospheric Environment, 35, 3385-3394, 2001.

Lang-Yona, N., Shuster-Meiseles, T., Mazar, Y., Yarden, O., and Rudich, Y.: Impact of urban air pollution on the allergenicity of Aspergillus fumigatus conidia: Outdoor exposure study supported by laboratory experiments, Science of The Total Environment, 541, 365-371, http://dx.doi.org/10.1016/j.scitotenv.2015.09.058, 2016.

Levy, H.: Normal Atmosphere: Large Radical and Formaldehyde Concentrations Predicted, Science, 173, 141-143, 1971.

Li, X., Brauers, T., Haeseler, R., Bohn, B., Fuchs, H., Hofzumahaus, A., Holland, F., Lou, S., Lu, K. D., Rohrer, F., Hu, M., Zeng, L. M., Zhang, Y. H., Garland, R. M., Su, H., Nowak, A., Wiedensohler, A., Takegawa, N., Shao, M., and Wahner, A.: Exploring the atmospheric chemistry of nitrous acid (HONO) at a rural site in Southern China, Atmospheric Chemistry and Physics, 12, 1497-1513, 2012.

Li, G., Su, H., Li, X., Kuhn, U., Meusel, H., Hoffmann, T., Ammann, M., Pöschl, U., Shao, M., and Cheng, Y.: Uptake of gaseous formaldehyde by soil surfaces: a combination of adsorption/desorption equilibrium and chemical reactions, Atmos. Chem. Phys., 16, 10299-10311, 10.5194/acp-16-10299-2016, 2016.

Menetrez, M. Y., Foarde, K. K., Dean, T. R., Betancourt, D. A., and Moore, S. A.: An evaluation of the protein mass of particulate matter, Atmospheric Environment, 41, 8264-8274, http://dx.doi.org/10.1016/j.atmosenv.2007.06.021, 2007.

Meusel, H., Kuhn, U., Reiffs, A., Mallik, C., Harder, H., Martinez, M., Schuladen, J., Bohn, B., Parchatka, U., Crowley, J. N., Fischer, H., Tomsche, L., Novelli, A., Hoffmann, T., Janssen, R. H. H., Hartogensis, O., Pikridas, M., Vrekoussis, M., Bourtsoukidis, E., Weber, B., Lelieveld, J., Williams, J., Pöschl, U., Cheng, Y., and Su, H.: Daytime formation of nitrous acid at a coastal remote site in Cyprus indicating a common ground source of atmospheric HONO and NO, Atmos. Chem. Phys., 16, 14475-14493, 10.5194/acp-16-14475-2016, 2016.

Miguel, A. G., Cass, G. R., Glovsky, M. M., and Weiss, J.: Allergens in paved road dust and airborne particles, Environmental Science & Technology, 33, 4159-4168, 1999.

Mikhailov, E., Vlasenko, S., Niessner, R., and Pöschl, U.: Interaction of aerosol particles composed of protein and saltswith water vapor: hygroscopic growth and microstructural rearrangement, Atmos. Chem. Phys., 4, 323-350, 10.5194/acp-4-323-2004, 2004.

Monge, M. E., D'Anna, B., Mazri, L., Giroir-Fendler, A., Ammann, M., Donaldson, D. J., and George, C.: Light changes the atmospheric reactivity of soot, Proceedings of the National Academy of Sciences of the United States of America, 107, 6605-6609, 10.1073/pnas.0908341107, 2010.

Ndour, M., D'Anna, B., George, C., Ka, O., Balkanski, Y., Kleffmann, J., Stemmler, K., and Ammann, M.: Photoenhanced uptake of NO2 on mineral dust: Laboratory experiments and model simulations, Geophysical Research Letters, 35, 10.1029/2007gl032006, 2008.

Neves-Petersen, M.T., Petersen, S., and Gajula, G.P. (2012): UV Light Effects on Proteins: From Photochemistry to Nanomedicine, Molecular Photochemistry - Various Aspects, Dr. Satyen Saha (Ed.), InTech, DOI: 10.5772/37947. Available from: http://www.intechopen.com/books/molecular-photochemistry-various-aspects/uv-light-effects-on-proteins-from-photochemistry-to-nanomedicine.

Nikogosyan, D. N., and Gorner, H.: Laser-induced photodecomposition of amino acids and peptides: extrapolation to corneal collagen, IEEE Journal of Selected Topics in Quantum Electronics, 5, 1107-1115, 10.1109/2944.796337, 1999.

Notholt, J., Hjorth, J., and Raes, F.: Formation of HNO2 on aerosol surfaces during foggy periods in the presence of NO and NO2, Atmospheric Environment Part a-General Topics, 26, 211-217, 1992.

Oswald, R., Behrendt, T., Ermel, M., Wu, D., Su, H., Cheng, Y., Breuninger, C., Moravek, A., Mougin, E., Delon, C., Loubet, B., Pommerening-Roeser, A., Soergel, M., Poeschl, U., Hoffmann, T., Andreae, M. O., Meixner, F. X., and Trebs, I.: HONO Emissions from Soil Bacteria as a Major Source of Atmospheric Reactive Nitrogen, Science, 341, 1233-1235, 2013.

Petersson, A.-S., Steen, H., Kalume, D. E., Caidahl, K., and Roepstorff, P.: Investigation of tyrosine nitration in proteins by mass spectrometry, Journal of Mass Spectrometry, 36, 616-625, 10.1002/jms.161, 2001.

Prutz, W. A.: Tyrosine Oxidation by NO2 in aqueous-solution, Zeitschrift Fur Naturforschung C-a Journal of Biosciences, 39, 725-727, 1984.

Prutz, W. A., Monig, H., Butler, J., and Land, E. J.: Reactions of nitrogen dioxide in aqueous model systems – oxidation of tyrosine units in peptides and proteins, Archives of Biochemistry and Biophysics, 243, 125-134, 10.1016/0003-9861(85)90780-5, 1985.

Pummer, B. G., Budke, C., Augustin-Bauditz, S., Niedermeier, D., Felgitsch, L., Kampf, C. J., Huber, R. G., Liedl, K. R., Loerting, T., Moschen, T., Schauperl, M., Tollinger, M., Morris, C. E., Wex, H., Grothe, H., Pöschl, U., Koop, T., and Fröhlich-Nowoisky, J.: Ice nucleation by water-soluble macromolecules, Atmos. Chem. Phys., 15, 4077-4091, 10.5194/acp-15-4077-2015, 2015.

Ramazan, K. A., Syomin, D., and Finlayson-Pitts, B. J.: The photochemical production of HONO during the heterogeneous hydrolysis of NO2, Physical Chemistry Chemical Physics, 6, 3836-3843, 2004.

Reinmuth-Selzle, K., Ackaert, C., Kampf, C. J., Samonig, M., Shiraiwa, M., Kofler, S., Yang, H., Gadermaier, G., Brandstetter, H., Huber, C. G., Duschl, A., Oostingh, G. J., and Pöschl, U.: Nitration of the Birch Pollen Allergen Bet v 1.0101: Efficiency and Site-Selectivity of Liquid and Gaseous Nitrating Agents, Journal of Proteome Research, 13, 1570-1577, 2014.

Reisinger, A. R.: Observations of HNO2 in the polluted winter atmosphere: possible heterogeneous production on aerosols, Atmospheric Environment, 34, 3865-3874, 2000.

Ren, X., Brune, W. H., Oliger, A., Metcalf, A. R., Simpas, J. B., Shirley, T., Schwab, J. J., Bai, C., Roychowdhury, U., Li, Y., Cai, C., Demerjian, K. L., He, Y., Zhou, X., Gao, H., and Hou, J.: OH, HO2, and OH reactivity

during the PMTACS-NY Whiteface Mountain 2002 campaign: Observations and model comparison, Journal of Geophysical Research-Atmospheres, 111, 2006.

Riediker, Koller, and Monn: Differences in size selective aerosol sampling for pollen allergen detection using high-volume cascade impactors, Clinical & Experimental Allergy, 30, 867-873, 10.1046/j.1365-2222.2000.00792.x, 2000.

Ring, J., Kramer, U., Schafer, T., and Behrendt, H.: Why are allergies increasing?, Current Opinion in Immunology, 13, 701-708, 2001.

Salgado, M. S., and Rossi, M. J.: Flame soot generated under controlled combustion conditions: Heterogeneous reaction of NO2 on hexane soot, International Journal of Chemical Kinetics, 34, 620-631, 10.1002/kin.10091, 2002.

Selzle, K.; Ackaert, C.; Kampf, C. J., et al., Determination of nitration degrees for the birch pollen allergen Bet v 1. Analytical and Bioanalytical Chemistry 2013, 405 (27), 8945-8949.

Shiraiwa, M., Ammann, M., Koop, T., and Pöschl, U.: Gas uptake and chemical aging of semisolid organic aerosol particles, Proceedings of the National Academy of Sciences, 108, 11003-11008, 10.1073/pnas.1103045108, 2011.Shiraiwa, M., Selzle, K., Yang, H., Sosedova, Y., Ammann, M., and Poeschl, U.: Multiphase Chemical Kinetics of the Nitration of Aerosolized Protein by Ozone and Nitrogen Dioxide, Environmental Science & Technology, 46, 6672-6680, 2012.

Sörgel, M., Regelin, E., Bozem, H., Diesch, J. M., Drewnick, F., Fischer, H., Harder, H., Held, A., Hosaynali-Beygi, Z., Martinez, M., and Zetzsch, C.: Quantification of the unknown HONO daytime source and its relation to NO2, Atmospheric Chemistry and Physics, 11, 10433-10447, 2011.

Sörgel, M., Trebs, I., Wu, D., and Held, A.: A comparison of measured HONO uptake and release with calculated source strengths in a heterogeneous forest environment, Atmos. Chem. Phys., 15, 9237-9251, 10.5194/acp-15-9237-2015, 2015.

Sosedova, Y., Rouviere, A., Bartels-Rausch, T., and Ammann, M.: UVA/Vis-induced nitrous acid formation on polyphenolic films exposed to gaseous NO2, Photochemical & Photobiological Sciences, 10, 1680-1690, 2011.

Stadler, D., and Rossi, M. J.: The reactivity of NO2 and HONO on flame soot at ambient temperature: The influence of combustion conditions, Physical Chemistry Chemical Physics, 2, 5420-5429, 10.1039/b005680o, 2000.

Staton, S. J. R., Woodward, A., Castillo, J. A., Swing, K., and Hayes, M. A.: Ground level environmental protein concentrations in various ecuadorian environments: Potential uses of aerosolized protein for ecological research, Ecological Indicators, 48, 389-395, http://dx.doi.org/10.1016/j.ecolind.2014.08.036, 2015.

Stemmler, K., Ammann, M., Donders, C., Kleffmann, J., and George, C.: Photosensitized reduction of nitrogen dioxide on humic acid as a source of nitrous acid, Nature, 440, 195-198, 2006.

Stemmler, K., Ndour, M., Elshorbany, Y., Kleffmann, J., D'Anna, B., George, C., Bohn, B., and Ammann, M.: Light induced conversion of nitrogen dioxide into nitrous acid on submicron humic acid aerosol, Atmospheric Chemistry and Physics, 7, 4237-4248, 2007.

Su, H., Cheng, Y. F., Shao, M., Gao, D. F., Yu, Z. Y., Zeng, L. M., Slanina, J., Zhang, Y. H., and Wiedensohler, A.: Nitrous acid (HONO) and its daytime sources at a rural site during the 2004 PRIDE-PRD experiment in China, Journal of Geophysical Research-Atmospheres, 113, 2008b.

Su, H., Cheng, Y., Oswald, R., Behrendt, T., Trebs, I., Meixner, F. X., Andreae, M. O., Cheng, P., Zhang, Y., and Poeschl, U.: Soil Nitrite as a Source of Atmospheric HONO and OH Radicals, Science, 333, 1616-1618, 2011.

Sumner, A. L., Menke, E. J., Dubowski, Y., Newberg, J. T., Penner, R. M., Hemminger, J. C., Wingen, L. M., Brauers, T., and Finlayson-Pitts, B. J.: The nature of water on surfaces of laboratory systems and implications for heterogeneous chemistry in the troposphere, Physical Chemistry Chemical Physics, 6, 604-613, 10.1039/B308125G, 2004.

Villena, G., Wiesen, P., Cantrell, C. A., Flocke, F., Fried, A., Hall, S. R., Hornbrook, R. S., Knapp, D., Kosciuch, E., Mauldin, R. L., McGrath, J. A., Montzka, D., Richter, D., Ullmann, K., Walega, J., Weibring, P., Weinheimer, A., Staebler, R. M., Liao, J., Huey, L. G., and Kleffmann, J.: Nitrous acid (HONO) during polar spring in Barrow, Alaska: A net source of OH radicals?, Journal of Geophysical Research: Atmospheres, 116, n/a-n/a, 2011.

Vogel, B., Vogel, H., Kleffmann, J., and Kurtenbach, R.: Measured and simulated vertical profiles of nitrous acid - Part II. Model simulations and indications for a photolytic source, Atmospheric Environment, 37, 2957-2966, 2003.

Weber, B., Wu, D., Tamm, A., Ruckteschler, N., Rodriguez-Caballero, E., Steinkamp, J., Meusel, H., Elbert, W., Behrendt, T., Soergel, M., Cheng, Y., Crutzen, P. J., Su, H., and Poeschi, U.: Biological soil crusts accelerate the nitrogen cycle through large NO and HONO emissions in drylands, Proceedings of the National Academy of Sciences of the United States of America, 112, 15384-15389, 2015.

Wong, K. W., Tsai, C., Lefer, B., Haman, C., Grossberg, N., Brune, W. H., Ren, X., Luke, W., and Stutz, J.: Daytime HONO vertical gradients during SHARP 2009 in Houston, TX, Atmospheric Chemistry and Physics, 12, 635-652, 2012.

Yang, H.; Zhang, Y. Y.; Pöschl, U., Quantification of nitrotyrosine in nitrated proteins. Analytical and Bioanalytical Chemistry 2010, 397 (2), 879-886.

Zhang, Y. Y.; Yang, H.; Pöschl, U., Analysis of nitrated proteins and tryptic peptides by HPLC-chip-MS/MS: site-specific quantification, nitration degree, and reactivity of tyrosine residues. Analytical and Bioanalytical Chemistry 2011, 399 (1), 459-471.

Zhang, Q., and Anastasio, C.: Free and combined amino compounds in atmospheric fine particles (PM2.5) and fog waters from Northern California, Atmospheric Environment, 37, 2247-2258, 2003.

Zhou, X. L., Beine, H. J., Honrath, R. E., Fuentes, J. D., Simpson, W., Shepson, P. B., and Bottenheim, J. W.: Snowpack photochemical production of HONO: a major source of OH in the Arctic boundary layer in springtime, Geophysical Research Letters, 28, 4087-4090, 2001.

Zhou, X. L., Civerolo, K., Dai, H. P., Huang, G., Schwab, J., and Demerjian, K.: Summertime nitrous acid chemistry in the atmospheric boundary layer at a rural site in New York State, Journal of Geophysical Research-Atmospheres, 107, 2002a.

Zhou, X. L., Gao, H. L., He, Y., Huang, G., Bertman, S. B., Civerolo, K., and Schwab, J.: Nitric acid photolysis on surfaces in low-NOx environments: Significant atmospheric implications, Geophysical Research Letters, 30, 2003.

Atmos. Chem. Phys. Discuss., doi:10.5194/acp-2017-277, 2017
Manuscript under review for journal Atmos. Chem. Phys.
Discussion started: 28 March 2017

Atmospheric Chemistry and Physics Discussions

Tables and Figures

Tab 1: Details on the different experiments, aims and experimental conditions (coating, applied NO_2 concentration, number of lights switched on, relative humidity and time for each exposure step):

		Coating density (number of monolayers NML_f, thickness)	NO_2 [ppb]	no. of lamps	RH [%]	time per step [h]
A	***light induced decomposition of nitrated protein and HONO formation***					
1	light and NO_2 dependency	n-OVA 21.5 ± 0.8 µg cm^{-2} (68 NML_f , 298.05 nm)	0-20	0-1-3-7 VIS	50	1
B	***heterogeneous NO_2 transformation on BSA***					
2	NO_2 dependency	BSA 16.1±0.4 µg cm^{-2} (50 NML_f , 217.6 nm)	0-20-40-60-100	7 VIS	50	0.5-1
3	light dependency	BSA 31.4±1.4 µg cm^{-2} (99 NML_f , 435.2 nm)	20	0-1-3-7 VIS	50	0.5-1
4	coating thickness	BSA 16.1±0.4 µg cm^{-2} (50 NML_f , 217.6 nm), 22.5±0.8 µg cm^{-2} (71 NML_f , 310.8 nm), 31.4±1.4 µg cm^{-2} (99 NML_f, 435.2 nm)	20	7 VIS		0.5-3
5	RH dependency	BSA 17.5±0.4 µg cm^{-2} (55 NML_f, 241.7 nm)	25	0-7VIS	0-50-80	0.25-1
6	time effect	BSA 17.5±0.4 µg cm^{-2}	100	7 VIS	75	20
7	time effect	BSA 17.5±0.4 µg cm^{-2}	100	4 VIS + 3 UV	75	20

NML_f numbers of monolayers in flat orientation

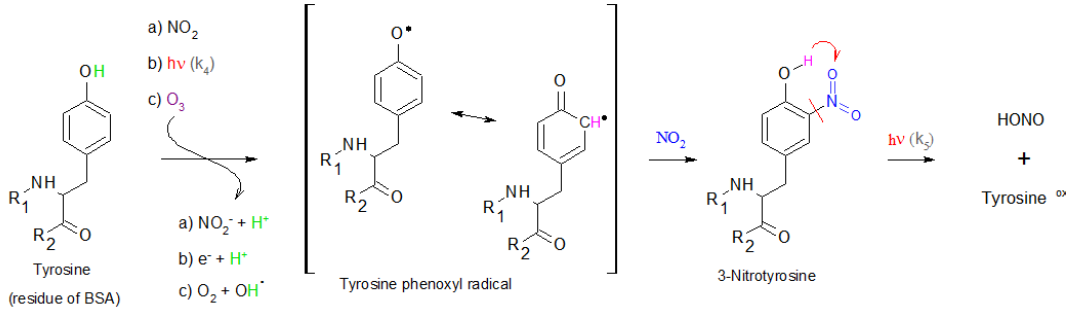

Fig. 1: Reaction mechanism of atmospheric BSA nitration and subsequent HONO emission (formation of the tyrosine phenoxyl radical and following NO_2 addition to 3-nitrotyrosine was adapted from Houée-Levin et al. (2015) and Shiraiwa et al. (2012); intramolecular H-transfer adapted from Bejan et al., 2006).

Atmos. Chem. Phys. Discuss., doi:10.5194/acp-2017-277, 2017
Manuscript under review for journal Atmos. Chem. Phys.
Discussion started: 28 March 2017

Atmospheric Chemistry and Physics Discussions

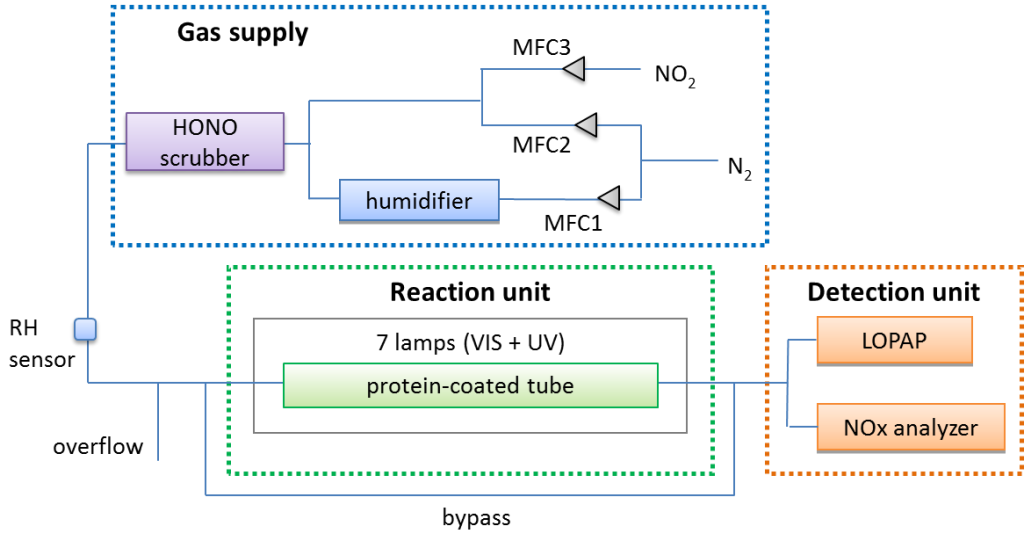

Fig. 2: flow system and set-up, MFC = mass flow controller

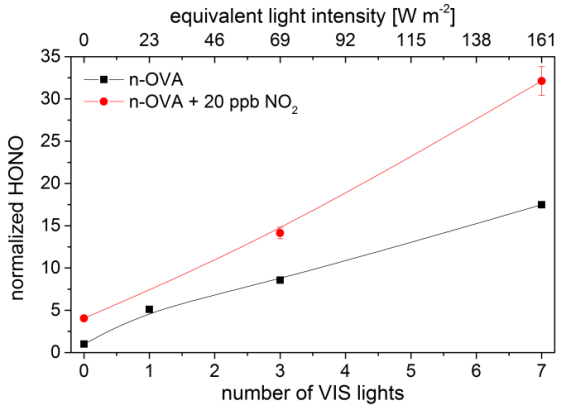

Fig. 3: Light enhanced HONO formation from proteins nitrated in the liquid phase prior to the flow tube experiments (n-OVA: ND 12.5%, coating 21.5 µg cm^{-2}) with and without additional NO_2 in the purging air at 50% RH (HONO is normalized to the HONO concentration measured without NO_2 and no light ($[HONO]_{lights;\ NO2}/[HONO]_{dark;\ NO2=0}$)) .

Atmos. Chem. Phys. Discuss., doi:10.5194/acp-2017-277, 2017
Manuscript under review for journal Atmos. Chem. Phys.
Discussion started: 28 March 2017

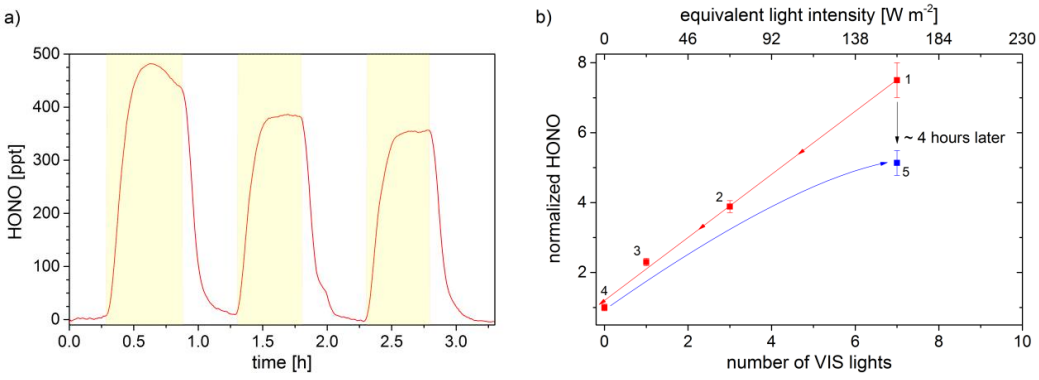

Fig. 4: a) Light enhancement of HONO formation on BSA surface (22.5 µg cm^{-2}), yellow shaded areas indicate periods in which 7 VIS lamps were switched on (RH = 50%, NO_2 = 20 ppb); b) Dependency of HONO formation on radiation intensity at 20 ppb NO_2 and 50% RH (BSA = 31.4 µg cm^{-2}). The experiment started with 7 VIS lights switched on, sequentially decreasing the number of lights (red symbols, nominated 1-4), prior to apply the initial irradiance again (blue symbol, 5). HONO was normalized to the HONO concentration in darkness ($[HONO]_{lights}/[HONO]_{dark}$). Error bars indicate standard deviation of 20-30 min measurements, standard deviation of point 5 covers 2.75 h measurement.

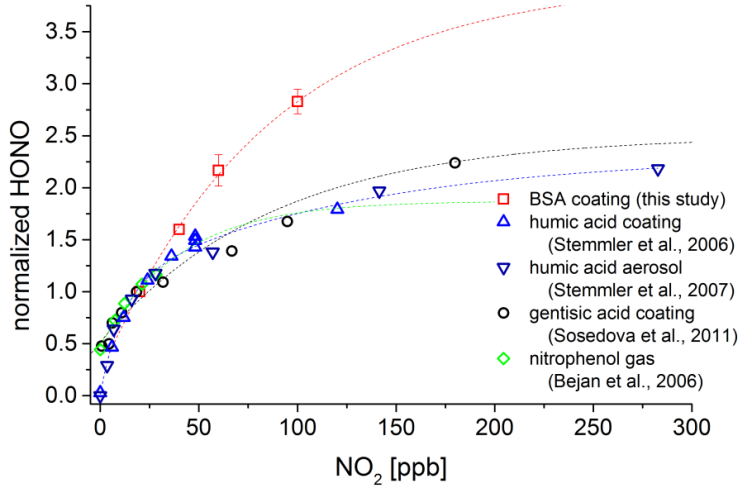

Fig. 5: Comparison of HONO formation dependency on NO_2 at different organic surfaces. HONO concentrations are normalized to the HONO concentration at 20 ppb NO_2 ($[HONO]_{NO2}/[HONO]_{NO2=20ppb}$). Red square = BSA coating (16 µg cm^{-2}) at 161 W m^{-2} and 50% RH (this study), blue triangles pointing up = humic acid coating (8 µg cm^{-2}) at 162 W m^{-2} and 20% RH (Stemmler et al., 2006), dark blue triangles pointing down = humic acid aerosol with 100 nm diameter and a surface of 0.151 m^2 m^{-3} at 26% RH and 1x10^{17} photons cm^{-2} s^{-1} (Stemmler et al., 2007), black circles = gentisic acid coating (160-200 µg cm^{-2}) at 40-45% RH and light intensity similar as in the humic acid aerosol case (Sosedova et al., 2011), green diamonds = ortho-nitrophenol in gas phase (ppm level) illuminated with UV/VIS light.

Atmos. Chem. Phys. Discuss., doi:10.5194/acp-2017-277, 2017
Manuscript under review for journal Atmos. Chem. Phys.
Discussion started: 28 March 2017

Atmospheric Chemistry and Physics Discussions

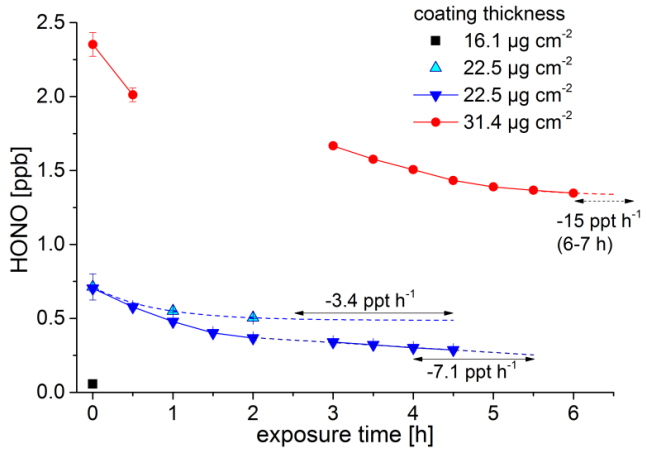

Fig. 6: HONO formation on three different BSA coating thicknesses, exposed to 20 ppb of NO_2 under illuminated conditions (7 VIS lamps). The HONO concentrations were normalized to reaction tube coverage (black: 100% of reaction tube was covered with BSA, blueish: 70% of tube was covered and red: 50% of tube was covered with BSA). The middle thick coating (22.46 µg cm^{-2}) was replicated and studied with different reaction times (cyan and blue triangle). Solid lines (with circles or triangles) present continuous measurements, when those are interrupted other conditions (e.g. light intensity, NO_2 concentration) prevailed. Dotted lines show interpolations. Arrows indicate the intervals in which the shown decay rates were determined. Error bars indicates standard deviations from 10-20 measuring points (5-10 min).

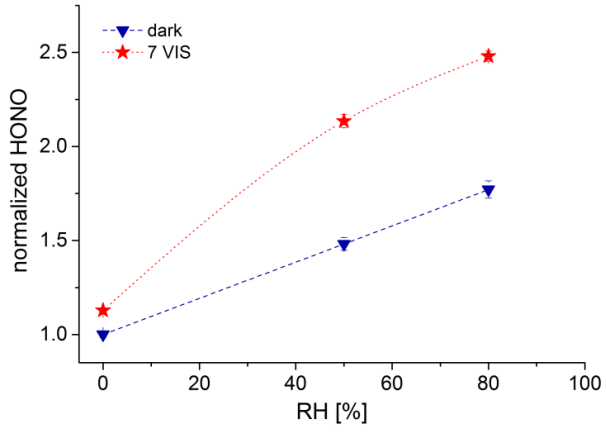

Fig. 7: Dependency of humidity on the transformation of 25 ppb NO_2 in darkness (blue triangle) and with 7 VIS lights (red star). HONO was normalized to HONO concentrations in darkness under dry conditions ($[HONO]_{lights\ on\text{-}off;\ RH}/[HONO]_{dark;\ RH=0}$).

Atmos. Chem. Phys. Discuss., doi:10.5194/acp-2017-277, 2017
Manuscript under review for journal Atmos. Chem. Phys.
Discussion started: 28 March 2017

Atmospheric Chemistry and Physics Discussions

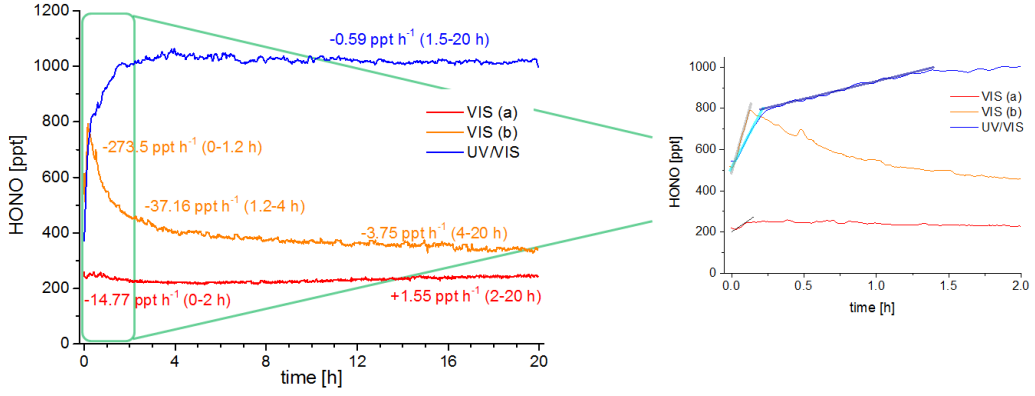

Fig. 8: Extended (20 h) measurements of light-enhanced HONO formation on BSA (three coatings of 17.5 µg cm^{-2}) at 80% RH, 100 ppb NO_2. HONO decay rates [ppt h^{-1}] are shown with time periods (in brackets) in which they were calculated, suggesting a stable HONO formation after 4 hours. Right: zoom in on the first 2 hours. Straight lines (black, grey, light and dark blue) show the regressions of which d[HONO]/dt were used in the kinetic studies.

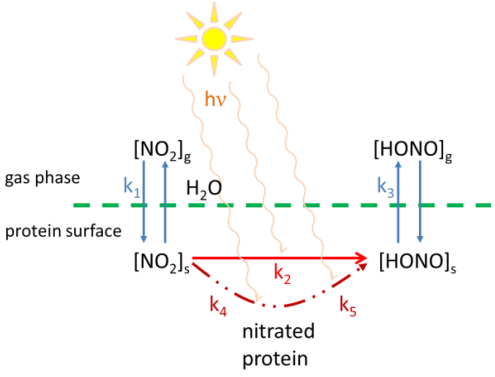

Fig. 9: Schematic illustration of the underlying Langmuir-Hinshelwood-mechanism of light induced HONO formation on protein surface.